THE MODULATION OF BACKSCATTERED MICROWAVE RADIATION BY OSCILLATING WATER DROPS

A Dissertation
Presented to the Faculty
of the New Mexico Institute of
Mining and Technology

In Partial Fulfillment
of the Requirements for the
Degree of Doctor of Philosophy
in Geoscience

Don J. Latham
June 1968

TABLE OF CONTENTS

LIST OF FIGURES

LIST OF TABLES

ABSTRACT

One of the problems in the field of cloud physics is obtaining knowledge of cloud and rainfall drop size distribution. The feasibility of utilizing modulation of backscattered radar by oscillation of drops is considered as a possible source of information.

Water drops of diameters 3-6 mm, freely suspended in a vertical wind tunnel, have been studied by cinematographic and microwave techniques. These studies show: 1) that the frequency of oscillation of a drop depends on size approximately as calculated by Rayleigh, 2) that backscattered 3 cm wavelength radiation is modulated by the oscillation, and 3) the modulation in backscattered intensity is on the order of 3 ± 1 db.

These results show that sizes of single drops can be inferred from measurements of their frequencies. Much more work, both theoretical and experimental, is necessary before this process can be used in the field.

ACKNOWLEDGMENTS

The author wishes to thank his advisor, Dr. Marx Brook for his many kindnesses and unflagging patience.

Thanks are also extended to the staff of the New Mexico Tech Computer Center, to Dennis Williams for his excellent drawings, and to the many people who listened with patience.

Special thanks to the author's wife, who never complained.

THE MODULATION OF BACKSCATTERED MICROWAVE RADIATION BY OSCILLATING WATER DROPS

INTRODUCTION

One of the more pressing needs in the study of cloud physics at the present time is that of determining, as a function of time, the size distribution of liquid water drops in clouds and rainfall by a remote method.

Several methods have been used to investigate the spectrum of drop sizes, both at the ground and in clouds (Pearson and Martin, 1957). Of these, the only remote methods which have been proposed are those of Bartnoff and Atlas (1951), Boyenval (1960), and Bridges and Feldman (1966), all using radar.

The method of Bartnoff and Atlas yields the dropsize distribution as the result of three simultaneous measurements: 1) the average echo return intensity, 2) the audio frequency spectrum of the pulse-to-pulse variation in echo intensity, and 3) the attenuation along the radar beam.

The first of these measurements has been used to estimate rainfall by use of empirically determined "Z-R" relationships,

where Z, proportinal to $n_i D_i^6$ (n_i is the number of scatterers of the ith size and D_i is the diameter of this size), is the return power from a region of cloud or rainfall, and R is the rainfall rate. This relationship is usually given as $Z = AR^b$ where A and b are experimentally determined. The use of a Z-R relationship assumes, however, that the drop-size distribution is repeatable. Cartmill (1963) and Wexler and Atlas (1963) have proposed the use of two differing wavelengths to partially alleviate this requirement.

The second measurement is based on the assumption that the pulse-to-pulse variation in echo intensity from an assembly of particles is caused by rearrangement of the scatterers because of differing velocities of the scatterers. Thus, the audio-frequency spectrum should become broader as the drop-size spectrum increases. This fluctuation spectrum has been shown to be related to the Doppler spectrum of the assembly (Atlas, 1964).

The third measurement of this trio, measurement of attenuation, suffers from many difficulties, the main one being that of measuring the attenuation over the same path as that of the backscattered radiation used in the first measurement.

Another remote method of measuring drop-size distribution, proposed by Boyenval (1960), using a Doppler technique is feasible. This method depends on the fact that the terminal velocity of drops varies with size. Hence, in the absence of vertical or horizontal wind components, the Doppler spectrum of an array will yield the drop-size spectrum.

Bridges and Feldman (1966) have proposed a simultaneous two-frequency attenuation, one-frequency reflectivity technique. This method suffers from the same disadvantages as the Bartnoff-Atlas technique due to the necessity of making attenuation measurements.

Ideally, a remote sensing technique for obtaining drop-size spectra calls for the measurement of some property of drops which is a function (at least to first order) of size alone, independent of such variables as position or velocity relative to the observation point, temperature, external pressure, and impurity content (It is assumed here, of course, that drops in clouds or rain are at terminal velocity, and that the consequences of this fact can be included in "function of size").

In this paper, we propose a mechanism utilizing the modulation of scattered microwave energy produced by changes in shape of an oscillating water drop.

The oscillations in shape of liquid drops have been observed qualitatively, and theoretical relations between frequency and size (mass) have been obtained (Rayleigh, 1877). Experimental verification of these relations have been made by Lenard (1887), Schmidt (1913), and Garner and Lane (1959).

The feasibility of utilizing this property of drops rests on two main points: 1) obtaining a relationship between drop size and oscillating frequency for the case of drops falling at terminal velocity in air, and 2) demonstrating that the scattered microwave energy from an oscillating drop contains the desired information (oscillation frequency, hence, drop size) and that this information can be retrieved.

The investigation of these two points, and the conclusions to be drawn therefrom, are the purpose of this study.

DROP SHAPE

Since a falling water drop has a free surface, dynamic effects are expressed by changes in shape of the surface. These dynamic effects are most easily expressible in terms of pressure.

The deformation of falling drops was first noted by Lenard who attempted to calculate the surface tension constant for falling water drops by measuring their oscillation frequencies (1887) and later measured the fall velocity of drops in a vertical wind tunnel (1904). This tunnel was capable of holding the drops for only 1 - 2 seconds, and the resultant velocities obtained were not very reliable. The drops were observed to resemble oblate spheroids of revolution with the axis of revolution parallel to the direction of fall. Lenard concluded that raindrops would not oscillate to any great extent, there being, in his estimation, no driving force present. Furthermore, he proposed that the shape of the drop was produced by internal circulation.

Schmidt (1913) made visual observations on falling raindrops, noted the oscillations and generally flattened shape, and attempted to find the oscillating frequencies without much success.

To the author's knowledge, the first photographs of falling drops which appear in the literature are those taken by Flower (1928). These are still photographs and show the drop to be an oblate ellipsoid with a slightly flattened bottom. Flower also notes the presence of oscillations.

The next mention of drop shape as shown by photography (generally thought to be the first) is a picture of a falling drop obtained by Edgerton and Killian (1939). Again, an oblate shape with flattened bottom is shown. No mention is made of oscillation.

An attempt to predict the shape of drops was made by Spilhaus (1948). He assumed the shape to be an oblate ellipsoid,

and calculated the axial ratio and fall velocity based on the equalization of surface tension forces with aerodynamic forces. Although his assumptions as to the surface tension forces are wrong (see McDonald, 1954), Spilhaus managed to fit his values of terminal velocity to those of Laws (1941) by a suitable choice of a parameter relating the pressure at the equator of the drop to the stagnation pressure ($1/2\ \rho v^2$). Oscillation and internal circulation are not mentioned.

Hinze (1949 a, b), by considering small perturbations about the spherical shape and solving the hydrodynamic equations for this case, predicted flattening of a drop falling in air. His conclusions deal mostly with breakup and its relation to the Weber number of the drop. (His solution contains a term dealing with oscillations which will be treated later.) Internal circulations, caused by tangential stress at the boundary, were presumed negligible in comparison to the normal stresses.

Blanchard (1949, 1950), constructed a vertical wind tunnel in which he supported drops of 5 - 9 mm diameter (diameter of a sphere of water of mass equivalent to the drop). He found that the drops were flattened oblate spheroids, and noted oscillations in shape. Axial ratios of the drops were measured. Internal circulation was found experimentally to be negligible.

Imai (1950) calculated a first order correction to shape by considering the balance of surface tension forces for the distorted surface with aerodynamic forces calculated for a sphere. This technique yielded a shape correction and a relation between terminal velocity and equivalent diameter. The relation found correlated well with the measurements of Gunn and Kinzer (1949) up to 2 mm diameter.

Savic (1953), by considering the aerodynamic forces around a sphere in balance at the surface of the drop with surface tension

and hydrostatic forces, predicted qualitatively the flattening of the bottom of a falling drop and the general shape, including a "dimpling" of the bottom of the drop for large diameters ($\geq$ 2 mm). The forces were assumed to be unchanged by the distortion. Oscillations were thus not considered. Internal circulation was assumed negligible.

The first extensive experiment on the shape of drops was performed by Magono (1954), in which drops in the range 2 - 7 mm diameter were allowed to fall 12 meters through stagnant air and photographed. The shape of all drops was found to be that of an oblate spheroid flattened on the bottom. A considerable spread in the axial ratios for a given equivalent diameter was noted, this spread increasing with increasing diameter. The reason for this spread was surmised to be oscillations of the drop caused by the initial perturbation due to formation from a hollow needle.

The most definitive work on the shape of drops is that of McDonald (1954). The forces acting on a drop are summarized by him as follows: 1) surface tension, 2) internal hydrostatic pressure, 3) electrical (due only to charge on the drop, not external fields), 4) internal circulation, and 5) aerodynamic.

The surface tension pressure at any point on the surface is given in terms of the principal radii of curvature at that point by the relation,

$$\Delta p_s = \sigma \left(\frac{1}{R_1} + \frac{1}{R_2} \right), \qquad (1)$$

where p_s is the pressure difference across the surface, σ is the surface tension constant and R_1 and R_2 are the principal radii of curvature at the point (Lamt, 6th edition). If R_1 and R_2 are taken as positive when the interface is convex from outside, then Δp_s is the interior pressure minus the exterior pressure. For a sphere, we have $p_s = 2\sigma/r$, where r is the radius.

The hydrostatic pressure, p_h, is of course given by ρgz, where z is the height above the bottom of the drop. Again for a sphere, $p_h = 2 \rho gr$. This pressure at the bottom of a spherical drop becomes equal to the surface tension pressure for a drop of 6 mm diameter.

The electrostatic tension, T, on the surface of a spherical drop bearing a charge density, γ, is $T = 2 \pi \gamma^2$. An upper limit for γ, and hence T, can be obtained by setting the value of the electric field at the surface equal to the breakdown value of air. If this is done, the maximum value of T may be calculated. This value at sea level is $\sim$400 dyne/cm^2 and at 500 mb level is $\sim$ 200 dyne/cm^2. The surface tension pressure is equal to the sea level value at a diameter (for a sphere) of $\sim$7 mm. It is noted by McDonald, however, that charges on drops in the natural environment seldom reach values sufficient to give 200 dynes/cm^2. He makes no mention of the action of external fields.

Based on the assumptions that 1) shear stress is continuous across the interface, 2) surface air velocity is near zero at the base of the boundary layer compared to just outside the boundary layer and 3) that the drop remains spherical (to simplify computations), McDonald calculates the circulation velocity at the "waist" of the drop to be $\sim$ 3% of the terminal velocity. Circulation velocity has been experimentally shown (Garner and Lane, 1959 b) to be less than 1% of terminal velocity.

The exact mathematical calculation in closed form of the pressure distribution around a body having the shape of a drop is not possible for the range of Reynolds numbers (500 - 1000) under consideration. McDonald thus proposes a statement of the problem enabling him to calculate the pressure distribution at points on the drop. This model is subsequently checked by adding

up the surface pressure increments around the drop in zones and comparing the total pressure drag thus found with the weight of the drop.

The model may be stated thus: if surface charges and internal circulation are neglected, the shape of the drop will be that for which aerodynamic pressure, surface tension pressure, and internal pressure satisfy the hydrostatic equation just inside the surface of the drop.

By measuring the radii or curvature from photographs (those of Magono), McDonald calculates the pressure distribution at points around the surface.

The general pattern of the pressure profile, proceeding along the surface from the stagnation point toward the top of the drop, shows the following characteristic features: the pressure falls rapidly, reaching zero at a point well below the maximum cross-section of the drop, beyond which it approaches a large negative value. The pressure then becomes less negative, approaching a low negative value in the region of maximum cross-section and remaining at this low value with irregular fluctuations, assuming a slightly more negative value at the top of the drop. (These characteristics have been confirmed by Finlay, 1957.)

From this profile, McDonald concludes that flow separation is occurring around a drop, comparing the flow around drops to flow around spheres. Qualitatively, flow separation explains the shape of drops quite adequately. Oscillations of drops are not mentioned.

Some experimental work on the shape of drops is that of Jones (1959), who photographed natural raindrops with cameras at right angles. The axial ratios of over 1000 drops were measured and tabulated as a function of equivalent diameter.

Figure 1 presents the results of his experiment, along with the experiments of Blanchard and Magono and the theoretical calculations of Spilhaus, Savic, Hinze, and Hughes and Gilliland (1952). The latter is an empirical relation based on drag coefficient, Reynolds number, and the measurements of terminal velocity of Laws (1941).

Some drops in Jones' work were observed to have an axial tilt, which he presumed to be caused by local turbulence and wind shear.

Of primary importance to this study is the tremendous variation in measured axial ratio for a given drop equivalent diameter. If we denote the vertical axis of the ellipsoid as b and the horizontal axis as a, the b/a ratios vary from 1.35 (prolate ellipsoid) to 0.45 (oblate ellipsoid), even larger than Magono's observations of 0.9 to 0.7 for stagnant air. These figures conclusively illustrate the point that raindrops, at least in the range 2 mm - 7 mm diameter must be oscillating with a very large amplitude.

Before proceeding to a consideration of the literature on velocity, oscillations, and wakes, completeness requires mention of deformation of drops in the Stokes law region. This deformation in creeping flow has been calculated by Saito (1913), Taylor and Acrivos (1964) and Matunobu (1966). The results of these calculations show that even in the Stokes region ($Re \ll 1$), deformation of the drop into an oblate spheroidal shape can be expected.

Terminal Velocity of Drops in Air

Although attempts (Imai, 1950, Spilhaus, 1948) have been made to calculate the terminal fall velocity of drops in air, the only reliable figures available are experimental.

Terminal velocity experiments have been made by Lenard (1904),

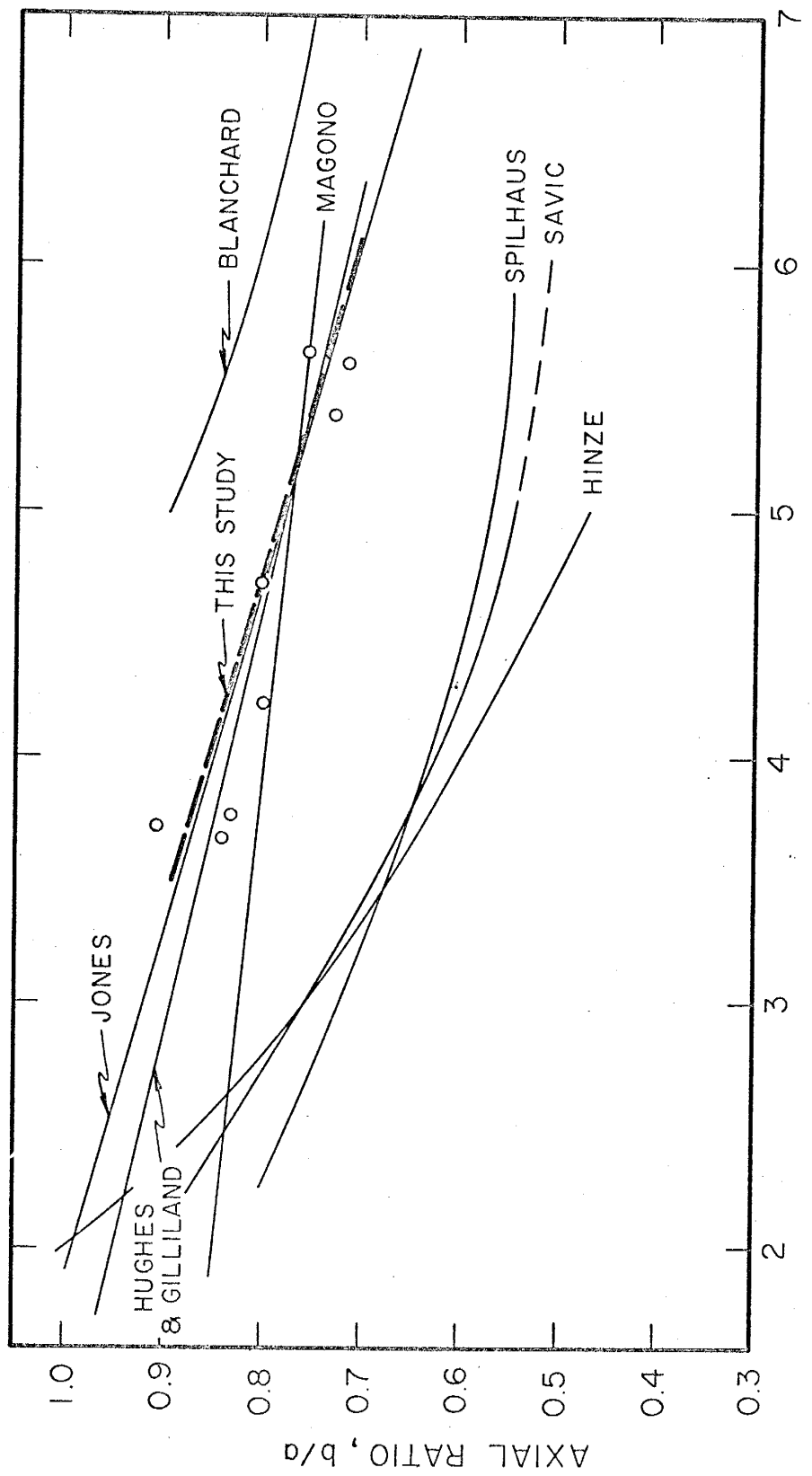

Fig. 1: A summary of the shape of drops as measured by axial ratio. (The circles are data points obtained in this study.)

Schmidt (1909), Flower (1928), Laws (1941), Gunn and Kinzer (1949), Davies (unpublished, mentioned in Best, 1950), and Van Der Leeden, Nio, and Suratman (1956). Best (1950) has generated empirical formulae for terminal velocities for varying atmospheric conditions based on the measurements of Davies and Gunn and Kinzer. The most complete and definitive measurements are those of Gunn and Kinzer and these will be used in this paper where ever the use of this quantity is necessary.

DROP OSCILLATION

Theoretical

The first theoretical treatments of the oscillation of free motionless drops appears in Rayleigh (1877). From dimensional analysis, he shows the period to be proportional to $\sqrt{\frac{\rho V}{\sigma}}$, where ρ is the density of the fluid, V is the volume of the drop, and σ is the surface tension constant. His method of evaluation of the period of oscillation may be found in Appendix I. Basically, the technique consists of expressing the radial coordinate of the surface as a series, $r = a_o + \sum_{n=1} a_n P_n (\cos \theta)$, finding the potential and kinetic energies of the motion and applying Lagrange's method to the result, giving

$$w^2 = n (n - 1) (n + 2) \frac{\sigma}{R^3} , \qquad (2)$$

where w is the frequency of the oscillation in rad/sec, and n is the order of the Legendre polynomial in the expansion for the surface. For n = 2, the oscillations are prolate spheroid - oblate spheroid with a sphere as the equilibrium shape. The n = 1 mode, of course, merely implies a uniform translation of the body as a whole, while the n = 0 mode is that of adding or subtracting mass from the body.

Lamb (1879) approaches the problem of a drop of liquid in a second liquid of differing density using another method. Expanding the surface in surface harmonics and assuming a sine dependence of the time variation, he finds the internal and external velocity potentials, and, from these, the variable portions of the internal and external pressures. The curvature of the surface is then found, and the pressure difference equated to the sum of curvatures times the

interfacial tension (see equation 1). Lamb's result is given by

$$w^2 = n(n+1)(n-1)(n+2)\frac{\sigma}{[(n+1)\rho + n\rho']R^3} \qquad (3)$$

where n, ρ, R, σ, and w are the same as for (2) and ρ' is the density of the external fluid. For $\rho' = 0$, Rayleigh's result is recovered.

Later in his book, Lamb discusses the damping of these oscillations. The technique used to estimate the damping time is, assuming irrotational flow within the drop, equating the rate of dissipation of energy to the time rate of change of total energy. A damping time

$$\tau = \frac{1}{(n-1)(2n+1)} \frac{R^2}{\nu} \qquad (4)$$

is thus obtained, where ν is the kinematic viscosity of the liquid. Lamb notes that, since a time average over many periods yields eq. (4), this solution is not correct for aperiodic damping.

Hinze (1949 a) in solving the hydrodynamic equations around a slightly perturbed sphere, obtains a frequency dependence identical to that of Lamb and Rayleigh, but the damping time is found to be

$$\tau = \frac{1}{n(n-1)} \frac{R^2}{\nu} \quad . \qquad (5)$$

Hodgkinson (1953) has utilized Lamb's formation of kinetic energy, potential energy, and dissipation rate to formulate the equation of motion for the surface of the drop. His results are identical to those of Lamb. Hodgkinson gives the diameter of the critically damped drop as 0.08μ.

Chandrasekhar (1959) has calculated the damping of a viscous globe under the action of gravitational forces, and Reid (1960), has shown that Chandrasekhar's treatment can be applied to surface

shown that Chandrasekhar's treatment can be applied to surface tension forces as well. The diameter of the critically damped drop is given by the formula

$$\frac{W_o R^2}{\nu} = 3.69, \qquad (6)$$

where W_o is the Rayleigh/Lamb frequency. This formula yields, according to Reid, a critically damped diameter of 0.46 mm. Reid, however, has an arithmetic mistake, for formula (6), when calculated, gives 0.45 μ. (The discrepancy can easily be explained if Reid forgot to include the value of ν in the final calculation.)

The most recent calculation of oscillation frequency and amplitude is that of Golovin (1964 a, b). Golovin considers two cases: 1) a Hill vortex within the drop (1964 a) and potential flow within the drop (1964 b). In each case, the drop is considered stationary in a field of uniform velocity. He finds expressions for the velocity of flow inside and outside the drop. The pressures are then obtained from the Bernoulli equation and the difference in these is equated to Lamb's formulation of the surface tension pressure difference.

In each of these two cases, Golovin obtains an extremely complex differential equation which, if the external velocity is reduced to zero, does yield frequencies as predicted by Rayleigh. The differential equations do not admit of even a reasonable computer solution, although if assumptions are made, a frequency is obtained which is in general 50% lower than that predicted by Rayleigh.

Table I presents damping calculations from Lamb, Reid, and Hinze. The size of drop corresponding to aperiodic decay (critical damping) is given, along with the size drop which yields a 1% lowering of frequency of oscillation with respect to the undumped

frequency. The frequency formula is the same for all investigators.

TABLE I

Damping figures for n = 2 (prolate - oblate) mode of oscillation of water drops in air

Investigator	Diameter of Critically damped Drop (Microns)	Diameter of Drop for which frequency lowers by 1% (Microns)	Time for 2 mm di Drop to reach 37% of initial amplitud (Seconds)
Lamb	0.063	3.15	0.158
Reid	0.045	2.25	0.222
Hinze	0.0133	0.66	0.752

Clearly, the frequency of oscillation of large drops will be lowered $\ll$ 1% by internal viscous damping.

Experimental

There are only three experimental measurements of oscillation of drops available, those of Lenard (1887), Schmidt (1913), and Garner and Lane (1959), although qualitative descriptions have been made by many investigators (see section on shape). Lenard and Schmidt found in general that the period of natural oscillations exceeded the period as predicted by Rayleigh.

Garner and Lane, using photographs of drops taken by a 64 frame per second camera, concluded that Rayleigh's formula holds, but the error given was approximately 25%, hence this measurement can hardly be relied upon.

Two measurements of oscillation have been made for liquid-liquid systems (for which relation (3) should hold if damping is neglected). Kaparthi and Licht (1962) note a frequency peak at about 5 cps for various systems, i. e., the oscillating frequency increases with

increasing drop size, peaks, and then decreases again as drop size increases. Consideration of their experimental technique, however, reveals that the stroboscope flash rate for all pictures taken was ten flashes per second, yielding a Nyquist frequency of 5 cps. No mention is made of the Nyquist frequency or of the consequences of the low flash rate.

Schroeder and Kintner (1965), have examined photographs of large drops taken at a film frequency of 64 frames/second, for two liquids of close density. They find a mean departure of approximately 16% from Lamb's theory. This departure is explained by finite amplitude, and by using a correction for this, the mean departure can be reduced to 9%. There seems to be, however, a more systematic pattern to the departure from theory, possibly due to the neglect of viscosity effects on the part of the authors (viscosity effects are not mentioned). Of interest is their finding that at large sizes, the prolate-oblate oscillations give way to "random wobblings", and that for Reynolds numbers less than 200, oscillations ceased in all cases. They note that Re 200 is the minimum necessary for vortex wake shedding to take place.

Drop Wakes

The interaction of a drop with its wake was first noted in the literature by Gunn (1949) (although mention is made of the unpublished observation of this phenomenon by Davies in 1939 (Lane and Green, 1956). The phenomenon is shown to be one of resonance, wherein the frequency of eddy shedding of the drop as predicted by Moller (1938) coincides with the natural frequency of the drop as predicted by Rayleigh. This phenomenon occurs for drops of approximately 1 mm diameter at a Reynolds number of about 250. Drops in this region were observed to fall very erratically, in a generally spiral pattern, with the axis in the direction of fall.

This observation shows that the wake of the drop and the drop itself must surely interact. A similar phenomenon (i. e., spiralling of a falling object) has been noted by Shafrir (1965) and Goldburg and Florsheim (1966).

Shafrir has made measurements of the spiral path taken by solid spheres of differing densities falling in water. For Re 10^3 (covered in his work) the frequency of the spiralling oscillation generally increased with Re, the frequency for Re 10^3 being 0.5 Hz. As mentioned previously, Moller shows increasing eddy shedding frequency with increasing Reynolds number.

Goldburg and Florsheim (1966), for solid bodies of various shapes, find that oscillation of the body-as-a-whole sets in at a Reynolds number of approximately 150 - 200, the same value of Reynolds number found for initiation of "vortex loop" wakes.

Although no information on wake behavior in liquid-air systems is available, there is some available on liquid-liquid systems. This data enables some qualitative conclusion to be made as to the liquid-air system because of the presence in both cases of a free boundary on the moving particle.

Magarvey and Bishop (1961), have classified the wakes behind liquid drops moving at terminal velocity through water. This classification is based on photographs taken of dye stripped off the drops. Figure 2 shows this classification superimposed on a graph of the Reynolds number curve for drops as spheres (based on Gunn and Kinzer, 1949), and the Reynolds number as corrected to the major axis of an oblate spheroid (based on Jones, 1959). This figure shows that the size drop considered by Gunn (1949) is within the range of vortex wake formation.

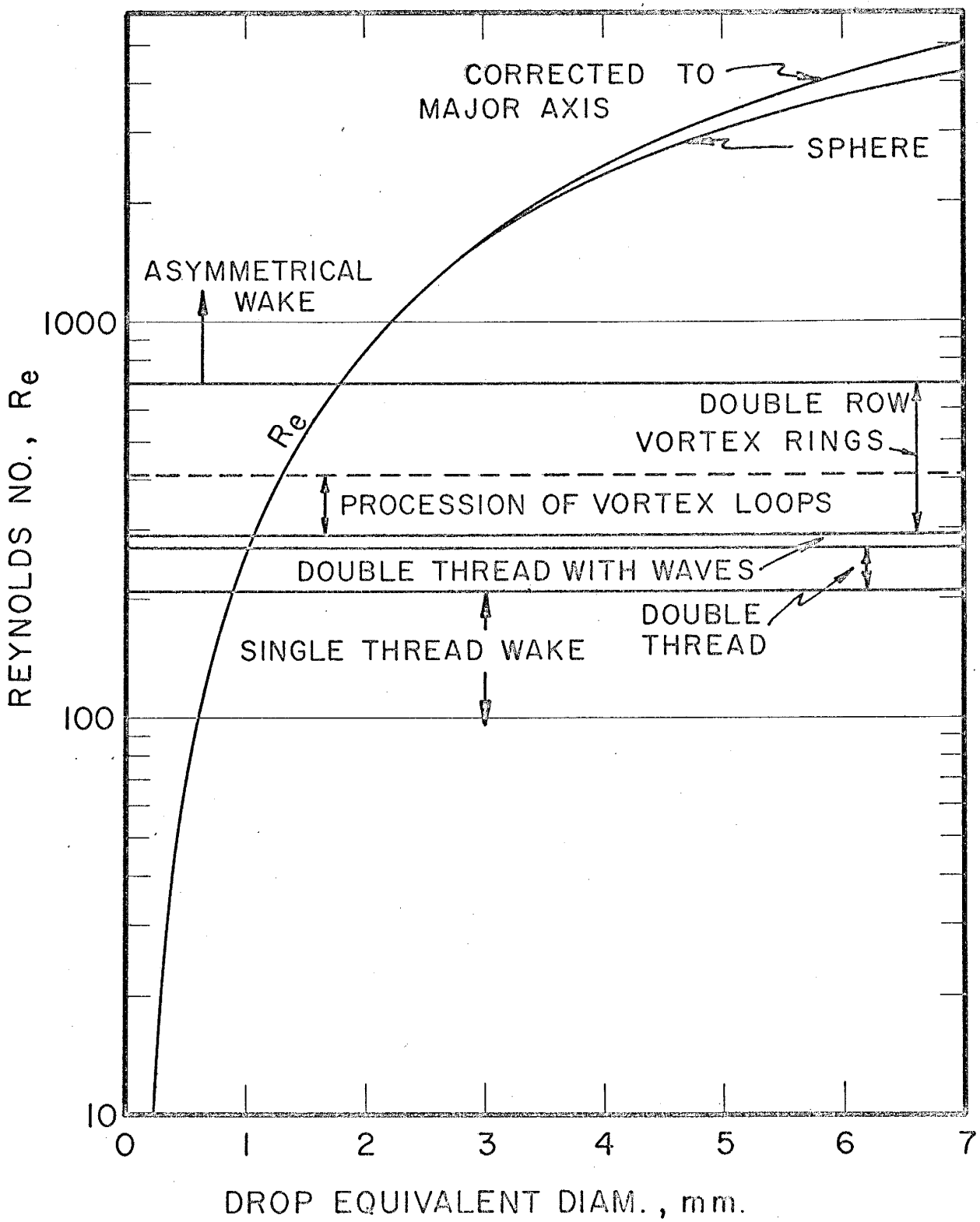

Fig. 2: Reynolds # vs. drop equivalent diameter.
(Data from Gunn and Kinzer, 1949, classifications from Magarvey and Bishop, 1961)

Cinematographic shadowgraphs of wakes behind drops in liquid-liquid systems have been taken by Winnikow and Chao (1966). These show that oscillations begin for Reynolds numbers greater than 400. In addition, estimates were made of the frequency of prolate-oblate oscillations. The photographs showed that the frequency of oscillation was some 20% lower than the predicted frequencies of Lamb, and that the wake shedding frequencies were in general very close in value to the oscillation frequencies, i.e., decreased in frequency with increasing size of drop, contrary to Moller's trend for solid spheres. The lowering of experimental frequency as compared to theory is attributed to viscous effects.

Recapitulation

The general picture obtained from the foregoing survey may be summarized as follows:

1) Drops moving at terminal velocity in air probably oscillate.

2) The oscillating frequency may be shifted somewhat from the ideal case, but this shift is almost certainly not due to viscous damping, and must be due to finite amplitude, aerodynamics, internal hydrostatic head, external electric fields, or a combination of these.

3) The amplitude of these oscillations varies considerably, both with drop size and in time for the same size drop. The time variation of amplitude is probably not due to damping, but to wake characteristics or turbulence in the region around the drop.

4) Extremely large drops ($\geq$ 5 mm dia) may not oscillate in the prolate-oblate mode but may oscillate about axes 90° apart in the horizontal plane or may display eccentric rotation about the vertical axis with differing horizontal axes which remain constant, (Blanchard, 1950). The first of these is of small amplitude (Finlay, 1957) and the second occurs in large drops having low viscosity and surface tension (Blanchard, 1950; Garner and Lane, 1959).

5) For drops larger than 0.8 mm (Re 200), the driving force for oscillation is probably the wake of the drop itself, as can be demonstrated in liquid-liquid systems (Winnikow and Chao, 1966), although coalescence and the wakes of other drops may excite oscillations. The excess surface energy available, for example, by the process of coalescence of two drops of the same diameter, is 80% of the surface energy of one of them.

Photographs of Class IV loop wakes (Magarvey and Bishop, 1961) show existence of the wake for more than 5 seconds after the passage of the drop. Thus the turbulence in the air due to one drop is available to excite another, even if the population is sparse.

There is probably very little natural air turbulence of the proper size (Colgate, 1966; D. Lilly, private comm.) available for excitation.

The oscillation of drops smaller than 0.8 mm diameter is possible, but the means of excitation must be coalescence, or turbulence from other drops. (A further possibility is that small drops which have been formed by the breaking-up of large drops may oscillate).

6) It is probable that drops greater than 0.8 mm diameter (Reynolds # $\geq$ 200) will travel in a spiral path. The relationship between velocity and frequency of this path may be extremely complex.

7) In regions of cloud where high electric fields are present, the frequency of oscillation will be lowered. Sample (1965) has given a method of finding the eigenvalues for a drop in an external field, neglecting aerodynamic forces. Some of the effects of oscillation on drop behavior in high fields may be found in Ausman and Brook (to be published).

SHAPE AND MICROWAVE SCATTERING

Although much work (Atlas, 1964) has been done on meteorological targets (water drops, ice, snow), very little of this work takes into account the shape of the particle. In addition, most work on shape of scatterer deals with ice and wet ice, and is not germane to the present work because of the large difference in refractive index at microwave frequencies of ice and water.

Scattering Solution in Use

For microwave work, the scattering solutions used have been those of Rayleigh, Gans, Mie, and, more recently, Stevenson (1953 a, b).

The Rayleigh theory holds for spherical particles whose diameters are very much less than the wavelength of radiation used ($D \leq 0.06\lambda$), for cloud drops and 3 cm radar, particles less than 1.8 mm dia. This theory predicts that the return from a particle is proportional to D^6, and the return from an array of such scatterers is proportional to $\sum n_i D_i^6$.

The Mie theory is a general one which can deal with spherical particles whose diameter is not less than the wavelength. The functions describing the backscattered energy are complex, the return from any given particle size (or aggregate thereof) depending in a rather nasty way on the ratio (diameter of scatterer) / wavelength. The result of the application of the Mie theory to water spheres has been tabulated by Herman er al. (1961) for wavelengths of interest in radar meteorology.

The Gans theory is an approximate treatment of scattering from spheroids for, again, sizes of scatterer much smaller than wavelength. This theory has not been experimentally verified.

The scattering theory of Stevenson (1953 a) is the most complete theory to date. This theory will not be expounded in the present paper,

as the degree of complexity makes this impracticable. Basically, the technique used is the expansion of the incident and scattered fields in terms of the ratio/dia/wavelength, enabling the solution to Maxwell's equations to be put into a more tractable form for computation. The application of Stevenson's formulation has been improved by Senior (1966).

Application of Theory

The application of the Gans and Stevenson theories to non-spherical scatterers are sparse. Calculations for water particles have been made by Atlas, Kerker, and Hitschfeld (1953) and Mathur and Mueller (1955). Other work has been done, but only on ice (or wet ice) particles and non-water substances (see Atlas, 1964).

As has been shown by Mathur and Mueller (1955), the Rayleigh-Gans development is not reliable for values of the parameter α ($=2\pi D/\lambda$, where D = diameter of scatterer and λ = wavelength of radiation) greater than 0.3, giving, for λ = 3 cm an upper limit of 1.5 mm diameter. The Stevenson approximation, involving higher order terms, has been shown by them to be valid up to α = 1.0, giving a diameter of 5 mm, close to the largest rain and cloud particles.

The Gans theory, as applied in Atlas, Kercher, and Hitschfeld (1953), however, serves, as they note, to qualitatively predict the behavior of the scattered radiation.

Suppose a coordinate system so oriented that the axis of symmetry and the x-axis are in the same direction, the direction of fall of the drop (see Fig. 3). Further assume that the drop is an oblate spheroid. Let the incident radiation be plane-polarized. Two cases will be considered: 1) vertical polarization, i. e., the electric vector in the x-z plane, and 2) horizontal polarization, the electric vector parallel to the y-axis. For the problem of this paper, the propagation vector lies along the z-axis. In the real case, it must be noted that

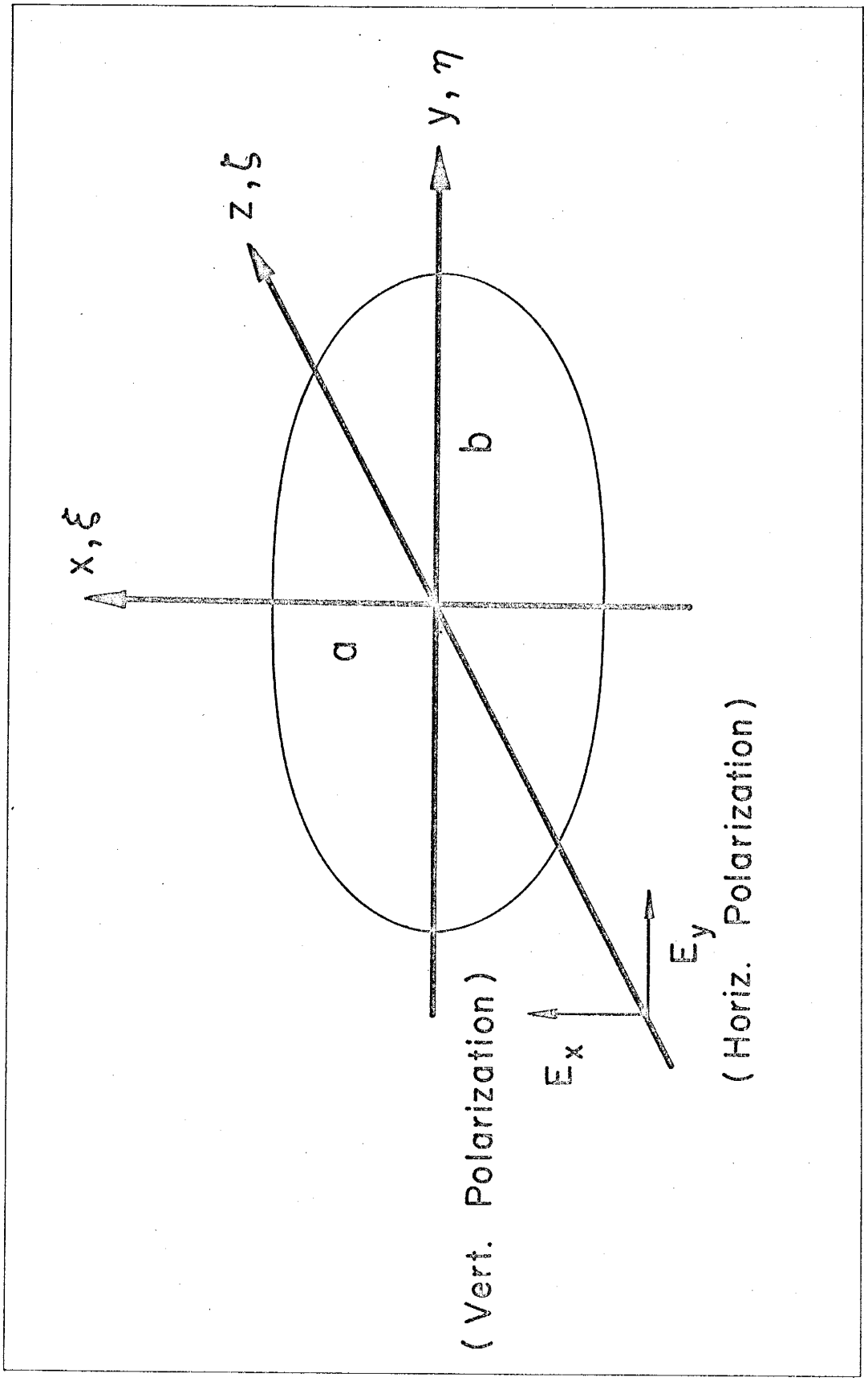

Fig. 3: Geometry of scattering

the propagation vector can have its origin anywhere in the lower half of the x-z plane.

Qualitatively, then, the following picture is obtained. For horizontal polarization, the back-scattered intensity will be greater than that for an equal-volume sphere, and will be the same for any angle of the incident propagation vector. For vertical polarization, the intensity will be the same as for the horizontal case if the propagation vector is parallel to the x-axis, decreasing as the propagation vector moves in the direction of the z-axis, passing through the value for the equivalent sphere at some angle depending on the axial ratio of the drop, and becoming less than the spherical value for the propagation vector along the z-axis. No depolarization can be expected to arise from the orientations discussed since one "long" axis of the particle is always perpendicular to the polarization of the incident radiation.

For the case of vertical or horizontal polarization with the polarization vector along the z-axis (the case for the experiments of this paper) the Gans theory predictions for extremes of cross-sections of oscillating drops can be obtained from Atlas et al, (1953) Fig. 5. For axial ratio extremes of 0.5 to 1.4 (Jones, 1959), the intensity for vertical polarization varies (normalized to an equivolumetric sphere) from 0.35 to 1.2 or 5.35 db. For horizontal polarization and the same extremes, theoretically the intensity will vary by 6.0 db. This change in return intensity should be easily seen in the laboratory. The change in intensity for horizontal polarization should not differ for differing angles of the incident radiation. The vertically polarized intensity difference will, however, gradually decrease to some small value, then increase to the horizontally polarized value as the incident radiation direction moves from the z-axis to the x-axis.

For idealized prolate-oblate oscillations (i.e., at any instant in time the shape is a perfect spheroid), no cross-polarized effects will be noticed. Real drops, on the other hand, have a flattened bottom, and cross-polarization effects will probably be noted, even though the electric vector may be perpendicular or parallel to the vertical axis.

Mathur and Mueller (1955) show that the Rayleigh-Gans type approximation tends to overestimate the back-scatter cross-section by some 10% for a value of α of ~ 0.8 (4 mm dia. drop) for conducting spheroids. They have calculated, from Stevenson's equations (1953 b), the return from oblate and prolate spheroids for the case of vertically and horizontally incident radiation along the x-axis and z-axis. Again, for the "perfect ellipsoid" considered, no cross-polarized terms originate. Calculation of polarization differences gives ~ 3 db for horizontal polarization and ~ 7 db for vertical polarization--again a detectable change for the laboratory. Note, however, that vertical polarization seems to give a much larger change than horizontal according to calculations made from Stevenson's formulae. In any case, rough calculations based on Jones' (1959) axial ratios show that oscillations should be detectable by microwave methods in the laboratory.

Experimental Work

Other than the work of Labrum (1952) on half-drops in wave-guides (which substantiates the Rayleigh approximation), one experimental paper appears in the literature (Gerhardt, et al., 1961).

In this experiment, water drops and ice particles were illuminated by 3.2 cm radiation in an anechoic chamber and the back-scattered energy measured with a receiver. The results of this experiment agree very well with the Mie scattering theory as calculated by Stephens (1960), some small excess in cross-section being noted. Of interest to this

paper is the mention of variations amounting to approximately 3 db due to drop oscillations. These oscillations were undoubtedly due to the method of drop release, as the distance of fall necessary to establish terminal velocity (9-10 meters, e.g., Hitschfeld, 1951) was not reached.

Scattering from an Oscillating Drop

A theory of scattering of electromagnetic energy from an oscillating drop has not been developed. Here, Gans' theory (as outlined by Atlas, et al., 1953) will be used to obtain at least a qualitative feeling for the behavior of back-scattered radiation from such a drop.

Suppose for the moment that the drop has an equilibrium shape which is an oblate spheroid of axial ratio b_o/a_o. Further suppose that the drop oscillates such that $a = a_o + A\cos(wt + \xi)$. Then, applying the constant volume condition (further assuming that all states of the drop are oblate spheroids), $a^2 b = R^3$ (where R is the radius of the sphere of equivalent mass). A ratio

$$\beta = \frac{b}{a} = \frac{R^3}{a^3} = \frac{R^3}{a_o + A\cos(wt + \xi)^3}$$

can thus be obtained, and

$$\beta = \frac{R^3}{a_o^3}\left(1 - \frac{3A}{a_o}\cos(wt + \xi)\right) \qquad (7)$$

to first order in $\frac{A}{a_o}$.

Consider radiation incident along the z-axis with the body (ξ) axis being the same as the x-axis (see Fig. 3), and let the other two body axes be along z and y as shown. Two incident polarizations may be defined as vertical and horizontal (Fig. 3). Further, let the

radiation have unit amplitude at the scatterer. In general, the electric field at the scatterer has components E_ξ, E_η, E_ζ. The dipole set up in the spheroid will have components f_ξ, f_η, f_ζ, given by

$$f_\xi = gE \quad , \quad f_\eta = g'E_n, \quad f_\zeta = g'E \tag{8}$$

where g and g' are given by Gans (as quoted in Atlas, et al., 1953) as:

$$g = m_o^2 \frac{3V}{4} Le^{-i\varphi} = \frac{m_o^2 V(m'^2 - 1)}{4\pi + (m'^2 - 1) P} \tag{9}$$

$$g' = m_o^2 \frac{3V}{4} L'e^{-i\varphi} = \frac{m_o^2 V(m' - 1)}{4\pi + (m'^2 - 1) P'} \tag{10}$$

and P and P' are geometric factors defined for oblate spheroids as:

$$P = 4\pi - 2P' = \frac{4}{e^2} \left[1 - \sqrt{\frac{1 - e^2}{e^2}} \sin^{-1} e \right] . \tag{11}$$

In these formulae, m_o is the refractive index of the medium, m' is the ratio of refractive index of the body to that of the medium, V is the volume of the body, L, L', φ, φ', are defined by (9) and (10) and e is the eccentricity of the principal cross-section of the body; $e = \sqrt{a^2 - b^2 / a^2}$ (a, b as defined in Fig. 3).

Substitution of the index of refraction of water (m' = 7 - 3i) into (9) and (10) gives (m_o = 1):

$$g = \frac{V}{P_o} \left[.0617 - i(.0719) \right] \tag{12}$$

and

$$g' = \frac{V}{P'_o} \left[.0617 - i(.0719) \right] \tag{13}$$

where $P_o = P/4\pi$ and $P'_o = P'/4\pi$.

Then

$$g = \frac{1.19V}{P} e^{-i \tan^{-1}(1.08)} \tag{14}$$

$$g' = \frac{1.19V}{P'} e^{-i \tan^{-1}(1.08)} \tag{15}$$

are the values obtained for g and g'.

If the incident radiation is of unit amplitude, the induced dipole is simply equal to $\mathrm{Re}(g) \cos(2\pi\nu t + \varphi)$ for vertical, and $\mathrm{Re}(g') \cos(2\pi\nu t + \varphi)$ for horizontal polarization, where ν is the frequency of the incoming radiation, and φ an arbitrary phase angle.

The reradiated components can be expressed as

$$E_{rx} = \frac{d^2}{dt^2} \mathrm{Re}(g) \cos(2\pi\nu t + \varphi) \tag{16}$$

and

$$E_{ry} = \frac{d^2}{dt^2} \mathrm{Re}(g') \cos(2\pi\nu t + \varphi). \tag{17}$$

Taking the derivative,

$$E_{rx} = (\ddot{\mathrm{Re}}(g)) \cos(2\pi\nu t + \varphi) - 4\pi\nu \dot{\mathrm{Re}}(g) \sin(2\pi\nu t + \varphi) + (2\pi\nu)^2 \mathrm{Re}(g) \cos(2\pi\nu t + \varphi) \tag{18}$$

$$E_{ry} = (\ddot{\mathrm{Re}}(g)) \cos(2\pi\nu t + \varphi) - 4\pi\nu \dot{\mathrm{Re}}(g') \sin(2\pi\nu t + \varphi) + (2\pi\nu)^2 \mathrm{Re}(g') \cos(2\pi\nu t + \varphi) \tag{19}$$

The average reradiated intensity will be for vertical or horizontal polarization the square of (18) or (19), integrated over one cycle of the incident radiation. Since the frequency contained in g is , Re(g) will not vary over one period of , and

$$I_{rx} = \left(\frac{2\pi}{\lambda}\right)^4 \left[\mathrm{Re}(g)\right]^2 \tag{20}$$

$$I_{ry} = \left(\frac{2\pi}{\lambda}\right)^4 \left[\mathrm{Re}(g')\right]^2 . \tag{21}$$

From (14) and (15), $\mathrm{Re}(g) = \frac{1.19V}{P} = \frac{5R^3}{P}$ and $\mathrm{Re}(g') = 5R^3/P'$ where R is the radius of the equivalent sphere. Thus

$$I_{vert} = \left(\frac{2\pi}{\lambda}\right)^4 \left[\frac{5R^3}{P}\right]^2 \tag{22}$$

$$I_{hor} = \left(\frac{2\pi}{\lambda}\right)^4 \left[\frac{5R^3}{P'}\right]^2 . \tag{23}$$

From (11) and the definition of e, P may be written as:

$$P = 4\pi - 2P' = \frac{4\pi}{1-\beta^2}\left[1 - \sqrt{\frac{\beta^2}{1-\beta^2}}\sin^{-1}\sqrt{1-\beta^2}\right] . \tag{24}$$

For maximum and minimum values of β of 0.9 and 0.5, respectively, we obtain, for vertical polarization, $P_{max} = 4.9$ and $P_{min} = 7.3$ giving a difference of 1.7 db, a reasonable figure in the light of the value obtained previously from Atlas et al., (1953) for a much larger excursion on the maximum value. For horizontal polarization the ratio is 3.2 db. Note if $P = 4\pi f(\beta)$ that $P' \sim 1 - f(\beta)$, so that I_{vert} and I_{hor} can be considered to be out of phase by some amount depending on the behavior of $f(\beta)$.

If $\sin^{-1}\sqrt{1-\beta^2}$ is expanded to an order sufficient to maintain 1% accuracy for the extreme value of β, (24) can be rewritten:

$$P = 4\pi\left[\frac{1}{1+\beta} - \frac{797}{1680}\beta + \frac{23}{140}\beta^3 - \frac{5}{112}\beta^5\right]. \qquad (25)$$

To simplify computation, note that (7) can be rewritten:

$$= \frac{b_o}{a_o}\left[1 - \varepsilon\cos(wt + \phi)\right] \qquad (26)$$

where $\varepsilon = 3A/a_o$ and can be evaluated, as can b_o/a_o, from the data of Jones (1959). For a 4 mm dia. drop having extremes of of 0.5 and 0.9, $\varepsilon = 0.2$, $b_o/a_o = 0.7$, $\beta = 0.7\left[1 - 0.2\cos(wt + \phi)\right]$, and $I_v = .0256(\frac{1}{P})^2$ for 3 cm radiation. A Fourier analysis of I_v for this case shows: $I_v = 0.00386 - 0.00109\cos wt + 0.00019\cos 2wt - 0.00003\cos 3w$. The return intensity from a single oscillating drop is thus clearly shown to be modulated at the fundamental frequency of oscillation of the drop, with the second harmonic being an order of magnitude less.

EXPERIMENT

Since it can be inferred from previous work that drops of diameter 0.8 - 6 mm falling at terminal velocity in air probably oscillate, an experiment is in order to determine: 1) the possibility of detecting this oscillation by microwaves and 2) the relation of frequency to size. The experiment to do this may conveniently be divided into three stages: 1) design and construction of a vertical wind tunnel to support drops at their terminal velocity for a time sufficient to enable measurements to be made, 2) optical recording of the time history of a drop to enable its frequency to be measured, and 3) design and construction of a microwave system for measuring drop frequency and the amplitude of the modulated signal.

The Vertical Wind Tunnel

Four vertical wind tunnels for supporting drops have been mentioned in the literature. Of these, two, those of Lenard (1904) and Telford, Thorndike, and Bowen (1955) are not suitable for the present study, because drops will not remain in these tunnels for more than 2-3 seconds. The tunnels of Blanchard (1949, 1950) and Garner and Kendrick (1959), on the other hand, are capable of maintaining a drop in a stable position in the airstream for a considerable time (Blanchard reports drop residence times up to 40 minutes).

The basic feature of these tunnels is that the drop "sits" in the bottom of a potential well of moving air in a position such that the drop is at its terminal velocity with respect to the airstream. The fundamental requirements of such a tunnel are, then, that first, the vertical velocity gradient must be negative for some region as the height from the orifice of the tunnel increases, second, the velocity gradient must be positive as the radial distance from the proposed stable point increases.

The action of the vertical velocity gradient in maintaining the vertical position of the drop is easily seen. The drop is in balance when the upward drag force due to air motion just equals the weight of the drop. If the drop moves upward, the drag force decreases, and the drop

tends to return to the position of stability. If the drop moves downward, the drag force increases, and the drop tends to move upward toward the position of stability (see "Discussion" for further consideration of this motion).

Horizontal stability of the drop appears to depend on a horizontal gradient in the vertical velocity. Let the drop move such that the center of mass no longer lies on the airflow symmetry axis. The horizontal gradient gives rise to a force on the surface of the drop which decreases toward the axis of the flow. This force tends to move the drop toward the axis of the airflow.

Note that for flow around a drop, the pressure distribution, as given by McDonald (1954), is such that Bernoulli forces will be negligible.

Blanchard accomplishes the first by placing a screen disc in the center of the mouth of his tunnel, and the second by placing a flow retarding open cone some distance above the center of the tunnel. Garner and Kendrick use a shaped wire screen to obtain the horizontal gradient and a plexiglas cone enclosing the air flow (having the proper angle such that detachment of flow does not occur at the surface) to obtain the vertical gradient.

The tunnel of Garner and Kendrick, however, is constructed as a closed flow device (for making mass transfer measurements). Since photography and microwaves were to be used in the present experiment, it was felt that, although the experiment could be done with such a system, the disadvantage of "having things in the way" outweighed the advantage of having a more controlled environment.

As a result of this decision, the construction of a Blanchard-type tunnel was begun.

Two 250 cfm, 3200 rpm squirrel-cage blowers were obtained. For a 4" by 4" orifice, these yield a flow velocity at full capacity (without screening or flow straightening) of 25 m/sec. The largest drop to be supported is $\sim$ 6 mm dia., having a terminal velocity of about 10 m/sec, hence this flow rate is adequate. These blowers were

mounted in a box such that the output velocity could be regulated by controlling the input aperture. The blowers exhausted in to a chamber 9" x 9" x 12", and the tunnel portion was mounted on the top of this section.

Originally a 4" square tunnel was built, in an attempt to duplicate Blanchard's tunnel, with screens to reduce turbulence and a small round screen at the orifice, to provide the horizontal gradient. Very little success with this setup was obtained, and work was started on a tunnel having a 4" diameter cross-section.

The final design of the tunnel is shown in Figure 4. The major feature of this tunnel is the method used to create the horizontal gradient. This method consists of utilizing a radial array of nylon thread 5 mils thick. The end of the 4" I. D. plexiglas tube is slotted at regular angular intervals, and the thread (36 strands) stretched straight across between slots, the strands crossing in the center of the tube. The effect is thus one of impeding the flow more in the center of the jet than near the edges.

Two inches below this "spiderweb" is a nylon screen, a piece of petticoat stiffening having 0. 2 mm threads and hexagonal holes 1. 3 mm across.

Preceding this mesh is a piece of aluminum honeycomb material, having hexagonal cells 1/4 inch across and 7 inches long. The settling chamber leads directly into this section.

Before discussing the turbulence effects in the tunnel, the gross aspects of the flow will be described.

Measurements of the flow were made using a Hastings Air-Meter (hot-wire anemometer) and a hot-wire transducer having a 15 cm long, 0. 5 mm I. D. input tube bent at right angles 3 mm from the open end. The output end of this transducer exhausted into a leak. The upper cutoff frequency of the transducer was calculated to be $\sim$300 cps (Morse, 1948).

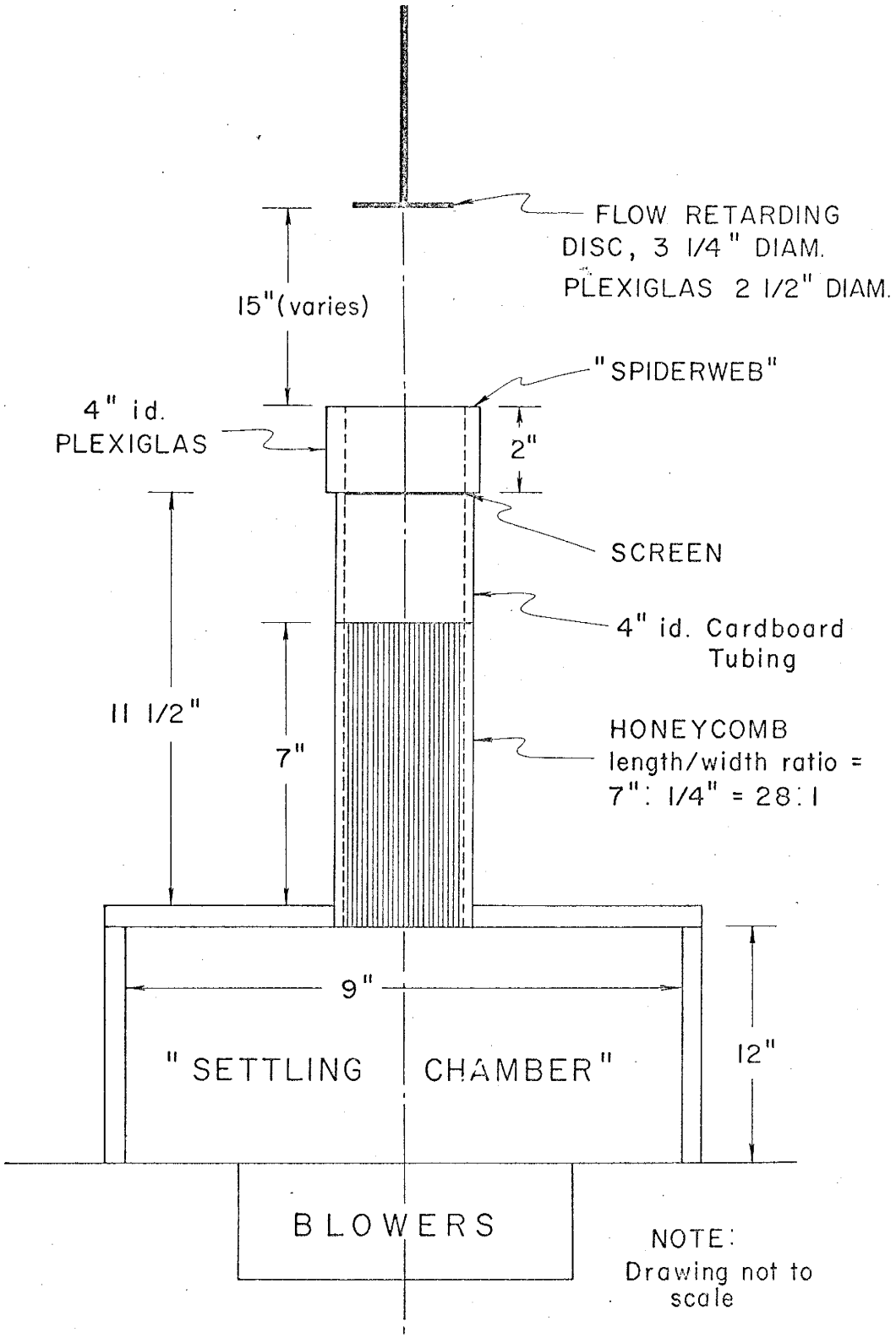

Fig. 4: Schematic of vertical wind tunnel.

Figure 5 shows the result of velocity measurements made along the vertical axis of the tunnel with the transducer, and Figure 6 typical horizontal cross-section in the region of drop stability. The horizontal measurement was made by moving the transducer through the airstream at a constant rate. The width of the line is, of course, due to turbulence in the stream. An integration time of 0.1 second was used on the transducer output to reduce this effect. The figures show clearly that the required velocity gradient to support a drop was achieved, although the turbulence is high.

The flow retardation plate, or "spoiler" is necessary even though the velocity gradient along the axis normally decreases with distance from the throat. The velocity without a retardation plate falls off directly as the distance from the throat (Squires, 1951). Since considerable turbulence is present in the flow, close control of the velocity along the axis would be extremely difficult. Then, too, turbulent mixing would insure that the horizontal gradient upstream would probably vanish, even reverse.

The presence of the "spoiler" plate, then, yields a much steeper vertical gradient than would otherwise be obtained, making control of the velocity of the flow at the throat much less critical. This "spoiler", of course, need not be solid; in fact, screen has been used, also a truncated cone, open in the middle. An adjustable iris from an optical bench was tried in the present tunnel, and worked fairly well, although because of the crudeness of the velocity control, the flat plate gives better results.

The turbulence in the tunnel used for this study is quite large, the fluctuations amounting, in the vertical direction, to approximately 20% of the rms velocity of the center stream for frequencies 10 cps and decreasing steadily as shown by the turbulence spectra of Fig. 7. (The spectra were obtained using the hot-wire transducer previously

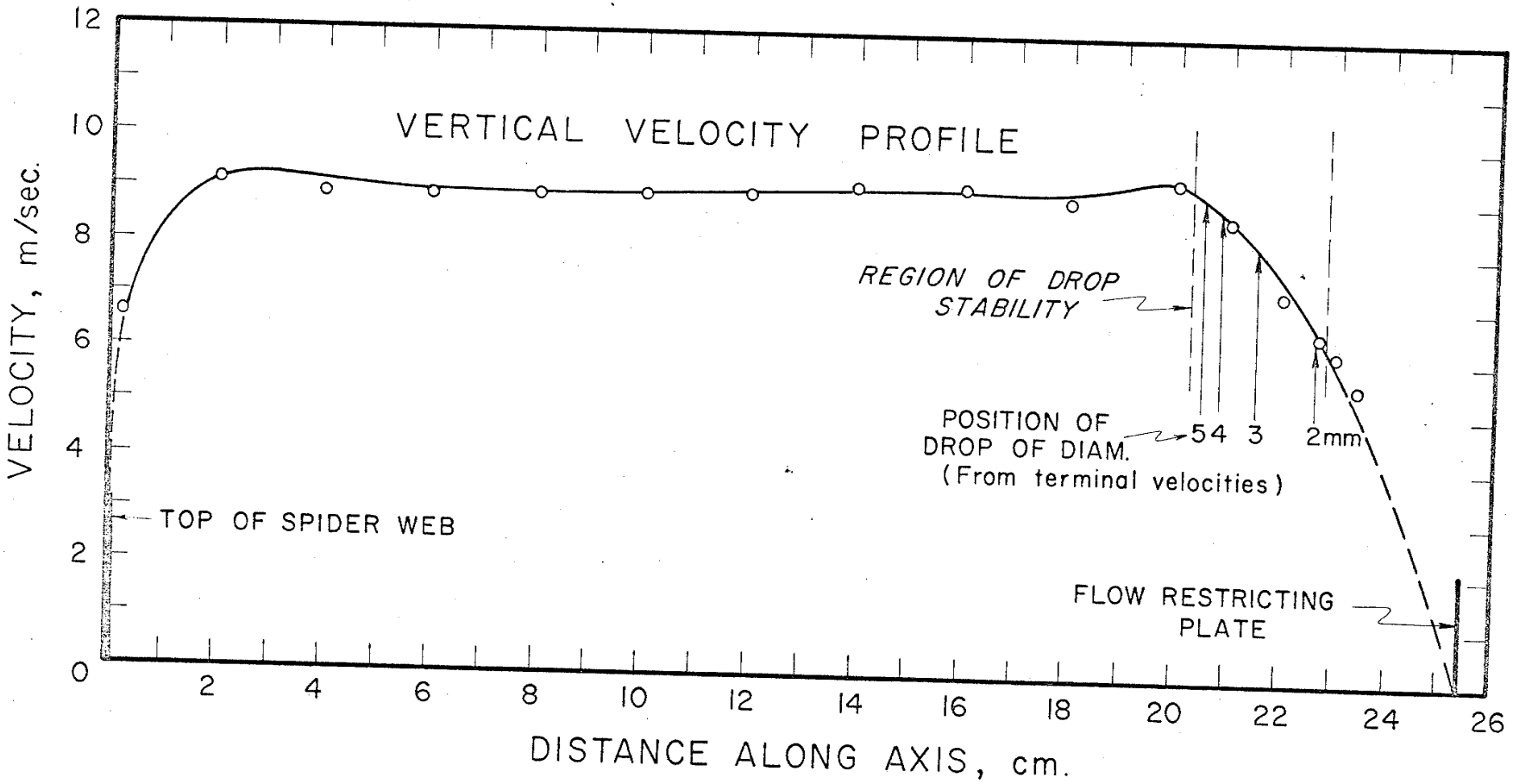

Fig. 5: Axial measurements of vertical velocity starting at the discharge orifice.

mentioned, the output being fed into a Nelson-Ross spectrum analyzer inserted in a Tektronix 535 oscilloscope. The output of the analyzer went to an x-y recorder.)

The 60 cps peak is due to "hum" in the system and must be disregarded. The somewhat smaller peak at 30-40 cycles is quite real, however. This peak may be due to the action of the throat and settling chamber as a Helmholtz resonator. A rough calculation places its frequency at 46 cps. The damping due to the presence of honeycomb and screening could, however, lower the frequency to this extent. The vertical profile (Fig. 5) shows that no standing waves exist in the air stream.

The honeycomb used in the lower portion of the tunnel has a lenght/diameter ratio of 28. The flow through this material is fully developed and reduction in fluctuating energy for this case can be estimated (Lumley, 1964) to be ~ 0.3. The honeycomb does, however, introduce turbulence with wave numbers on the order of the same size as the honeycomb orifices, about 1/4". These should damp out before the screen is reached (10 diameters). The screen introduces turbulence also, but again this should be damped by the time the spiderweb is reached. Turbulence generated by the web should also be damped out by the time the air stream reaches the region of drop stability.

On a qualitative basis, then, the turbulence in the stream must originate either outside the blowers (in which case these are merely "chopping" the incoming turbulence), or within the jet itself. Unfortunately, solutions for the free jet (Pai, 1954) are not applicable because of the presence of the "spoiler", and the spiderweb. The turbulence in the free round jet (rms longitudinal component) has been measured to be 12% of the orifice velocity for a distance from the orifice of 5 diameters, having a "notch" on the axis of the jet which disappears at ~ 20 diameters. The effect of the spiderweb is to eliminate this center "notch" giving rise

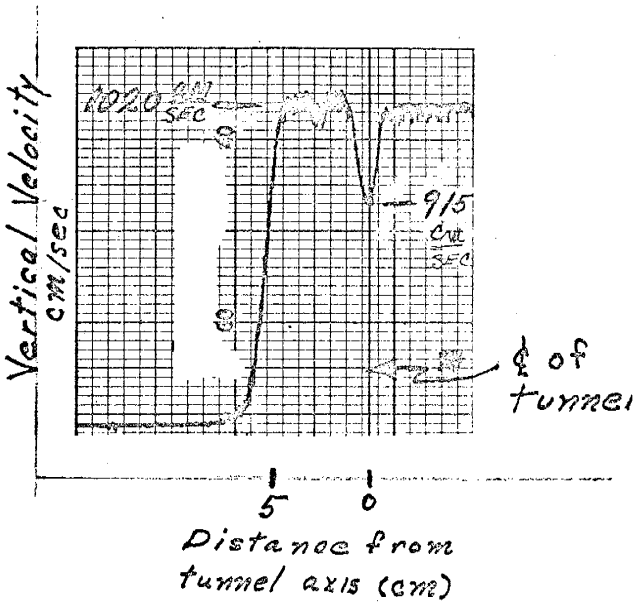

Fig. 6: Horizontal profile of vertical velocity.

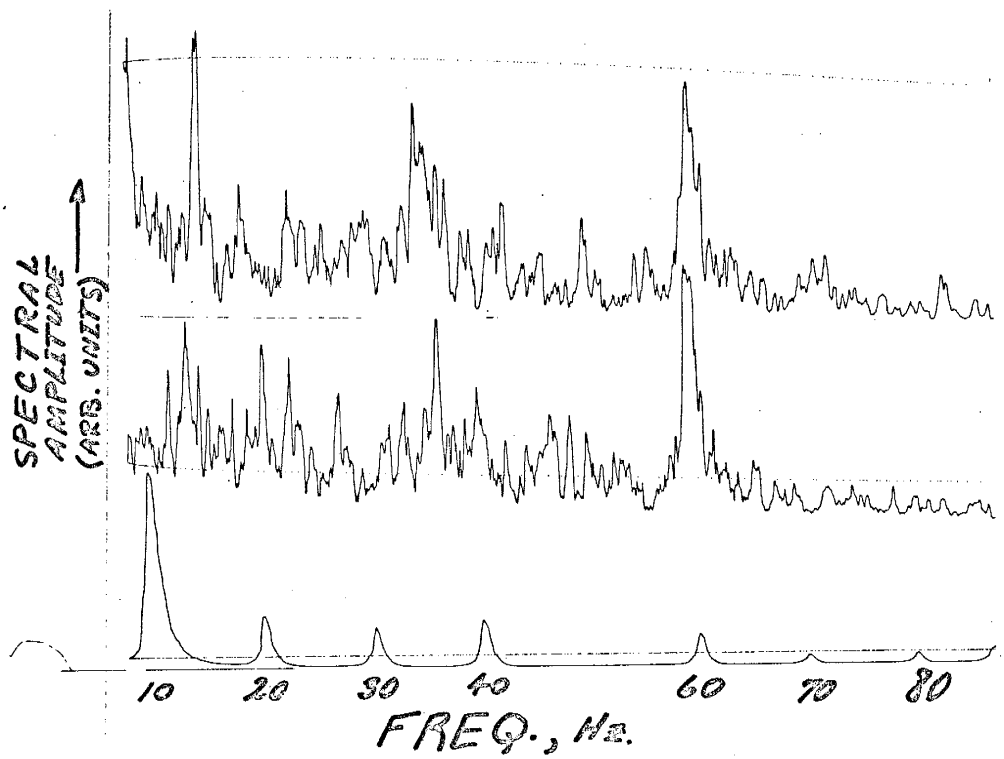

Fig. 7: Two vertical turbulence spectra at position of stability of drops.

to the somewhat higher turbulence found in this tunnel. Qualitatively, then, the jet itself can generate enough turbulence to explain the level found.

Of major interest to the experiment is the fact that the turbulence which does exist is sufficient to cause oscillations of the drops in the stream.

Photographic Experiment

Since standard motion-picture cameras were not available with fast enough framing rates, a special camera system was developed to take rapid photographs.

A Beattie-Coleman continuous-feed 35 mm film magazine and lens holder were obtained. The magazine was altered so that one pulse from a light-source-photoresistor combination was obtained for each standard film frame length as the film progressed through the magazine. This light pulse triggered a General Radio Strobotac which was arranged opposite the camera, giving bright-field illumination. A Zeiss Biotar f/1.5, 75 mm f.l. lens was placed on the lens holder, yielding approximately 1/3 magnification.

Another strobe unit was used, with a "light pipe" of plexiglas, to place accurate (output checked by counter) timing marks on the film. Film speed was thus found to correspond to a frame rate of 228 frames/sec (interval between photographs of 0.0044 sec). Some jitter in frame rate was apparent immediately after starting the camera, but was negligible after some 25-50 frames had been taken.

Calibration of the film was made by placing a glass plate, having on its surface a piece of tape with identifying data, on the wind tunnel axis. The tape was measured both full size and on the film. The tape edges were used with a ground glass screen in the lens holder to adjust the focus of the lens. The film used was 'fastax-perforated' Dupont Superior 4, ASA 320. This film was developed in D-19 for

approximately 12 minutes.

Wet and dry bulb temperatures were taken with a sling psychrometer held in the air stream.

For the photographic study, a chain analytic balance was used to measure the weight of the drop-forming syringe and needle before and after insertion of a drop into the wind tunnel, thus affording a measure of the drop weight.

A synopsis of the technique used is as follows:

1) The glass plate was inserted in the wind tunnel, focus checked, and a few frames taken.

2) The glass plate was removed, and a drop was inserted from the previously weighed syringe.

3) The camera was started, and 100 feet of film was exposed, requiring 11 sec.

4) The syringe was then reweighed, and the weight of the drop calculated and recorded.

5) The film was processed.

Microwave Experiment

A first attempt to observe frequency of oscillation by microwaves involved the use of a "zero-frequency i. f." In this technique, the return signal is beat directly against the outgoing signal, the mixing occurring in a crystal detector, and the output of the crystal detector subsequently amplified. This technique was not satisfactory because the signal-to-noise ratio was too low. The noise was primarily due to the operation of the crystal detector as a mixer in the low frequency range where crystal noise is large.

For this reason, a more suitable system was constructed in which the down conversion was performed at 60 HZ (Fig. 8). The primary feature of this system is that it is coherent, i. e., return signals from a scatterer bear a fixed phase relationship to the local oscillator frequency.

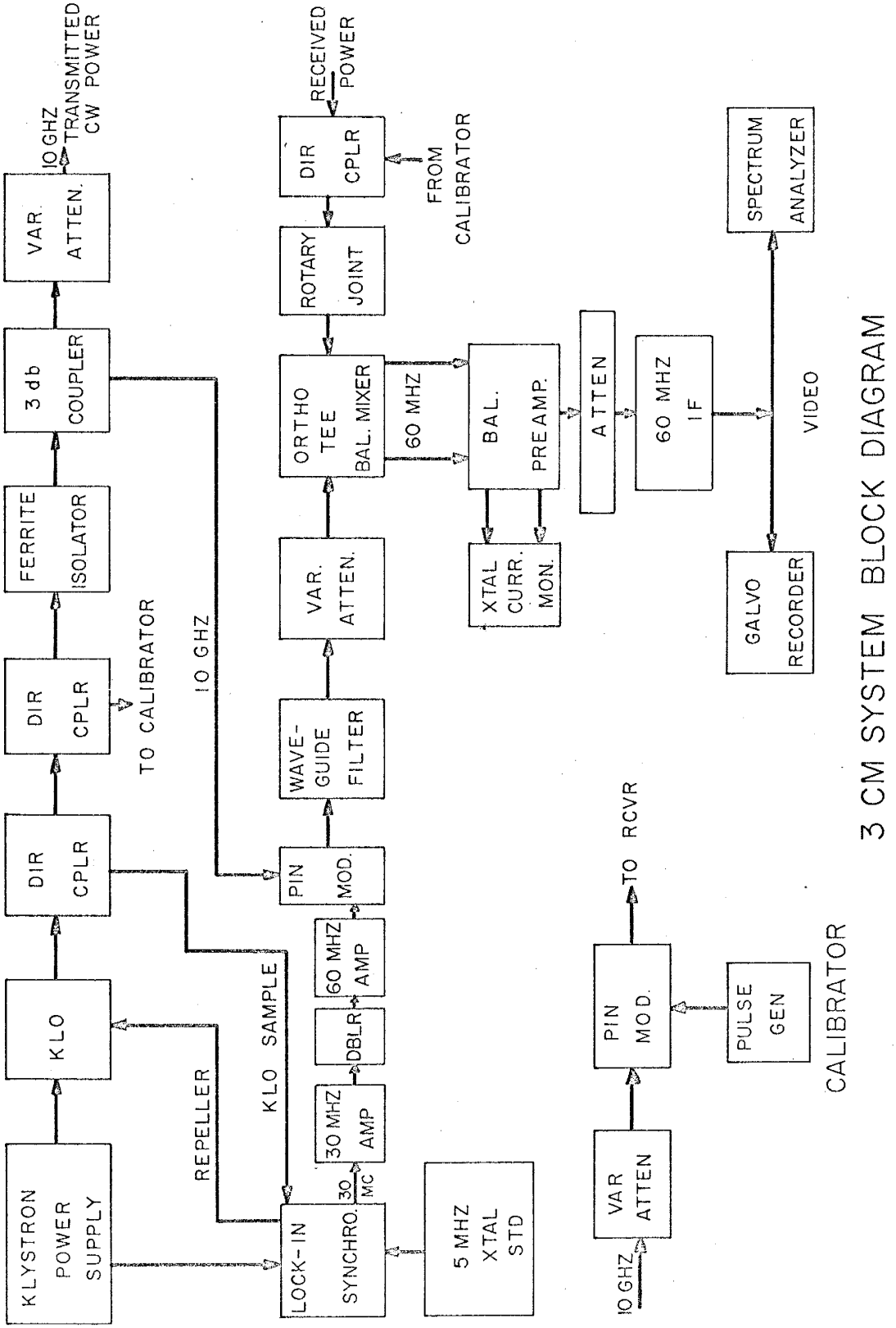

Fig. 8: Block diagram of microwave experimental system.

This very desirable end is accomplished as follows:

1) An extremely stable oscillator (1 part in 10^{10} per day) is formed by using a klystron oscillator, stable srystal oscillator, and phase lock synchronizer. A sample from the oscillator is compared with a harmonic of the 5 mHz crystal oscillator, giving a beat of 30 mHz in a phase sensitive detector. The resultant output voltage then modulates the klystron repeller in such a way as to reduce the phase sensitive detector output to zero.

2) The local oscillator frequency was derived from this very stable source to maintain the desired phase coherence between outgoing signal and local oscillator. The 30 mHz beat between the oscillator and crystal standard was amplified, doubled, and amplified again. The resulting 60 mHz signal, whose phase bears a fixed relationship to that of the klystron oscillator, drives a PIN diode modulator acting on 1/2 of the signal from the klystron. A bandpass filter, 70 db attenuation off center frequency, was then used to select the upper sideband, this sideband being used as the local oscillator signal for the receiver.

3) The local oscillator signal was coupled to an ortho-tee mixer, there mixed with the incoming signal from the scatterer, and the resultant 60 Hz signal plus sidebands amplified and detected by an RHG i.f. preamplifier and amplifier.

4) The video output of the amplifier was coupled to a Nelson-Ross audio spectrum analyzer set to cover the range 5 Hz to 100 Hz (roughly compatible with the Nyquist frequency of the photographic experiment 110 Hz). The analyzer was swept over this range at the slowest sweep rate of the Tektronix 535 oscilloscope, giving a sweep rate of 1Hz/sec. The width of the window in the analyzer was fixed at 0.5 Hz.

5) The video output was coupled to an oscilloscope and to a Hewlett-Packard digital voltmeter for an attempt at quantitative measurements.

6) The video output was also fed directly to a Honeywell galvanometer recorder.

7) The r.f. energy was transmitted and received through identical small waveguide horns, coupled to rotary joints to enable the polarization to be changed at will. These horns have a near field distance of 10 cm. The drop was supported in the wind tunnel at a distance of 30 cm from the horns.

8) The wind tunnel was covered on all sides, top and bottom with wedge-type absorbing material, the direct reflection being 40 db down from the radiation incident on it.

9) The transmitter and receiver horns were placed as close as possible to each other in a horizontal plane that also contained the drop.

10) For calibration purposes, the transmitter horn was replaced by a load, and a calibration signal, derived from the stabilized klystron, was applied in a standard fashion to the receiver by a directional coupler. The receiver sensitivity was found to be -111 dbm.

Several difficulties were at first encountered with this system. First, the i.f. output did not vary properly with the bias (gain) control. Second, 120 Hz hum was noted in the video output of the i.f. amplifier which did not succumb to the usual remedies (elimination of ground loops, etc.). Third, a much higher noise background than expected was noted when the transmitter was "off" (i.e., load in place of horn).

The first of these troubles was found to be caused by the output of the preamplifier overloading the input of the i.f. amplifier. As these units were supposedly identical being the same models (from the same company), this trouble took some time to diagnose. The remedy was the insertion of an attenuator between preamplifier and amplifier, 10 db being found satisfactory to allow the use of the gain control in a normal fashion.

The second problem that of hum, also took some time to find, as the first thought in cases of this type is of ground loops in the equipment. The source was finally found to be microwave radiation from the plasma in the fluorescent lights in the room. At this point the top of the anechoic enclosure was covered, alleviating this problem.

The third problem, that of "residual signal" was deduced to be due to insufficient filtering of the local oscillator signal generator, giving rise to energy at the transmitter frequency being propagated from the receiver horn, scattered, and detected. Another band-pass filter was inserted in the local oscillator path. This cut the radiation down, but did not eliminate it completely. Evidently, absolute quantitative scattering measurements are questionable when made with this apparatus.

Microwave Drop Frequency Measurements

The procedure for obtaining microwave data using the spectrum analyzer was as follows:

1) The receiver horn was adjusted to either vertical or horizontal polarization (the transmitter horn maintained with vertical polarization).

2) The drop was inserted in the tunnel at the beginning of a sweep of the spectrum analyzer.

3) The spectrum analyzer was allowed to complete its sweep.

4) The analyzer was immediately switched to a crystal-controlled frequency standard emitting a 10 Hz square wave. This served to calibrate the analyzer.

5) After (3), which step took only a few seconds, the drop was caught on a previously weighed bundle of filter paper. The bundle was sufficiently thick to absorb the whole drop without allowing any portion to be "strained" through the paper. The paper was then weighed on a Mettler electric balance.

6) The weight of the drop was recorded directly on the sheet containing the spectrum.

The procedure for taking data using the Honeywell recorder was as follows:

1) The transmitter and receiver horns were adjusted such that the polarization was at 45° to the drop axes for all runs.

2) A drop was placed in the tunnel.

3) The recorder drive was energized, and six seconds of video output was recorded. Time marks generated in the recorder were also on the data taken.

4) The drop was caught on filter paper and weighed , about 30 seconds after initial placement in the tunnel.

Microwave Backscatter Variation Measurements

The video output of the receiver used in this study was nonlinear with respect to power incident at the receiver horn. Thus, in order to measure definite power level changes it was necessary that the receiver be calibrated.

This calibration was accomplished by placing a termination on the transmitter in place of its horn, feeding energy derived from the stable klystron into the receiver (via directional coupler) at known power levels, and measuring the video output level. A graph was then drawn of power input vs. video voltage.

The experimental procedure was as follows:

1) The transmitter horn was replaced, and the polarization of receiver and transmitter adjusted to both vertical or both horizontal.

2) The transmitter power level was adjusted such that the video voltage was at a value corresponding to a nearly linear portion of the calibration curve ($\sim$-30dbm).

3) A drop was placed in the tunnel, and the peak-to-peak video voltage excursions were measured on an oscilloscope.

4) The appropriate variation in backscattered power was obtained utilizing the video-voltage vs. power curve.

EXPERIMENTAL RESULTS

Photographic Experiment

Portions of the photographs taken are shown in Appendix II. Each of these prints shows approximately 1/2 cycle of the oscillation of the larger drops, more for the smaller.

General results of the photographs can be summarized:

1) All drops photographed did oscillate, although it was possible to record only one projection.

2) These oscillations were approximately of the prolate-oblate type.

3) The larger drops generally displayed greater extreme amplitudes than did the smaller.

4) The oscillations vary in amplitude with time, but not in any regular pattern.

5) The drops occasionally displayed tilting of the major axis. This tilting was not of a regular nature.

6) The bottom of the drop is seen to be flattened, except during large vertical (prolate) excursions.

Frequency analysis of the shape was made by reading the widths and heights of the drop image with a ruler from an enlarged display of the negative. A sequence of successive values as shown by Table II were taken and a power spectrum analysis run on the height, width, and the axial ratio values.

The power spectrum program, used on the N M Tech IBM computer, was of the autocorrelation type. In this method, the sequence of values is compared to itself point by point as one "copy" of the record is "slid along" another. A discrete Fourier transform is taken of the comparison numbers (autocovariances), this tranform yielding the spectrum.

Appendix III presents the results of the power spectrum analysis

of the photographic data. Rayleigh frequency for a spherical drop of the same mass oscillating with small amplitude is shown as a constant frequency line. Each spectrum is "tagged" by the appropriate droplet mass in grams.

These spectra show several common features (listed quantitatively in Table II):

1) The existence of a small peak in the region below 10 Hz. This peak, with one questionable exception (0.027 gm spectrum) lies at 3 Hz, or appears as a zero Hz peak.

2) On the optical width spectra, and to a lesser extent on the height and ratio spectra, a small (subsidiary) peak, lower in frequency is associated with the major peak. The separation in Hz between these two peaks tends to increase with decreasing drop size.

3) The main peak generally lies close to the Rayleigh frequency. No systematic shift of this peak from the Rayleigh frequency is evident from the data.

4) The half-power width of the main peak lies between 3 and 7 Hz, with the lower value favored.

5) Second harmonic effects can be seen in some of these records, but are too small to enable any reliable measurements to be made.

6) A small peak appears on most records between 10 and 20 Hz.

A least squares fit of the main peak and the subsidiary peak to the formula, $f = k\sqrt{1/m}$ where f is the frequency associated with a peak, and m is the mass of the drop, yields, for the subsidiary peaks, $k = 6.4 \pm 0.8$ and for the main peaks, $k = 8.3 \pm 0.3$. The value of k given by the Rayleigh analysis is 7.92. Generally, then, the main peaks are higher than, and the subsidiary peaks lower than the Rayleigh frequency for a given drop.

TABLE II

Summary of Width Spectra

Drop mass gms.	Drop dia. mm.	Computed Rayleigh frequency Hz.	Low peak Hz.	'Subsidary' peak Hz.	Main peak Hz.	Separation main-Subsidary Hz.	Main peak Half power width Hz.	Mean axial ratio	Max axial ratio	Min axial ratio	No. points taken
0.026	3.68	49.6	3	44.5	50.5	8	4	0.84	1.4	0.48	240
0.027	3.72	48.1	-	38	49.5	11.5	7	0.91	1.3	0.59	120
0.028	3.77	47.5	-	30.4	46.5	16.1	7	0.83	1.2	0.50	120
0.039	4.21	40.1	-	29	39.2	10.2	7	0.80	1.3	0.41	120
0.055	4.72	33.8	3	27	33.1	6.1	4	0.78	1.1	0.45	240
0.082	5.39	27.6	3	18	24.5	6.5	3	0.73	1.2	0.39	240
0.092	5.60	26.0	3	19	26	7	3	0.71	1.0	0.43	240
0.094	5.64	25.8	3	23	27.5	4.5	3.5	0.75	1.2	0.36	240

Microwave Frequency Experiment

The data from the spectrum analyzer at first looked promising. Certainly there was some apparent effect on the backscattered radiation from the drop due to changes in cross-section.

These spectra were, unfortunately, useful only to show the presence of a phenomenon. The drop is excited at random, thus the amplitude of oscillation at any time is not known. Since the analyzer was set to sweep a rate of 1 Hz/sec, the spectral amplitude at any time depended upon the amplitude of oscillation at that time. The position of frequency peaks in such a spectrum are thus not necessarily related in any quantitative fashion to the true peaks. For this reason the method was abandoned, and continuous records were taken on the video output of the receiver and then digitized.

Spectral analysis of continuous recrodings of video output was accomplished by digitizing the records in steps of 0.005 sec using an x-y plotter, digital voltmeter, and accurate voltage source. The corresponding Nyquist frequency for this time interval is 100 cps. Two hundred forty (240) successive points were taken from each of the 20 usable records. The others had either questionable or no drop mass measurement. The results of these spectral analyses are given in Appendix IV and Table III. As in the photographically obtained data, several common features are seen:

1) A peak large compared to all other peaks on the record exists for all records. This peak is found to lie below 10 Hz. Favored values, 0 Hz and 2.5 Hz, independent of drop size, are obtained for this peak

2) All spectra show evidence of a pair of peaks at a frequency within a few cycles of the Rayleigh frequency. In all cases but one (0.0743 gm drop) the larger of this pair is higher in frequency than the smaller. The separation of these peaks shows no trend with respect to drop size.

TABLE III

Results of Microwave Spectral Analyses

Drop mass gms	Drop dia. mm.	Computed Rayleigh frequency Hz.	Low peak Hz.	"Subsidiary" peak Hz.	Main peak Hz.	Separation (Main-subsidiary) Hz.	Main peak half power width Hz.
3.35	0.0197	56.5	1.5	-	61	-	7
3.90	0.0309	44.5	-	38	44.5	6.5	4
4.14	0.0370	41.0	-	35	42	7	4
4.36	0.0434	38.0	2.5	32.5	42	9.5	5.5
4.45	0.0459	37.0	2.5	34	37	3	4
4.47	0.0467	36.8	-	30	37.2	7.2	6
4.62	0.0515	35.9	-	-	35.5	-	4
4.80	0.0579	32.8	3.8	26.5	34	7.5	4
4.85	0.0587	32.2	-	26.5	34	7.5	6
5.10	0.0692	30.0	-	28	33	5	5
5.10	0.0693	30.0	2.5	24	30.5	6.5	3.8
5.22	0.0743	29.2	-	23	28.2	5.2	3
5.33	0.0793	28.4	2.5	22	30.5	8.5	5
5.56	0.0900	26.5	2.5	23	28	5	4.5
5.66	0.0947	25.8	-	20	26.8	6.8	4
5.75	0.0995	25.1	2.5	-	28	-	9
5.80	0.1021	24.6	2.5	22	28	6	6.5
5.92	0.1088	24.0	2.5	-	25	-	4.5
6.29	0.1306	22.0	3.0	18.5	23	4.5	6.5
6.78	0.1630	19.5	2.5	14	19	5	3

3) The larger of the pair of peaks generally is close to the Rayleigh frequency. No systematic deviation of this peak from the Rayleigh frequency is evident from the data.

4) The value of the half-power width of the larger of the pair of peaks mentioned above lies between 9 Hz and 3 Hz, with a tendency to be in the lower portion of this region.

5) Traces of second-harmonic effects are found in all records. The small amplitude of these peaks however, precludes accurate measurement of their frequencies.

6) A small peak at 80 Hz can be seen in all records. This peak was caused by the folding over of the 120 Hz noise generated by the resonance of the galvanometer in the recorder. A small peak lying between 10 and 20 Hz also appears on all records.

A least-squares fit of the frequencies of each of the two peaks of the associated pair was made to the formula $f = k\sqrt{1/m}$ (where f and m are defined as before). For the lower peak of the pair, $k = 7.3 + .34$. The upper peak calculation yielded $k = 7.7 \pm .26$. The frequencies of the associated pair of peaks for the optical and microwave spectra are shown in Figure 9.

The results of the intensity measurements were qualitatively promising, but quantitatively not so, due to technical problem. One run was made in which simultaneous optical and intensity (relative) data were taken. The absolute level of the return power was not known, and the value of the oscillations in intensity was not calculable. The results of this run showed:

1) The maxima (and minima) in intensity variation correspond to maxima (and minima) in the drop dimension in the direction of polarization for parallel recsiver and transmitter polarization.

2) For cross-polarization, the maxima in return intensity correspond to the minima in the drop dimension parallel to the receiver polarization.

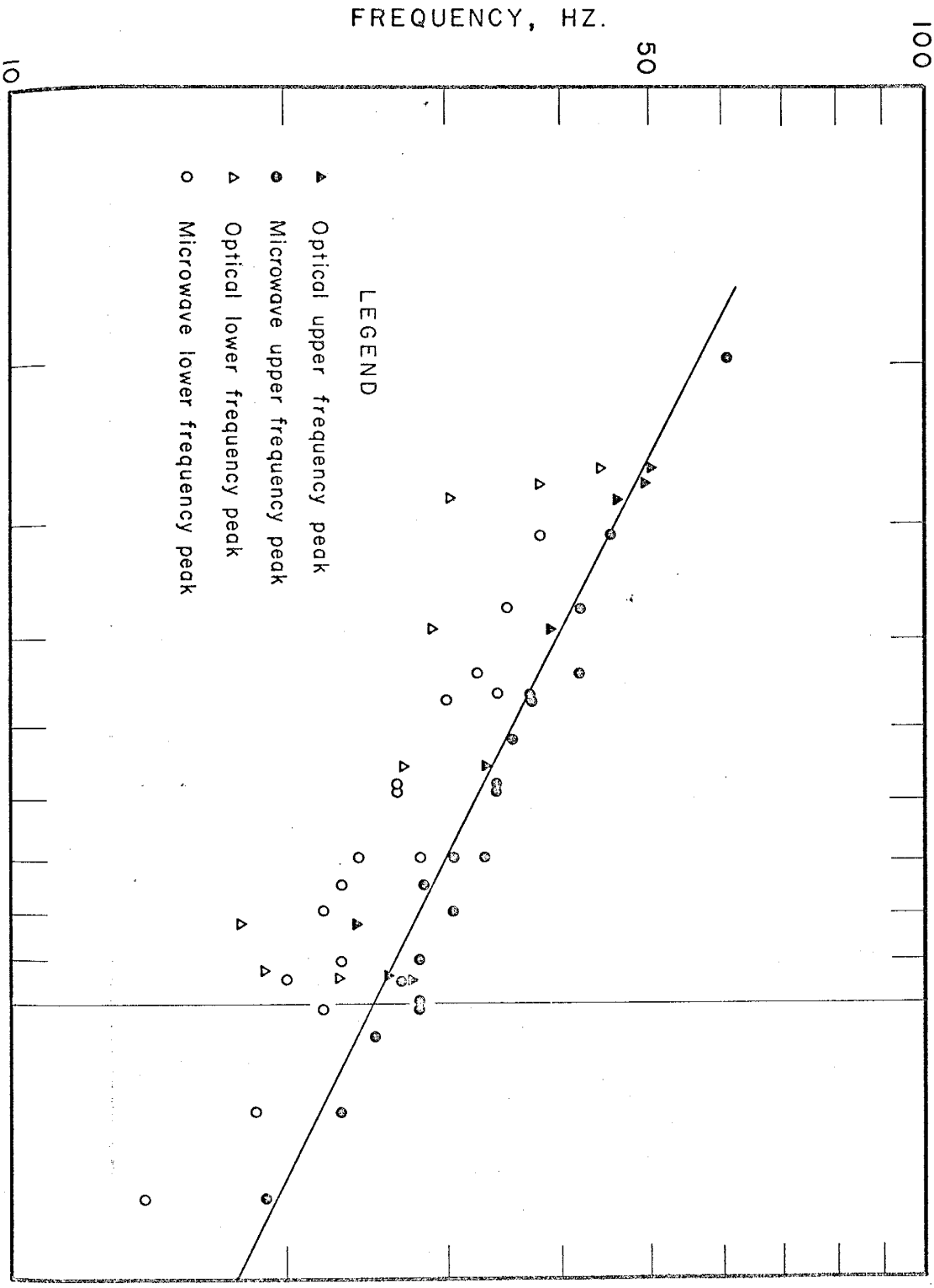
FREQUENCY, HZ.
10
50
100
.01
.05
.1
.2
DROP MASS, gm.
LEGEND
Optical upper frequency peak
Microwave upper frequency peak
Optical lower frequency peak
Microwave lower frequency peak
8

DISCUSSION

Motion of a Suspended Drop as a Rigid Body

Visual observation of a drop suspended in the wind tunnel conveys the impression that the drop executes a seemingly periodic motion along the vertical axis of the tunnel. The amplitude of this motion is not constant, but varies between one and two cm.

An estimate of the frequency of this periodic motion can be derived in the following manner:

Suppose for simplicity, that the drop motion is along the vertical axis of flow. (This is of course not strictly true; however, the vertical motion far exceeds the horizontal.) Let the coordinate along this axis be z, and the point $z = 0$ be the equilibrium point, i.e., that point for which the weight of the drop just balances the upward drag force on the drop (considered now as a rigid body). For drops in the range of interest, 3-6 mm diameter, the drag force is proportional to the square of the velocity of the air stream. A proportionality constant can thus be calculated from the relation, $k v_o^2 = mg$ where m is the mass of the drop, g is the gravitation constant and v_o is the velocity at $z = 0$ (terminal velocity).

Considering Figure 5, we find that, in the region of drop stability,

$$v = v_o - a z \tag{27}$$

where a, the slope of the velocity curve, can be calculated as 155 sec^{-1}.

The equation of motion of the drop along the flow axis can thus be written:

$$m\ddot{z} = F_{drag} - mg = k(v_o - az)^2 - mg, \tag{28}$$

where $\ddot{z}$ is the second time derivative of the coordinate. Expanding

the drag force, and recalling that $kv_o^2 = mg$ by definition, (28) becomes:

$$mz = -2akv_o z + ka^2 z^2, \tag{29}$$

the equation of motion of the drop about the equilibrium position, $z = 0$. If $ka^2 z^2 \ll 2akv_o$, the solution of this equation, which is that of an anharmonic oscillator, is given by:

$$z = A\cos\left(\sqrt{\frac{2akv_o}{m}}\,t + \varphi\right) - \frac{aA^2}{12v_o}\cos 2\left(\sqrt{\frac{2akv_o}{m}}\,t + \varphi\right) + \frac{aA^2}{4v_o} \tag{30}$$

where A and φ are constants determined by the initial conditions of the motion.

An upper limit on the allowed displacement for oscillatory motion can be found from eq. (29) by setting the z term equal to the z^2 term, giving $z = \frac{2v_o}{a}$ or ~ 10 cm for a 3 mm diameter drop. For values of z greater than this value, the motion becomes non-oscillatory. A more realistic value of the vertical amplitude is $z = 1$ cm which yields a ratio of 10 for the z to the z^2 term of eq. (29). The approximate solution, eq. (30), is therefore justified.

The frequency of the motion is thus given by (since $kv_o^2 = mg$)

$$f = \frac{1}{2\pi}\sqrt{\frac{2akv_o}{m}} = \frac{1}{2\pi}\sqrt{\frac{2ag}{v_o}}\,. \tag{31}$$

For a 3 mm diameter drop, this frequency is 3.1 Hz, and for a 6 mm diameter drop, 2.9 Hz. The frequency thus varies little over the diameter range of interest. Inserting an amplitude, A, of 1 cm into equation (30) yields an amplitude ratio of fundamental/second harmonic of 10^2. Second harmonic effects are thus very small.

Spectral Peaks Below 10 Hz

Analysis of both the microwave and optical spectra show the presence of a peak in the region below 10 Hz. From the above consideration, it appears that this peak is probably due to the translational motion of the drop in the air stream.

The presence of this peak in the microwave spectra can be explained by considering the illumination of the working volume. The horn used as a transmitting antenna does not provide uniform power along the vertical axis of the tunnel, hence the backscattered power varies as the position of the drop on the axis. This power variation produces a large amplitude variation in the receiver video at the frequency of motion of the drop.

The optical spectra were produced by measurements of drop shape parameters which were not related to a fixed point in the air stream. These spectra, then, should ideally show no effects produced by variation of the position of the drop in the wind tunnel. Since the drop does respond to changes in its environment, however, some coupling of the motion of the drop as a whole to the motion of the surface of the drop must occur, as demonstrated by the presence of a relatively small peak in the optical spectrum at the frequency of motion of the drop.

Rayleigh Peaks

The presence of peaks in the microwave spectra corresponding to peaks in the optical spectra known to be caused by vibration of the drop demonstrates that one of the main points of this paper has been achieved. Microwave backscatter from an oscillating drop does contain modulation at the frequency of vibration of the drop. The spectra obtained from microwave measurements can thus be used to obtain information concerning the nature of the drop vibrations.

The microwave spectra, in 17 out of 20 cases, show the presence of two peaks, generally within 10 Hz of each other, in the vicinity of the Rayleigh frequency of a spherical drop of equivalent mass. The frequency of the lower of these two peaks is between 5 and 7 Hz below the Rayleigh frequency for 13 cases. The higher frequency peak lies between 1 and 4 Hz above the Rayleigh frequency.

The difference between either peak and the Rayleigh frequency does not appear to depend upon the Rayleigh frequency (for the equivalent speherical drop) or upon the relative amplitude of the two peaks. Similarly, the frequency separation between the two peaks seems unrelated to the Rayleigh frequency and the relative amplitudes.

It is proposed that these two peaks result from two different modes of oscillation of the drop. The first proposed mode, corresponding to the higher in frequency of the peaks, is a prolate-oblate spherical mode, with a symmetry axis in the vertical direction. The second proposed mode can be described as an alteration along two normal axes in a horizontal plane with the vertical dimension constant. These two modes are of course coupled by the condition of constant volume of the drop. Note that in at least one case (e.g. microwave spectrum, 0.743 gm), most of the oscillation energy would appear to be in the lower frequency mode.

The amplitude of the lower frequency mode of oscillation will be dependent upon the angle from which the drop is viewed, since the horizontal axes are not fixed with respect to the lens or the horn.

Credence is lent to this view by a consideration of the optical spectra. The higher frequency peak appears in the spectra of both the height and width measurements. The low frequency peak in question appears relatively much larger in the width measurement spectra than in the height measurement spectra as is predicted by the modes proposed above.

The two modes proposed above are not, of course, the only modes which can exist in the vibration of the drop. The absence of other peaks of comparable size do indicate that these two modes are probably predominant.

Other Spectral Peaks

There are several other peaks apparent in both the optical and microwave spectra. One of these, the peak at 80 Hz in the microwave spectra, was explained earlier on the basis of the spectrum analysis method used. A very small peak at 60 Hz is almost unavoidable, due to power line interference, and can be seen in some of the microwave spectra. Some spectra, for example that for the 0.587 gm drop, show the effects of noise inherent in the digitizing process when the signal to noise ratio is low.

Second harmonic effects can be seen in almost all microwave and optical spectra. These peaks are all very small and appear broader than the Rayleigh peaks. Some second harmonic effect was expected following the earlier analysis of backscatter from a drop vibrating in a fundamental mode. The presence of second harmonic peaks in the optical spectra implies, however, that no statement can be made as to the relative amplitude of the fundamental and second harmonic terms in the microwave spectra.

There is evidence in both spectral classes of a small peak in the region around 20 Hz. This peak is possibly due to an influence on the drop of a predominant turbulence frequency. Again, more data is necessary before definitive statements are possible.

Spectral Line Width

Measurements on the spectra show that almost all large peaks possess a line width of $\sim$ 3-4 Hz, except for three optical spectra which have a line width of $\sim$ 7 Hz. These three optical spectra were

formed from half the data points used on all other spectra, microwave and optical. To check the hypothesis that the line width was due to the analysis and did not represent the true spectrum width, a sine wave was recorded, digitized, and analyzed. The recovered frequency was the same as that recorded, and the line width was found to be 3 Hz. The line width of the spectra obtained in this study must therefore be considered as an upper limit. The drop as an oscillating system thus can be said to have a Q ($f/\Delta f$) greater than 10, but how much greater is not determinable from the present measurements.

Amplitude of Oscillation

Visual observation, photographic records, and continuous records of the video output of the microwave receiver all demonstrate the extreme variability in time of the amplitude of the drop vibrations.

Inspection of the video records does show that the amplitude of the drop vibration is not appreciably affected by the motion of the drop in the wind tunnel. It appears probable that the drop vibrates in response to turbulence and pulse-like variations in the airflow past the drop. The excitation can thus be considered to be random, as would also be the case in the natural environment.

Comparison of the mean value of axial ratio for drops in the wind tunnel to those found in a natural environment by Jones (1959) shows a good agreement. In addition, the maximum and minimum values found in this study are close to those observed by Jones for naturally falling drops.

Amplitude of Microwave Modulation

As previously mentioned, the results of this portion of the experiment were not quantitative. The reasons for this are two-fold: first, the anechoic chamber used was of inadequate size to eliminate backscattered radiation from within the chamber and, second,

the presence of radiation from the receiver horn. The latter is one reason that no attempt was made to obtain even a "ball park" figure for the cross-polarized modulation intensity, since the energy originating from the receiver horn would add to the received back-scatter. In addition, depolarization by the enclosure walls was prohibitive.

The measurements do show, however, that more than 2.5 db intensity variation can be expected due to drop oscillation, and that the parallel and cross-polarized variations will be out of phase by 180°.

Error

A major error in frequency peak measurement is due to digitizing and spectrum analysis. The frequencies were read off the spectrum graphs, and thus have an uncertainty of about $\pm$ 1 Hz.

A source of error in the determination of the Rayleigh frequency to be associated with a given drop is in the measurement of the mass of the drop. An error analysis, using the Rayleigh formula as a guide, shows that

$$f = \mp 1/2\, f_o \left(\frac{\pm \epsilon}{m} \right) \qquad (32)$$

where f_o is the accurate frequency, m, the mass and $\pm \epsilon$, the error in the mass.

The balances used in this study are accurate to 0.0001 gm, hence little error in mass determination can be ascribed to this source. Catching the drop on filter paper and conveying this to the balance, however, introduces an error estimated at 0.0005 gm. Thus for the smallest drop measured, 0.0197 gm, the error in finding the Rayleigh frequency should be 0.7 Hz. or about 1%.

Another possible source of error in determining the Rayleigh frequency is the evaporation of the drop while in the airstream. Based on the measurements of Kinzer and Gunn (1951), the evaporation rate for the size of drops used and range of relative humidities encountered in this study is about 0.04 mg/sec. The drops were in the airflow for approximately 20 sec for both the optical and microwave experiments. The weight loss, then, is estimated as 0.8 mg, and the consequent error in determining the Rayleigh frequency could be as much as 2%.

Application of Backscatter Modulation

The application of the phenomenon investigated in this study to the determination of drop size spectra in clouds and rainfall presents several problems.

One of these is the possible error in inferred drop sizes introduced by the existence of two spectral peaks for each drop. The higher in frequency of these two peaks, as we have seen, is about 2 Hz greater than the Rayleigh frequency and the other peak $\sim$ 6 Hz less than the Rayleigh frequency.

If the mass of the smallest drop of this study were to be calculated, using the Rayleigh formula, from the higher frequency peak, the mass obtained would be 0.0182 gm, an error of 7.6%. The use of the lower peak would give a mass of 0.0231 gm, an error of 22.5%. In most of the cases of this study, however, the amplitude of the higher frequency peak is considerably larger than that of the lower frequency peak. Thus to a first approximation, it appears possible to use the Rayleigh formula to obtain drop sizes from frequency spectra.

For purposes of application, the importance of temperature as a source of error in the measurement of drop mass can be evaluated if the Rayleigh formula is used. Suppose a frequency is measured, corresponding to a true mass, m_0, and a true value of the surface tension constant, σ_0. Let the error in the value of σ due to ignorance of the true

temperature be ε . There will be a corresponding error in the mass, δ . Then

$$\frac{\sigma_o}{m_o} = \frac{\sigma_o \pm \varepsilon}{m_o \pm \delta}$$

and

$$\delta = \varepsilon\left(\frac{m_o}{\sigma}\right) \quad . \tag{33}$$

Now $m_0 \sim 0.1$ and $\sigma \sim 80$, thus $\delta \sim \varepsilon/800$, and if $\varepsilon \sim 4$ (a worst case), then $\delta \sim 0.0005$ or 0.5% error in mass. Thus, the error in mass determination introduced by temperature variations in much less than that which can be introduced through the use of the Rayleigh formula.

The effect of local electric fields will be of importance to an application, for in regions of high field, e.g. some parts of the thunderstorm, the drops will be considerably distorted from their shape with no field. This distortion may introduce a change in vibration frequencies, but an assessment of this effect is outside the scope of this investigation.

If the backscatter modulation method of determining drop sizes is to be applied, a problem of separating the desired information from rearrangement noise and the large mean signal level arises. One possible way to overcome this difficulty is to utilize the fact that the backscatter of microwave energy from vibrating drops is depolarized. Hence, if two receivers are used, one sensitive to radiation parallel in polarization to that out going from a radar, and one sensitive to perpendicular radiation, a cross-correlation of the two video signals (one shifted in phase by 180°) should cancel the rearrangement noise. An alternate solution to the rearrangement noise problem utilizes the simultaneous measurement of the amplitude of a very small portion of the amplitude modulation spectrum and the total Doppler spectrum. The amplitude spectrum measurement yields the number density of drops of a very

narrow range of sizes. This information can be used to correct the Doppler spectrum for updrafts or downdrafts, giving a Doppler spectrum of terminal velocities. A drop-size spectrum can then be obtained from the terminal velocity Doppler spectrum (Boyenval, 1960).

Further considerations of application will be discussed in a paper, now in preparation, by Dr. Marx Brook and the author.

CONCLUSION

Conclusions

In this study, an attempt has been made to show the feasibility of utilizing a heretofore ignored portion of the noise in the backscattered radiation from water drops, that due to oscillation in shape of the drops, to measure their size.

In the opinion of the author, this feasibility has been demonstrated:

1) The frequency of one mode of vibration of a water drop falling at terminal velocity in air has been shown to be proportional to $\sqrt{1/m}$ where m is the mass of the drop. The constant of proportionality found in this study is within 10% of that calculated by Rayleigh for the fundamental frequency of a drop--a result which is surprising considering the vast difference in the nature of the environment between this study and the idealized Rayleigh calculation.

The presence of another mode of drop vibration associated with the first mode but generally containing less energy has been demonstrated and a mechanism for these two modes proposed.

2) The backscattered microwave energy from a vibrating drop has been found to be modulated at the same frequencies; the modulation due to the first mode is generally a factor of 4 - 5 times greater than that due to the second.

3) The amplitude of microwave modulation observed in this study amounted to about 3 db.

4) Such intensity variation in backscattered microwave energy arising from drop vibrations should be detectable in radar returns from natural rain and should provide another means of inferring the size distribution of drops $\gtrsim$ 1mm diameter.

Recommendations for Further Study

If the modulation of microwave energy by drop vibrations is to be of use as a research tool, the following studies should be made:

1) Determination of the intensity variations in backscattered radiation for natural rain.

2) Depolarization measurements for single drops.

3) Theoretical calculations based on true drop shapes.

4) Theoretical and laboratory studies on ensembles of drops falling at terminal velocity.

5) Measurements of the effect of electric fields on the frequency of drop vibration.

APPENDIX I

The Rayleigh development of the frequency of oscillation of liquid drops (from Rayleigh, 1877).

Let the surface of the drop be given by:

$$r = a_0 + a_1 P_1(\mu) + a_2 P_2(\mu) + \ldots \qquad (1)$$

where $\mu = \cos\theta$ (spherical coordinates), and P_n is the nth order Legendre polynomial. Let $a_{n\neq o}$ be $\ll a_o$.

The volume of the drop is given by:

$$V = \int_0^{2\pi}\int_0^{\pi}\int_0^{r} r^2 \sin\theta \, d\theta \, d\phi \, dr = \frac{2}{3}\pi \int_{-1}^{1} r^3 \, d\mu$$

$$= \frac{2\pi a_0^3}{3}\int_{-1}^{1}\left[1 + \sum_{n=1}\frac{a_n}{a_0}P_n(\mu)\right]^3 d\mu$$

$$= \frac{2\pi a_0^3}{3}\left[\int_{-1}^{1} d\mu + 3\int_{-1}^{1}\left(\sum\frac{a_n}{a_0}P_n(\mu)\right)d\mu\right.$$

$$\left. + 3\int_{-1}^{1}\sum\frac{a_n^2}{a_0^2}P_n^2(\mu)\,d\mu + \int_{-1}^{1}\left(\sum\frac{a_n}{a_0}P_n(\mu)\right)^3 d\mu\right.$$

and:

$$V = \frac{4\pi a_0^3}{3}\left[1 + 3\sum_{n=1}(2n+1)^{-1}\frac{a_n^2}{a_0^2}\right] \qquad (2)$$

and, if a is the radius of the equilibrium sphere:

$$V = \frac{4\pi a^3}{3}$$

and, to first order in the sum:

$$a = a_0\left[1 + \sum_{n=1}(2n+1)^{-1}\frac{a_n^2}{a_0^2}\right] \qquad (3)$$

To find the surface tension energy (the potential energy of the system), the surface area S must be multiplied by the surface tension constant σ . For the surface area:

$$S = 2\pi\int r\sin\theta\left[r^2 + \left(\frac{dr}{d\theta}\right)^2\right]^{1/2} d\theta$$

where $\left[r^2 + \left(\frac{dr}{d\theta}\right)^2\right]^{1/2} d\theta$ is the element of length

perpendicular to r. If we expand this term:

$$S = 2\pi\int\left[r^2 + \frac{1}{2}\left(\frac{dr}{d\theta}\right)^2\right]\sin\theta\, d\theta$$

breaking the integral into two parts, the first integral is:

$$\int_{-1}^{1} r^2 d\mu = \int_{-1}^{1} \left[a_0 + \left(\sum_{n=1} a_n P_n\right)\right]^2 d\mu$$

$$= \int_{-1}^{1} \left[a_0^2 + 2\left(\sum a_n P_n\right) a_0 + \left(\sum a_n P_n\right)^2\right] d\mu$$

But

$$\int_{-1}^{1} P_n P_m \, d\mu = 2(2n+1)^{-1} \delta_{mn}$$

Where $\delta_{mn} = 1$, $m = n$, $\delta_{mn} = 0$, $m \neq n$,

and

$$\int_{-1}^{1} r^2 d\mu = 2a_0^2 + 2\sum (2n+1)^{-1} a_n^2$$

The second part of the surface integral is:

$$\frac{1}{2}\int \left(\frac{dr}{d\theta}\right)^2 \sin\theta \, d\theta = \frac{1}{2}\int_{-1}^{1} (1-\mu^2)\left[\sum a_n \frac{dP_n}{d\mu}\right]^2 d\mu$$

Since $(1-\mu^2)^{1/2}\left(\frac{dr}{d\theta}\right) = \frac{dr}{d\mu}$ A Legendre polynomial relation of help is:

$$\int_{-1}^{1} (1-\mu^2) \frac{dP_m}{d\mu} \frac{dP_n}{d\mu} d\mu = n(n+1) \int_{-1}^{1} P_m P_n \, d\mu$$

$$= \frac{2n(n-1)}{2n+1} \delta_{mn}$$

and the second part of the integral is thus

$$\frac{1}{2}\int_{-1}^{1}\left(\frac{dr}{d\theta}\right)^2 d\mu = \sum_{n=1} \frac{n(n+1)}{2n+1} a_n^2$$

and, adding the two portions,

$$S = 4\pi a_0^2 + 4\pi \sum_{n=1} (2n+1)^{-1} a_n^2$$

$$+ 2\pi \sum_{n=1} \frac{n(n+1)}{2n+1} a_n^2$$

Combining the sums, we obtain:

$$S = 4\pi a_0^2 + 2\pi \sum_{n=1} (2n+1)^{-1} (n^2+n+2)\, a_n^2$$

From (3), we see that

$$a^2 = a_0^2 \left[1 + \sum_{n=1} (2n+1)^{-1} \frac{a_n^2}{a_0^2} \right]^{-2}$$

$$\approx a_0^2 + 2 \sum_{n=1} (2n+1)^{-1} \frac{a_n^2}{a_0^2}$$

to first order in the sum. Then

$$a_0^2 = a^2 - 2 \sum (2n-1)^{-1} a_n^2$$

and

$$4\pi a_0^2 = 4\pi a^2 - 2\pi \sum 4 (2n+1)^{-1} a_n^2$$

Substituting this value of a_o into S, we obtain:

$$S = 4\pi a^2 + 2\pi \sum_{n=1} (n-1)(n+2)(2n+1)^{-1} a_n^2 \qquad (4)$$

for the surface area. The excess surface area is thus

$$\Delta S = 2\pi \sum_{n=1} (n-1)(n+2)(2n+1)^{-1} a_n^2$$

and corresponding potential energy of the distortion is:

$$P = \sigma \Delta S \qquad (5)$$

In order to use Lagrange's equations of motion, we must find the kinetic energy of the motion. Let the velocity potential be given by:

$$\psi = b_0 + b_1 r P_1(\mu) + \ldots + b_n r^n P_n(\mu) + \ldots \qquad (6)$$

The kinetic energy of the motion at any point on the surface is

$$\tfrac{1}{2}\rho v^2 = \tfrac{1}{2}\rho (\nabla\psi)\cdot(\nabla\psi)$$

and the total kinetic energy is

$$\tfrac{1}{2}\rho \iiint_V \nabla\psi \cdot \nabla\psi \, dv$$

But by Green's theorem:

$$\iiint_V \nabla\psi \cdot \nabla\psi \, dv = \iint_S \psi \frac{d\psi}{dn} \, dS$$

and, for the present case,

$$K = \frac{1}{2}\rho \iint_S \psi \frac{d\psi}{dr} r^2 d\phi d\mu$$

Now

$$\frac{d\psi}{dr} = 0 + b_1 P_1(\mu) + 2b_2 r P_2(\mu) + \dots + n b_n r^{n-1} P_n + \dots$$

Thus

$$K = \frac{1}{2}\rho \iint_S \left(\sum_{i=0} b_i r^i P_i(\mu)\right)\left(\sum_{j=0} j b_j r^{j-1} P_j(\mu)\right) \times \left(a_0 + \sum_{m=1} a_m P_m(\mu)\right)^2 d\phi d\mu$$

and, noting that only i = j = n will yield a value for K, and that for $r = a_o$,

$$K = \pi\rho \int \sum_n \left[b_n^2 a_0^{2n-1} P_n^2(\mu)\right] a_0 \left[1 + \Sigma \frac{a_m}{a_0} P_m\right]^2 d\mu$$

But, a_o only differs from a by second order (Eq. 3) and, in the expansion, terms involving first orders of P_m go to zero, we have:

$$K = 2\pi\rho a^2 \sum_n n a^{2n-1} b_n^2 (2n+1)^{-1}$$

At the surface of the body,

$$\left(\frac{d\psi}{dr}\right)_{r=a} = \left(\frac{d\zeta}{dt}\right)_{r=a}$$

(Note that Rayleigh uses the boundary condition on the surface of the sphere, not the perturbed body)

Then

$$\sum \frac{da_n}{dt} P_n(\mu) = \sum n a^{n-1} b_n$$

and term by term

$$\frac{da_n}{dt} \cdot \frac{1}{n a^{n-1}} = b_n$$

Thus K becomes

$$K = 2\pi\rho a^3 \sum (\dot{a}_n)^2 / n(2n+1) \qquad (7)$$

where the dot denotes the time derivative.

From (7) and (5), it can be seen that the kinetic energy is a homogeneous function of a_n°, Lagrange's method can be applied, giving

$$\ddot{a}_n + n(n-1)(n+2)\frac{\sigma}{\rho a^3} a_n = 0 \qquad (8)$$

which is oscillatory, having an angular frequency given by

$$\omega^2 = n(n-1)(n+2)\frac{\sigma}{\rho a^3} \qquad (9)$$

the frequency of oscillation of the drop surface.

APPENDIX II

Photographic Sequences

(The mass of the associated drop is shown below each sequence.)

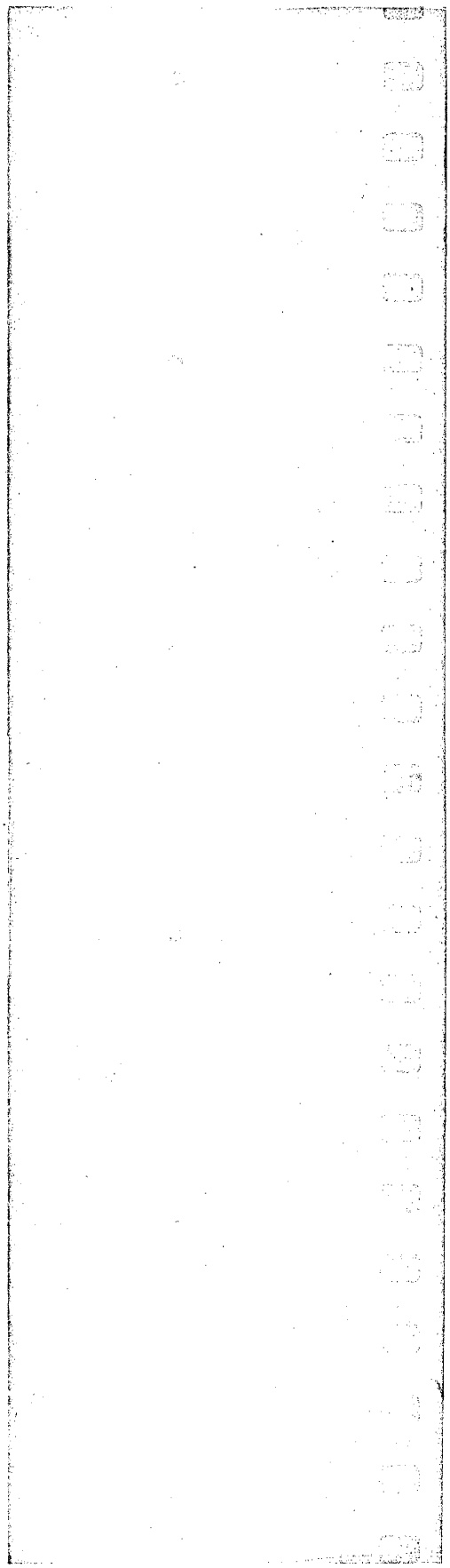

.028 gm

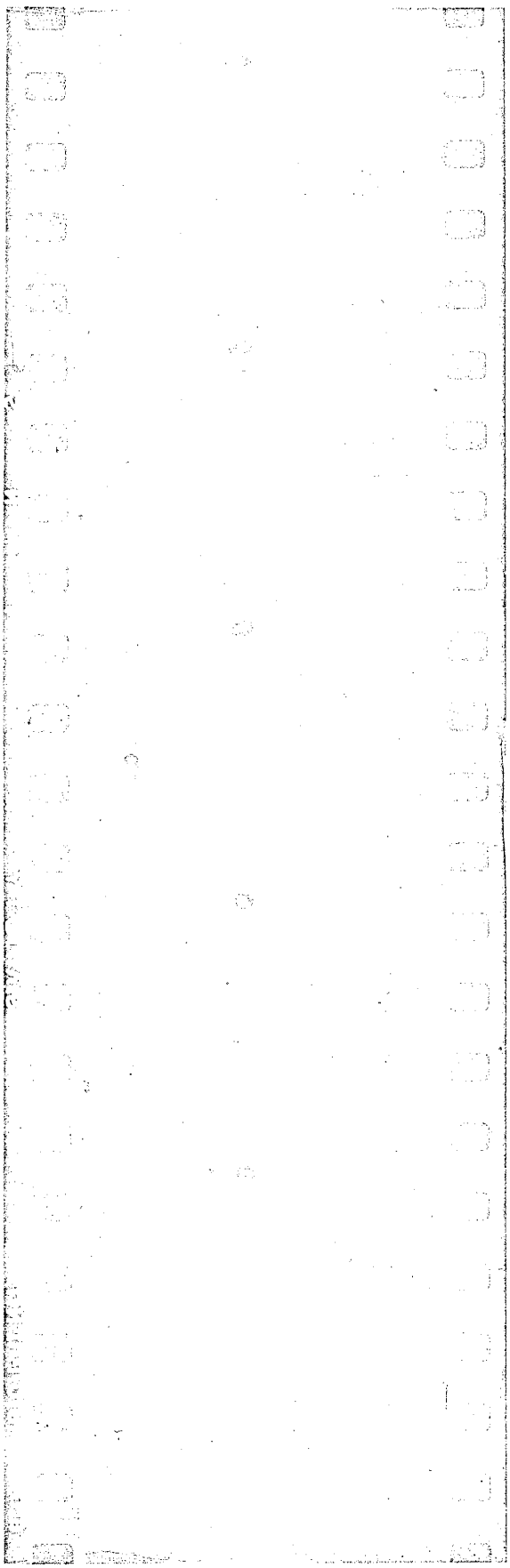

.039 gm

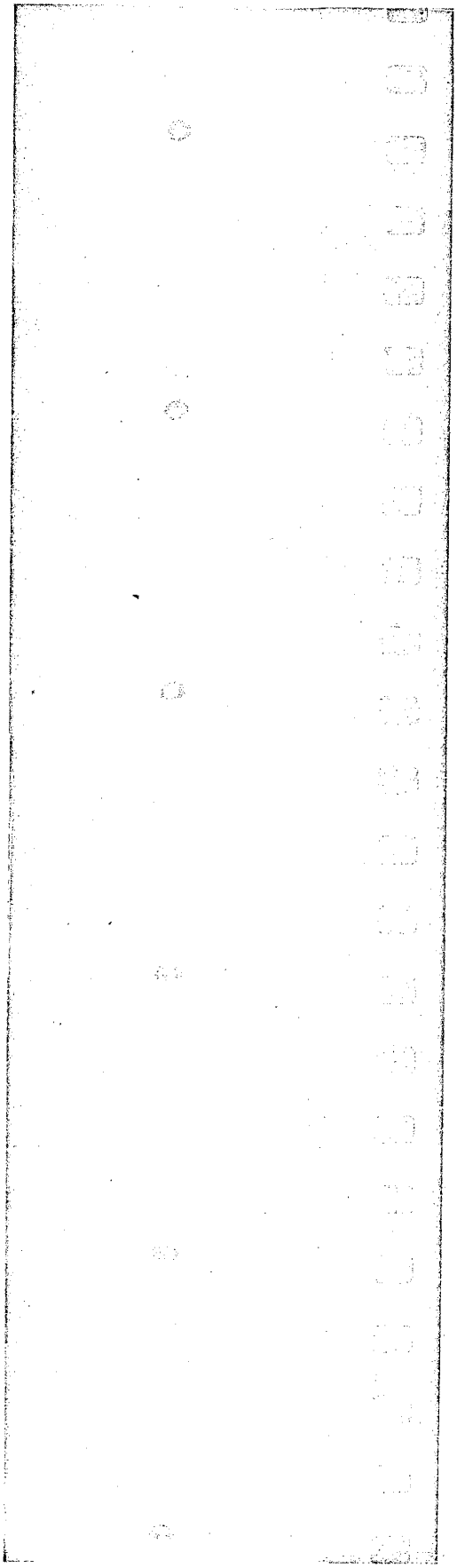

.082 gm

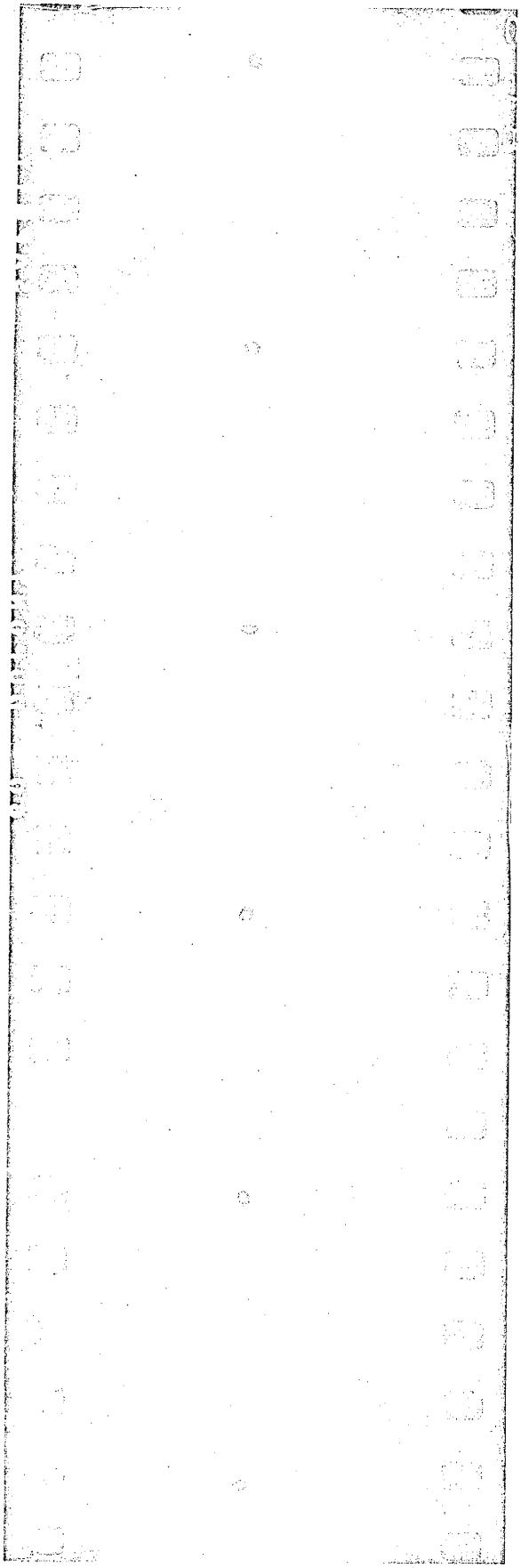

.027 gm

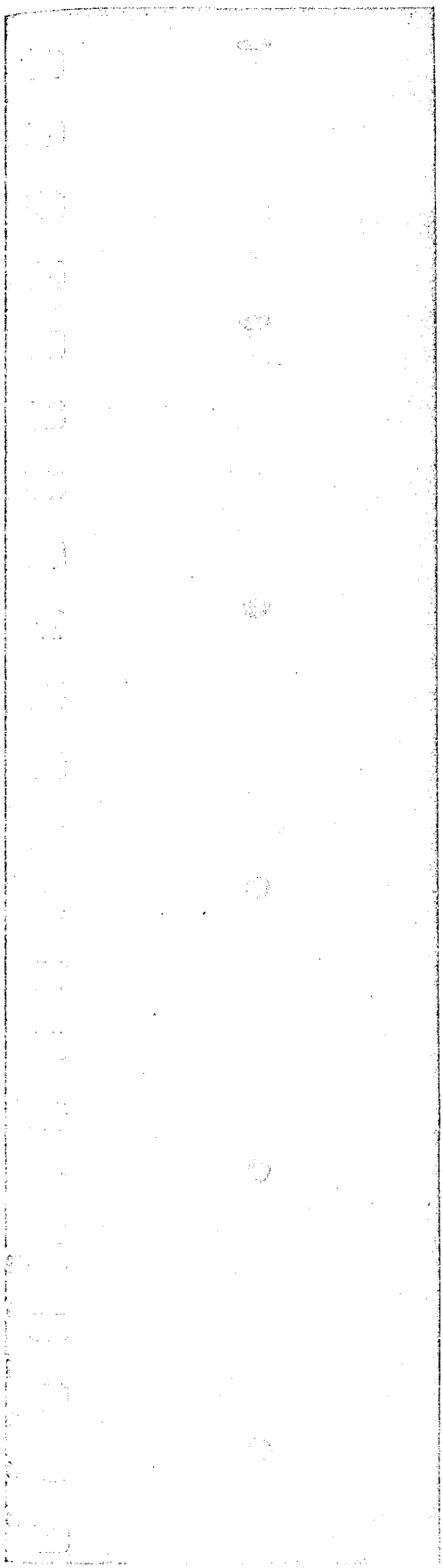

.055 gm

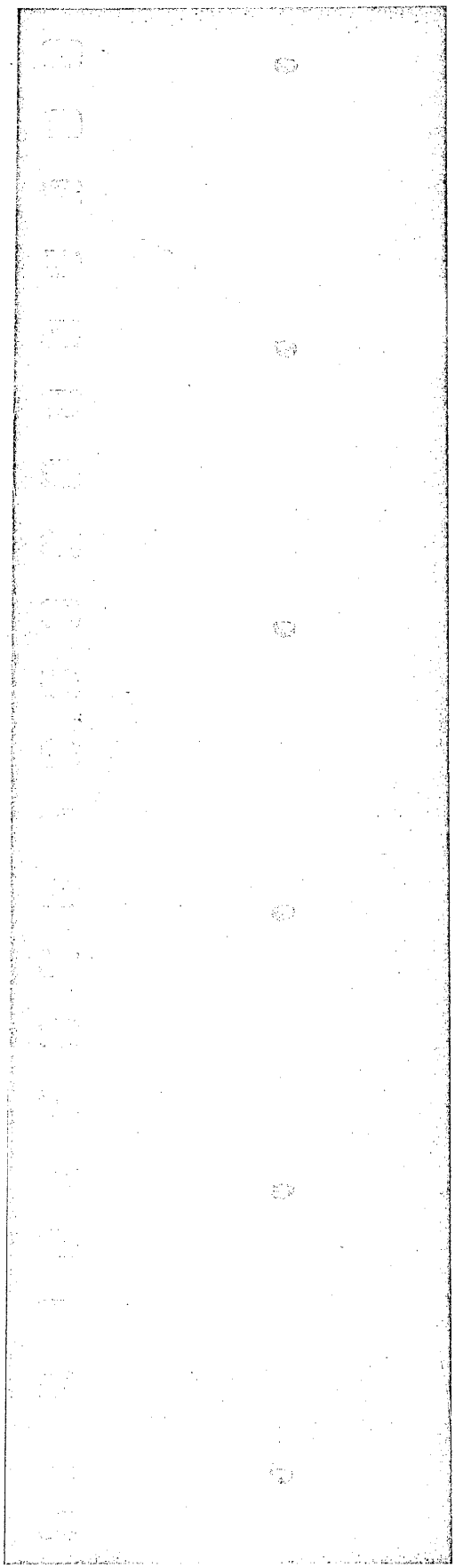

.094 gm

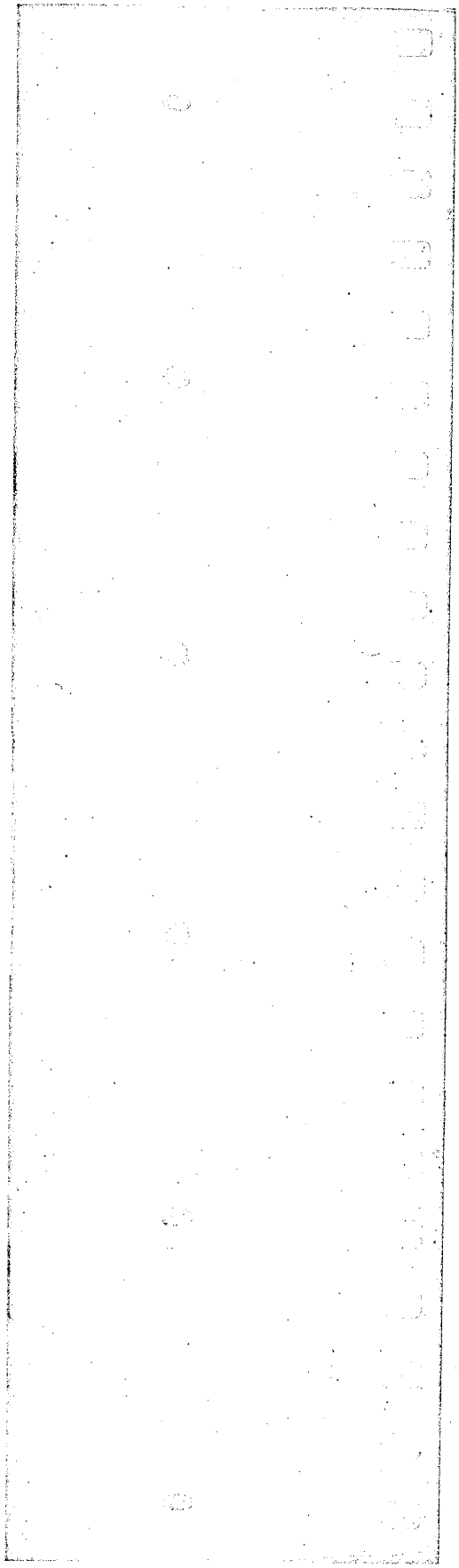

.093 gm

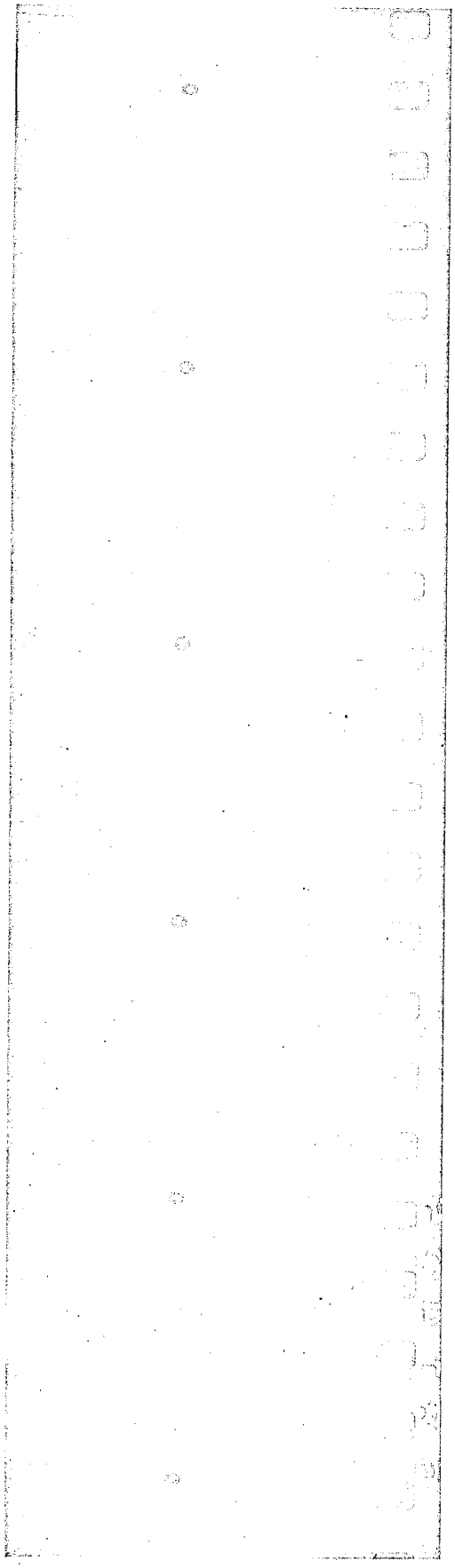

.026 gm

APPENDIX III

OPTICAL SPECTRA

Top of page: Spectrum of Drop Axial Ratio b/a

Middle of page: Spectrum of Drop Widths (2a)

Bottom of page: Spectrum of Drop Heights (2b)

(The Rayleigh frequency corresponding to the mass of the drop is shown as a solid constant frequency line.)

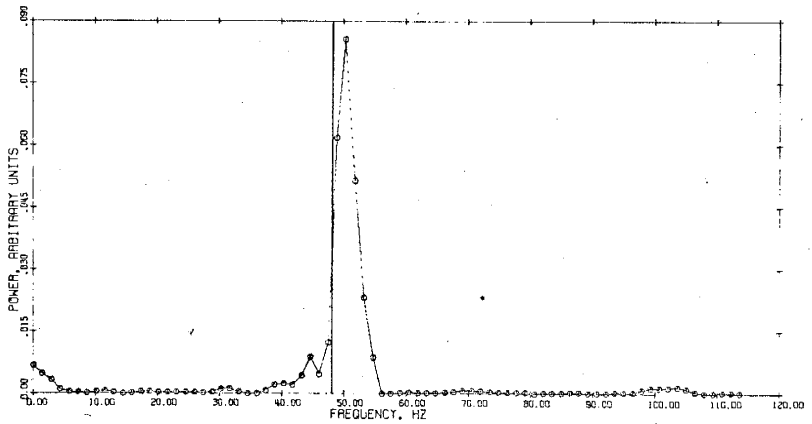

OPTICAL SPECTRUM WEIGHT 0.026 G.

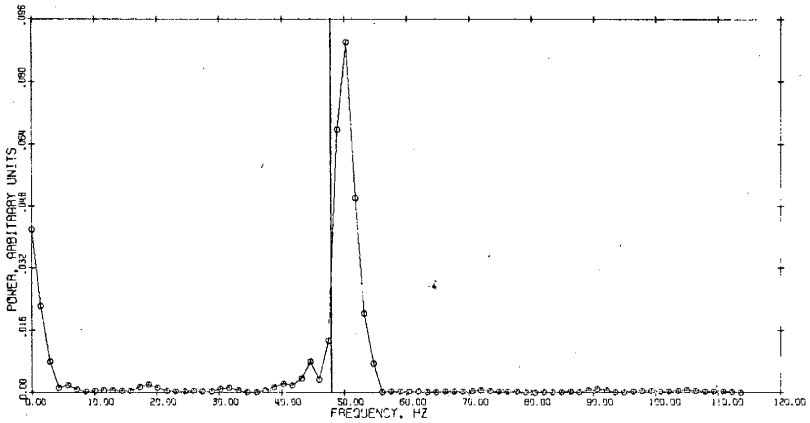

OPTICAL SPECTRUM WEIGHT 0.026 G.

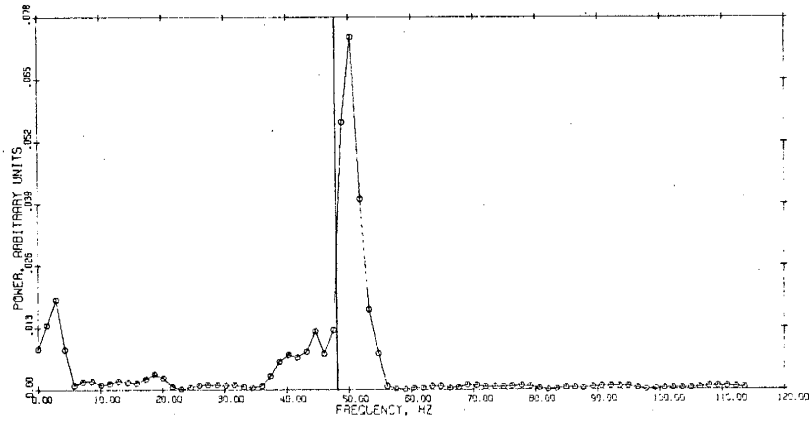

OPTICAL SPECTRUM WEIGHT 0.026 G.

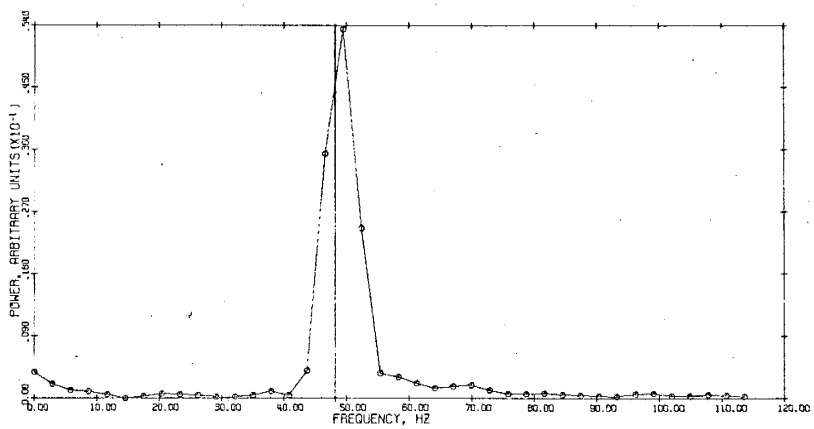

OPTICAL SPECTRUM WEIGHT 0.027 G.

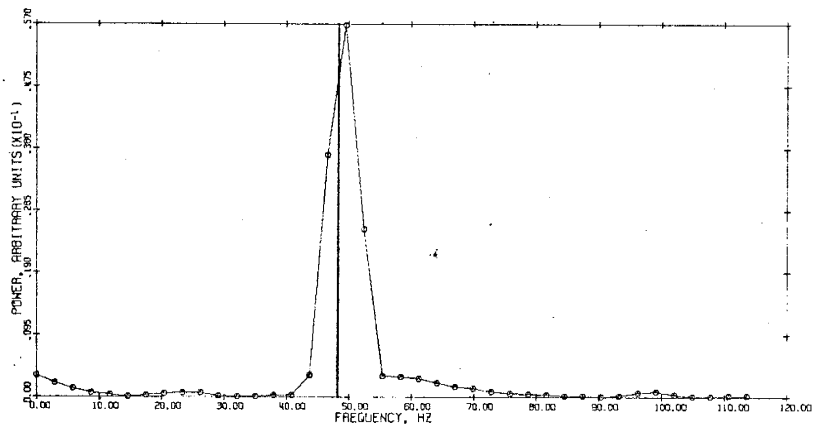

OPTICAL SPECTRUM WEIGHT 0.027 G.

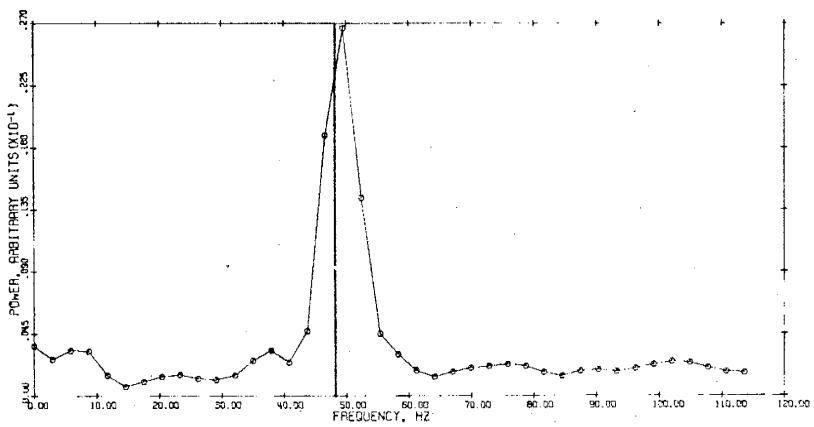

OPTICAL SPECTRUM WEIGHT 0.027 G.

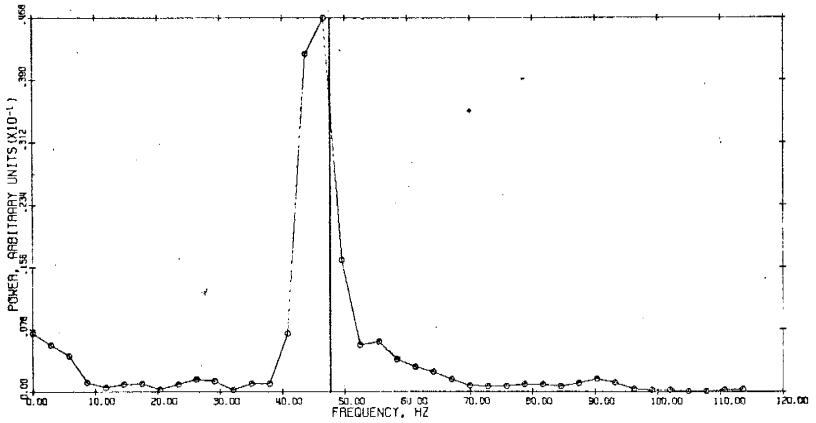

OPTICAL SPECTRUM WEIGHT 0.028 G.

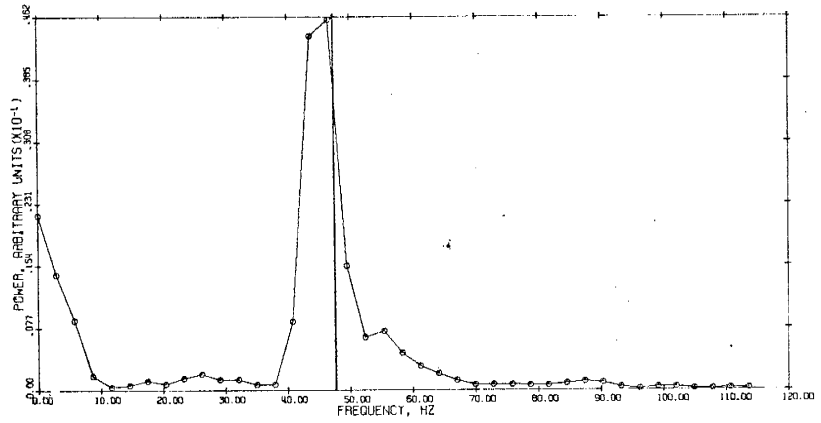

OPTICAL SPECTRUM WEIGHT 0.028 G.

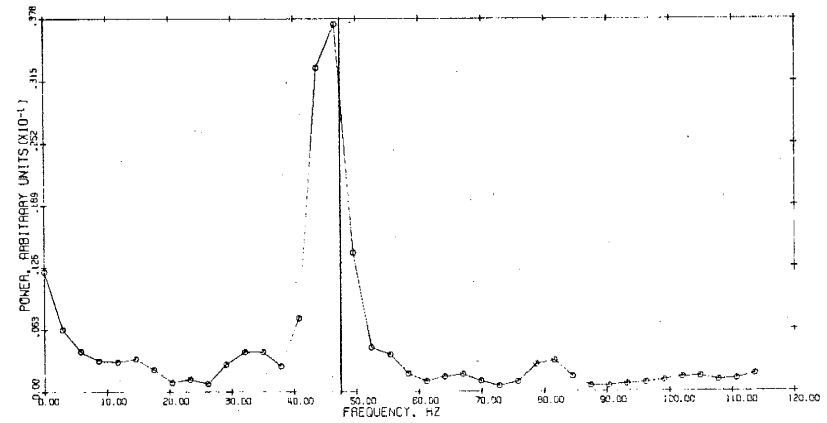

OPTICAL SPECTRUM WEIGHT 0.028 G.

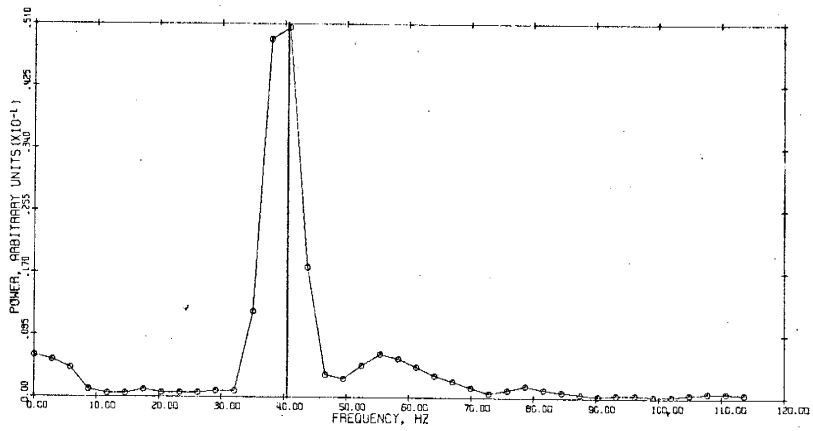

OPTICAL SPECTRUM WEIGHT 0.039 G.

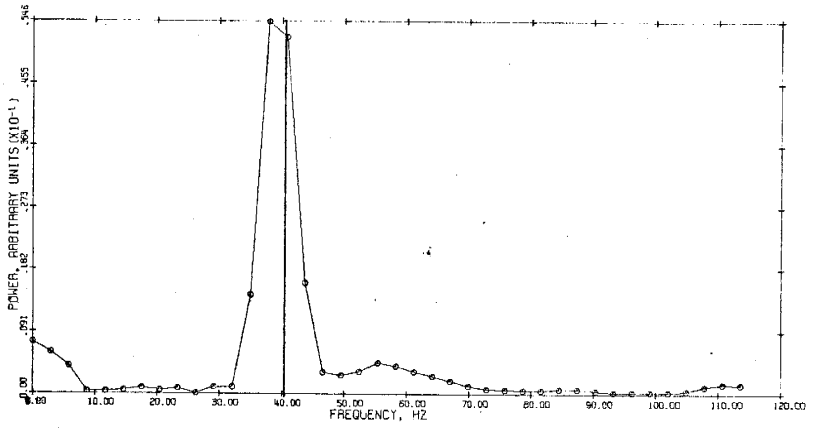

OPTICAL SPECTRUM WEIGHT 0.039 G.

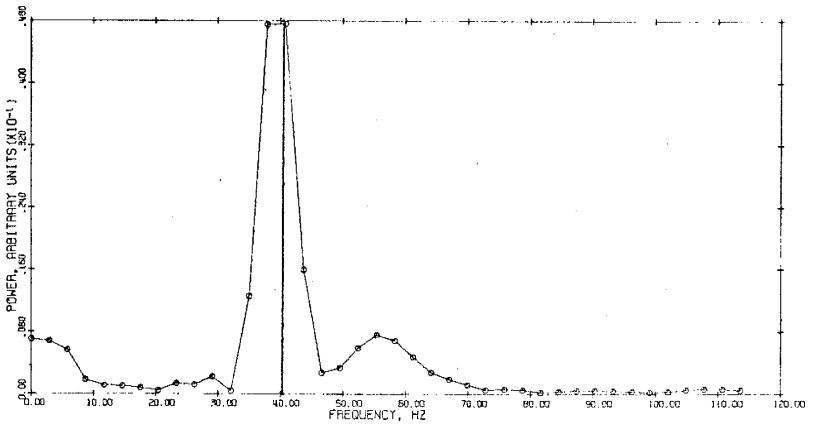

OPTICAL SPECTRUM WEIGHT 0.039 G.

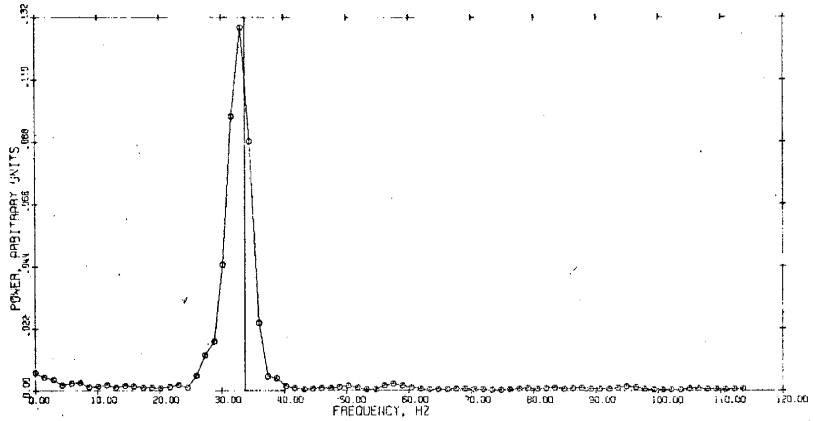

OPTICAL SPECTRUM, WT. = 0.055 GM.

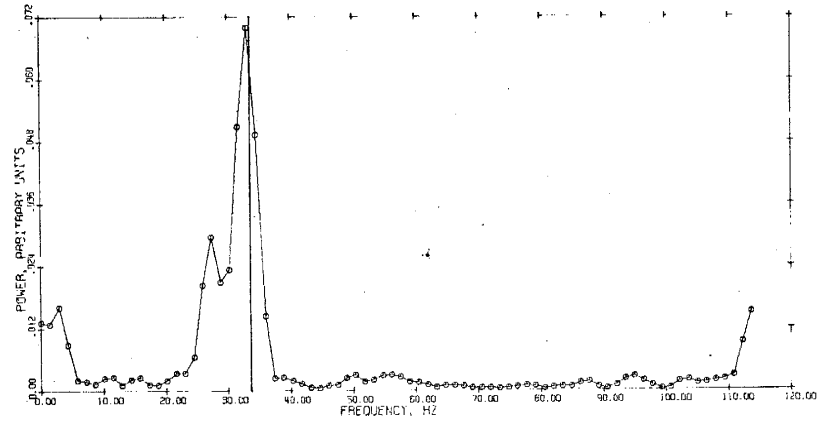

OPTICAL SPECTRUM, WT. = 0.055 GM.

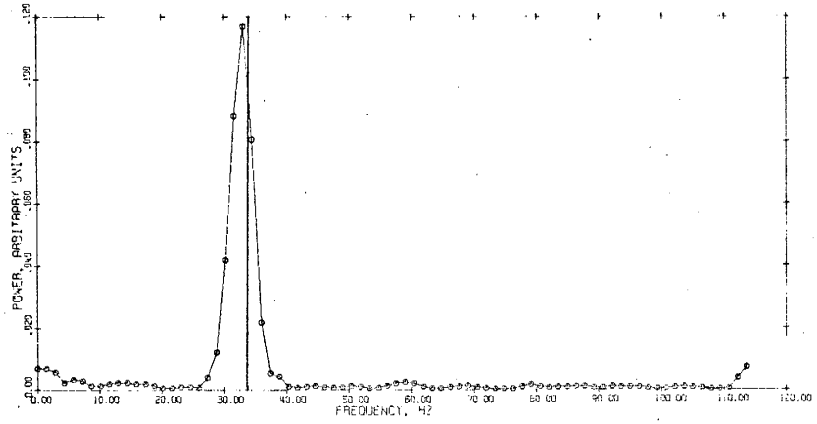

OPTICAL SPECTRUM, WT. = 0.055 GM.

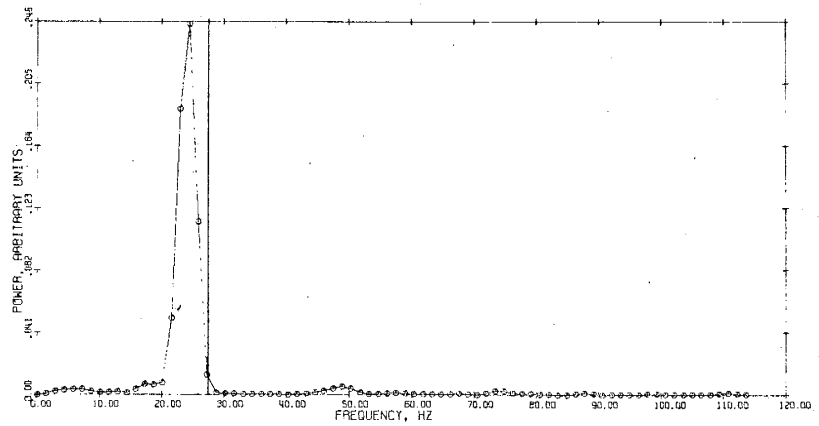

OPTICAL SPECTRUM WEIGHT 0.082 G.

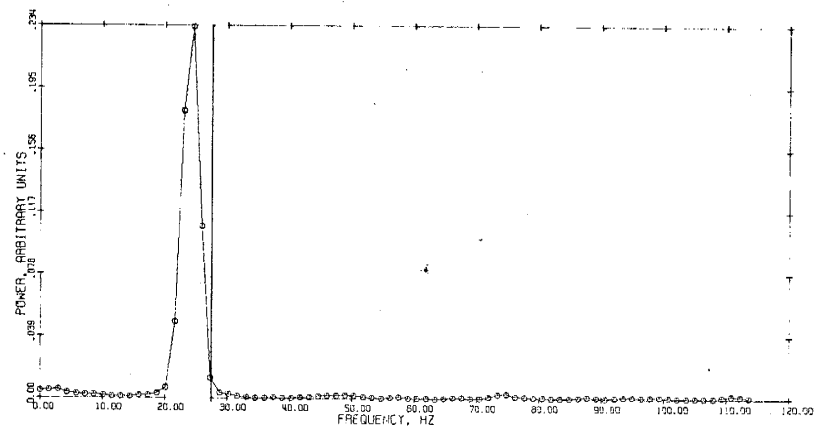

OPTICAL SPECTRUM WEIGHT 0.082 G.

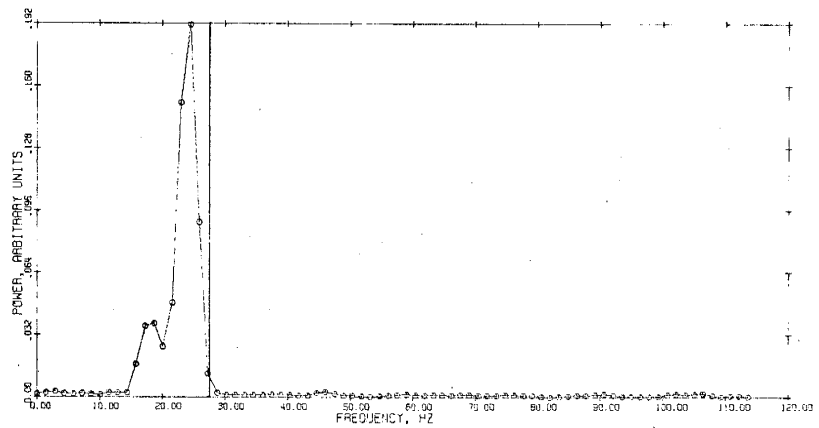

OPTICAL SPECTRUM WEIGHT 0.082 G.

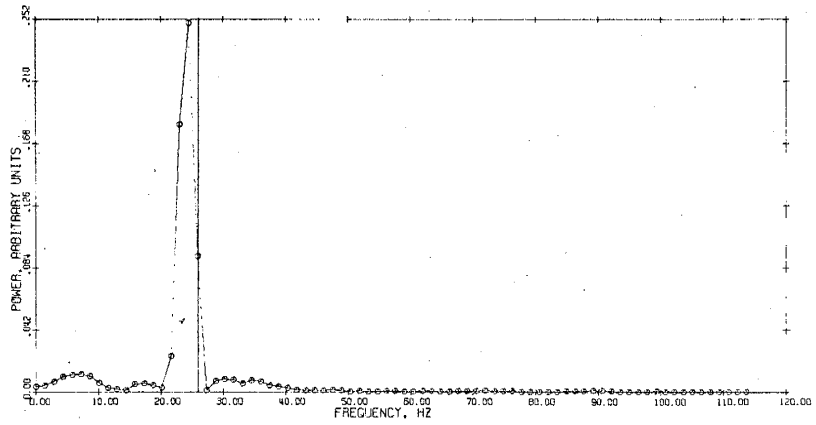

OPTICAL SPECTRUM WEIGHT 0.092 G.

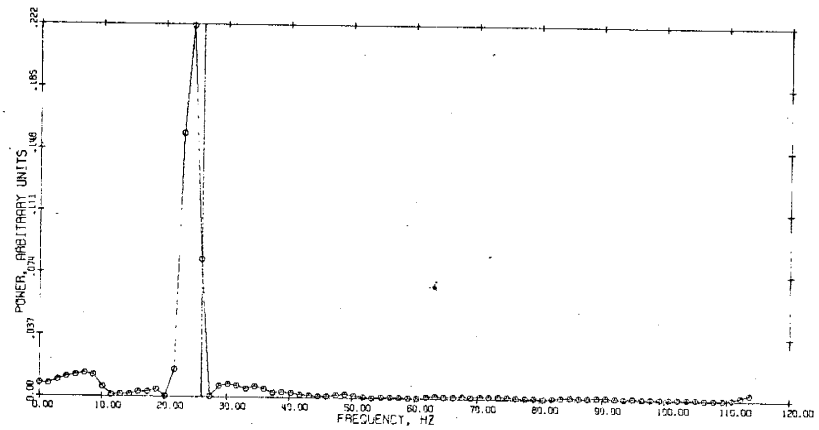

OPTICAL SPECTRUM WEIGHT 0.092 G.

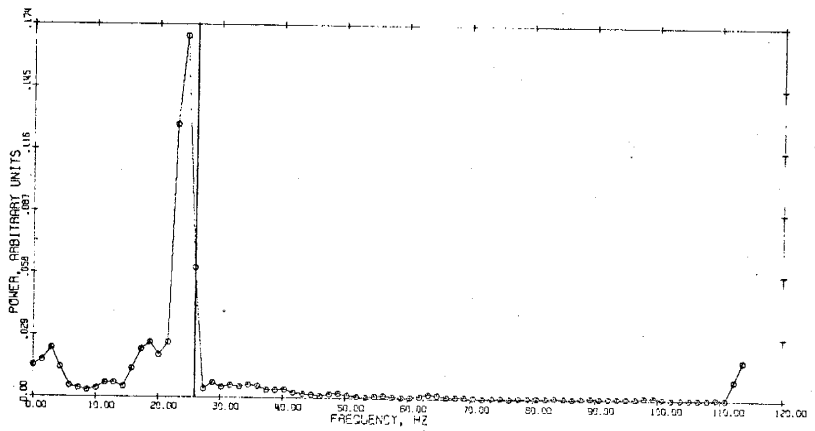

OPTICAL SPECTRUM WEIGHT 0.092 G.

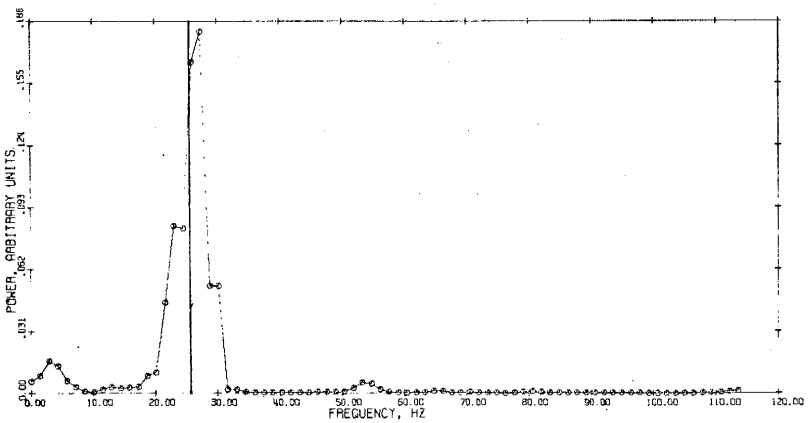

OPTICAL SPECTRUM WEIGHT 0.094 G.

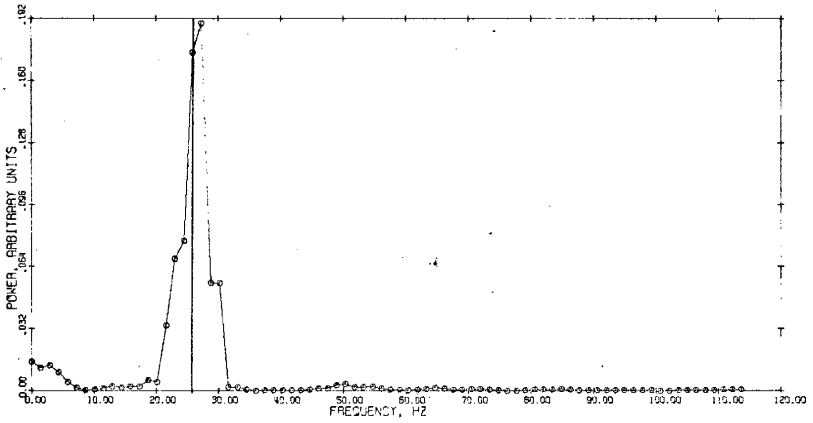

OPTICAL SPECTRUM WEIGHT 0.094 G.

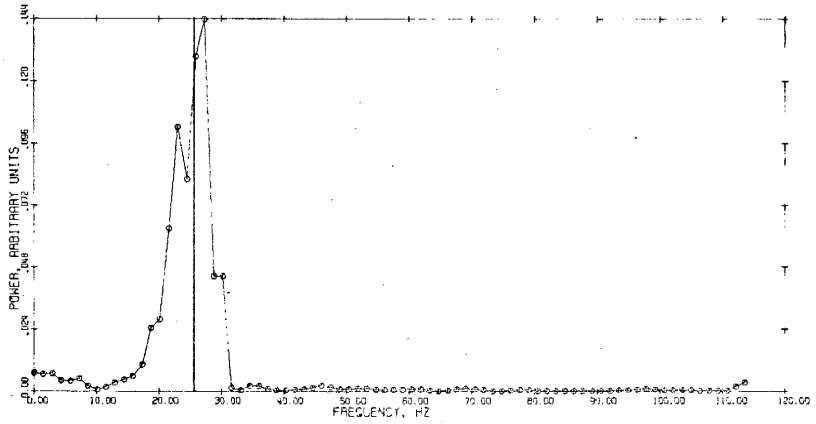

OPTICAL SPECTRUM WEIGHT 0.094 G.

APPENDIX IV

MICROWAVE SPECTRA

Top of page: Full Range Spectrum

Bottom of page: Spectrum for Frequencies 10 Hz.

(The Rayleigh frequency corresponding to the mass of the drop is shown as a solid constant frequency line.)

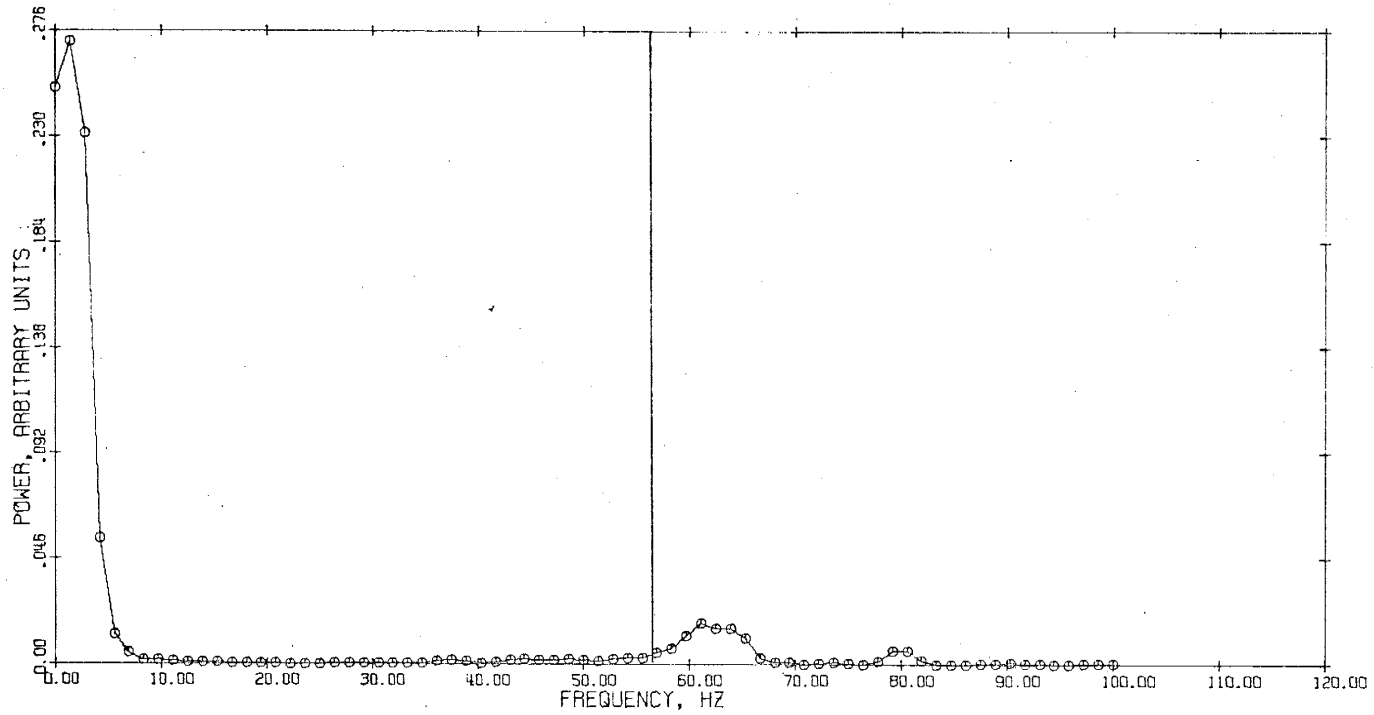

MICROWAVE SPECTRUM WEIGHT .0197 G.

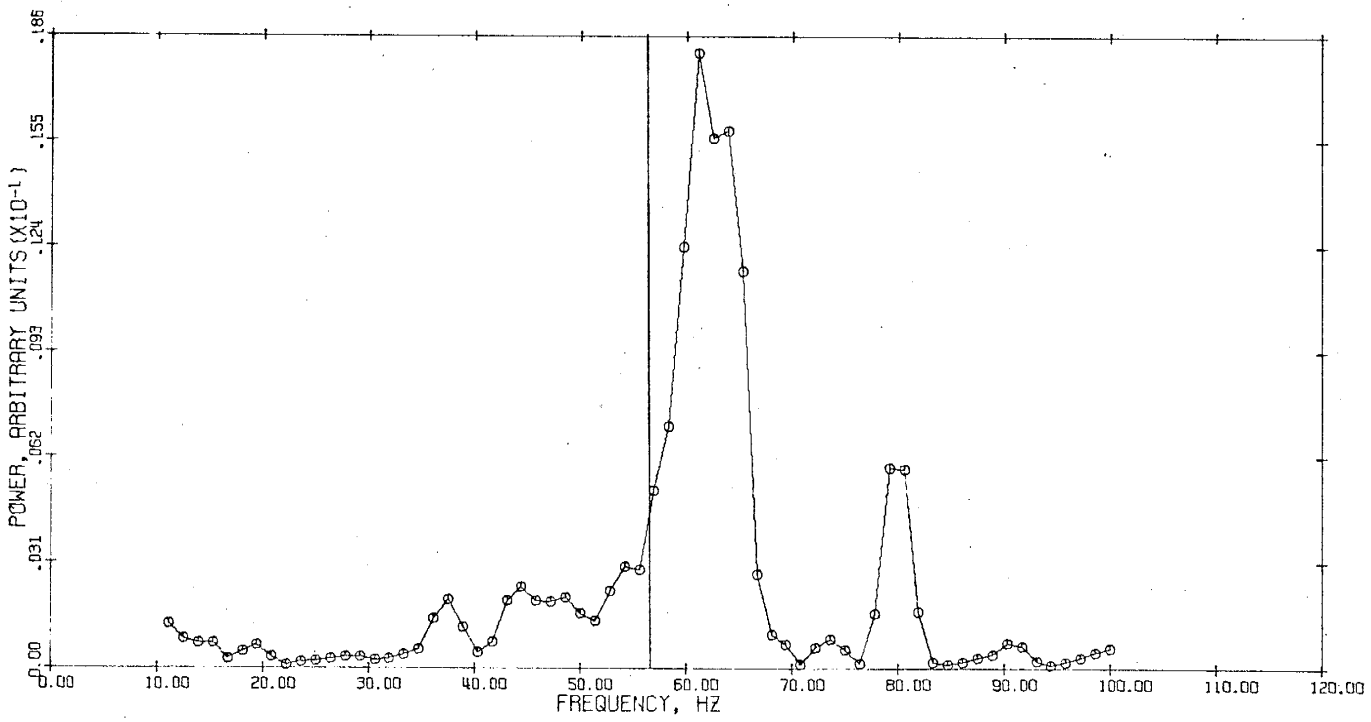

MICROWAVE SPECTRUM WEIGHT .0197 G.

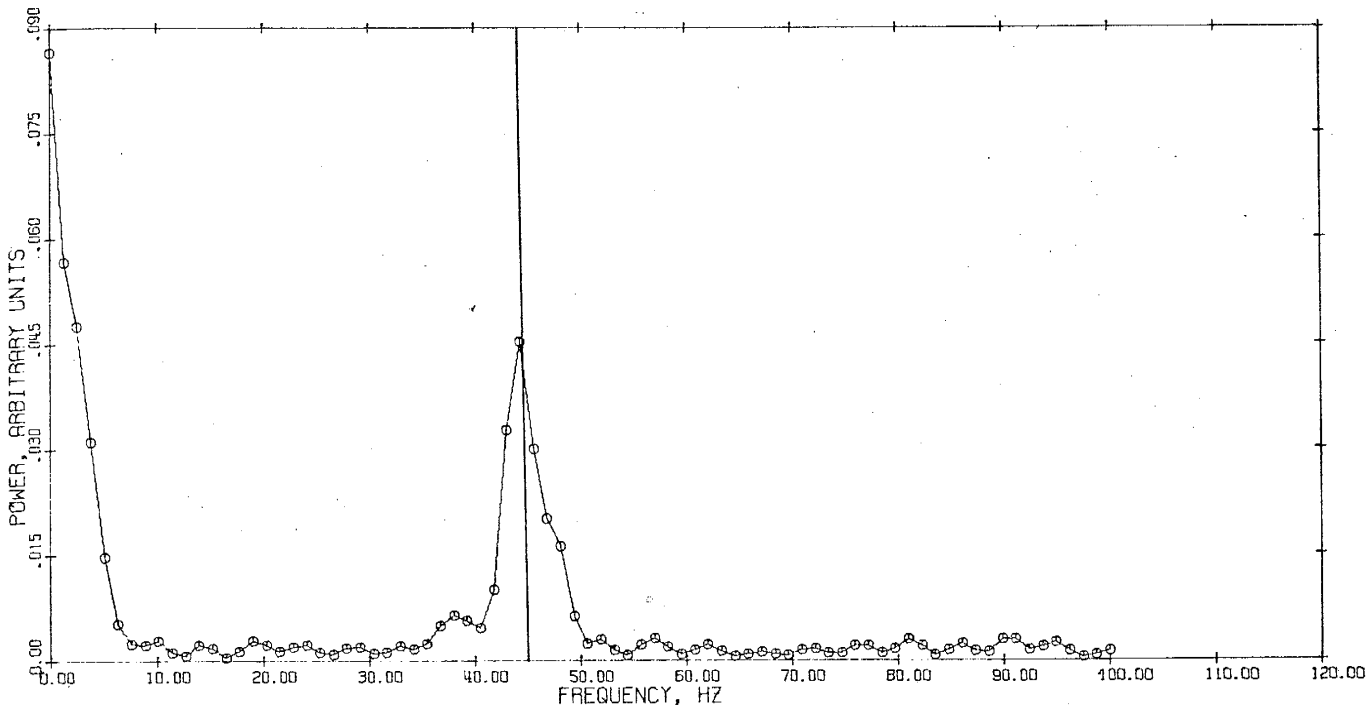

MICROWAVE SPECTRUM WEIGHT .0309 G.

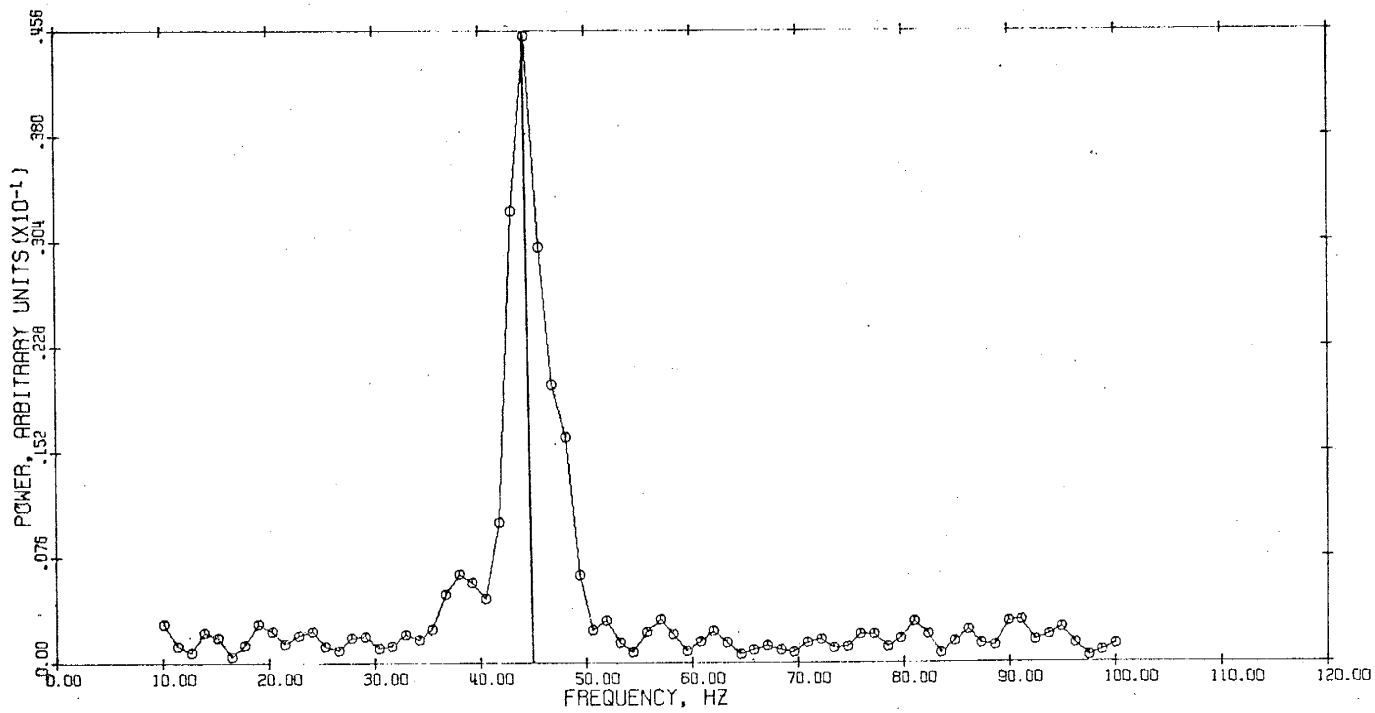

MICROWAVE SPECTRUM WEIGHT .0309 G.

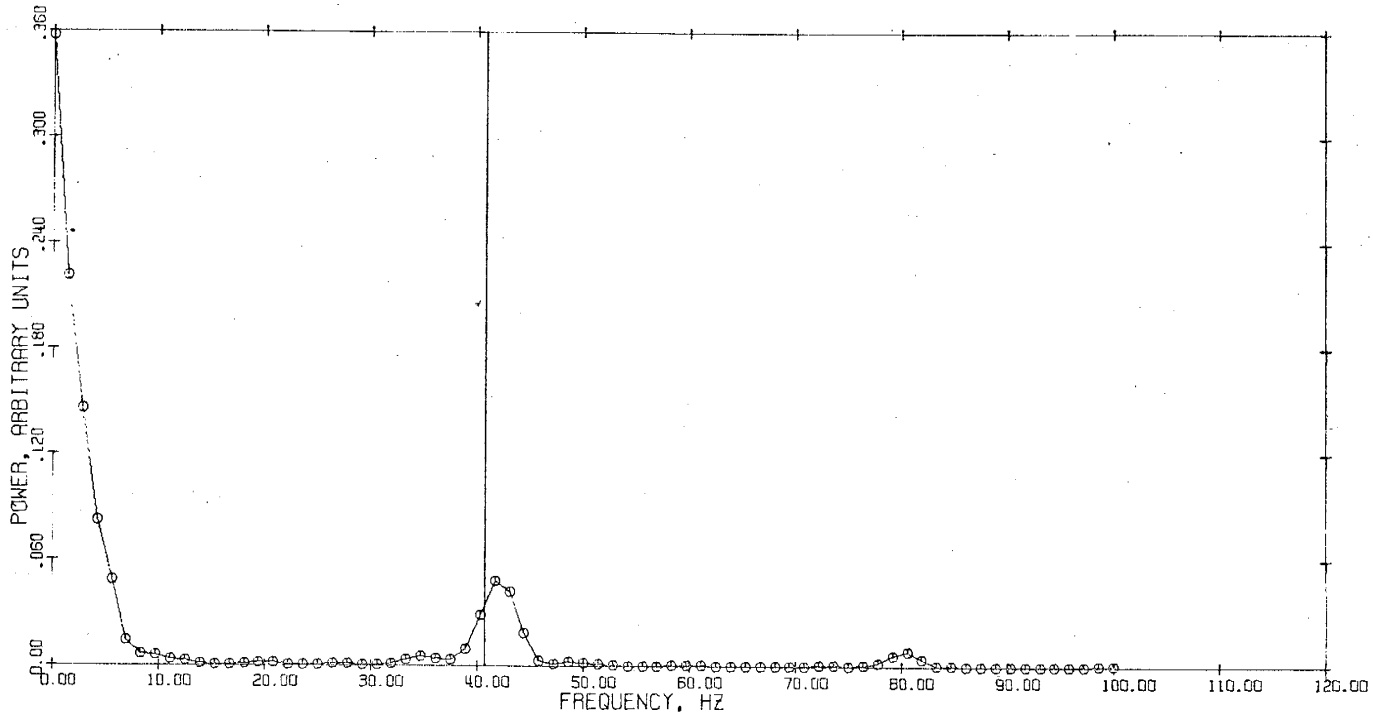

MICROWAVE SPECTRUM WEIGHT .0370 G.

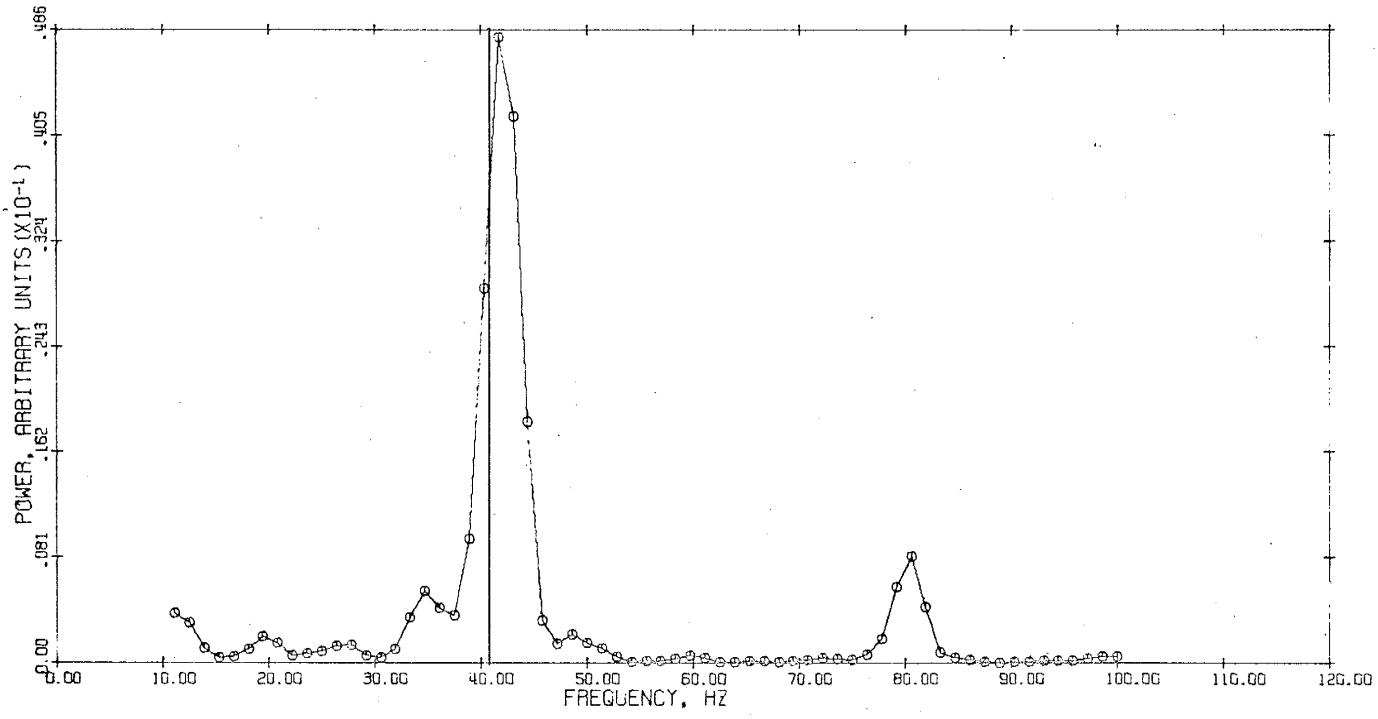

MICROWAVE SPECTRUM WEIGHT .0370 G.

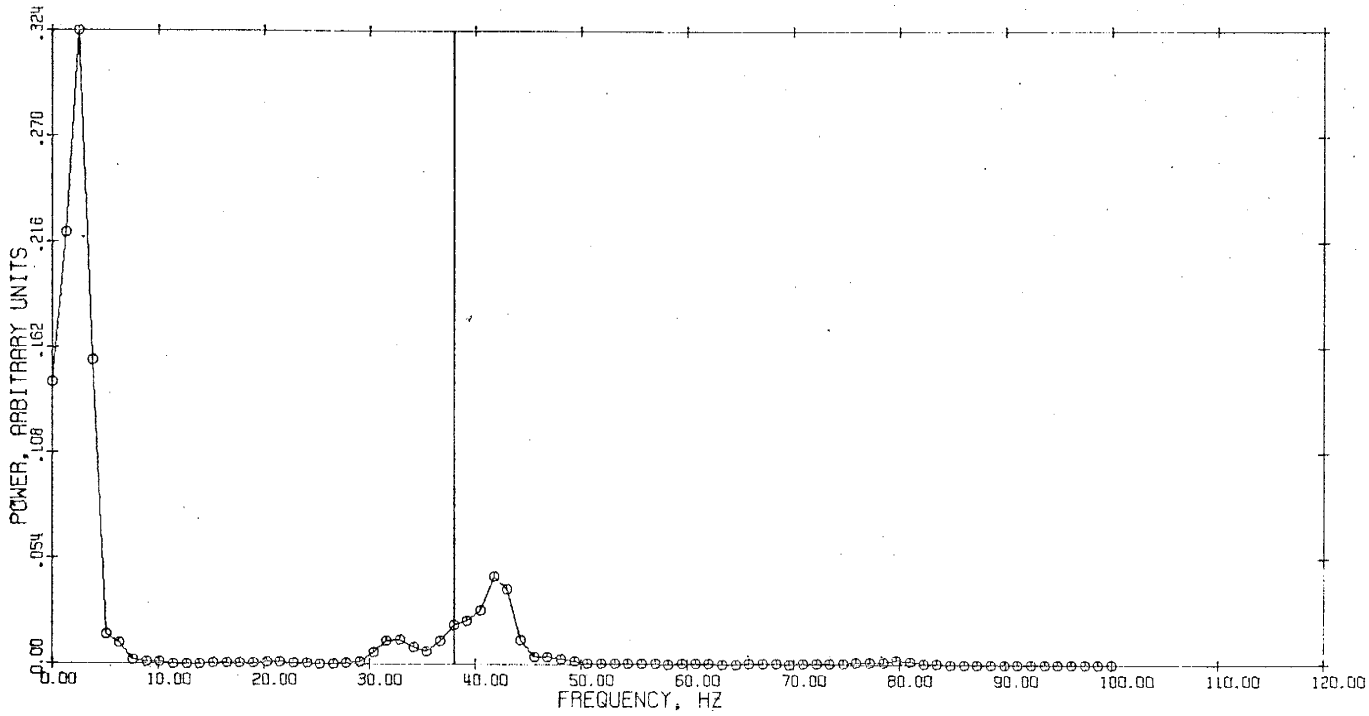

MICROWAVE SPECTRUM WEIGHT .0434 G.

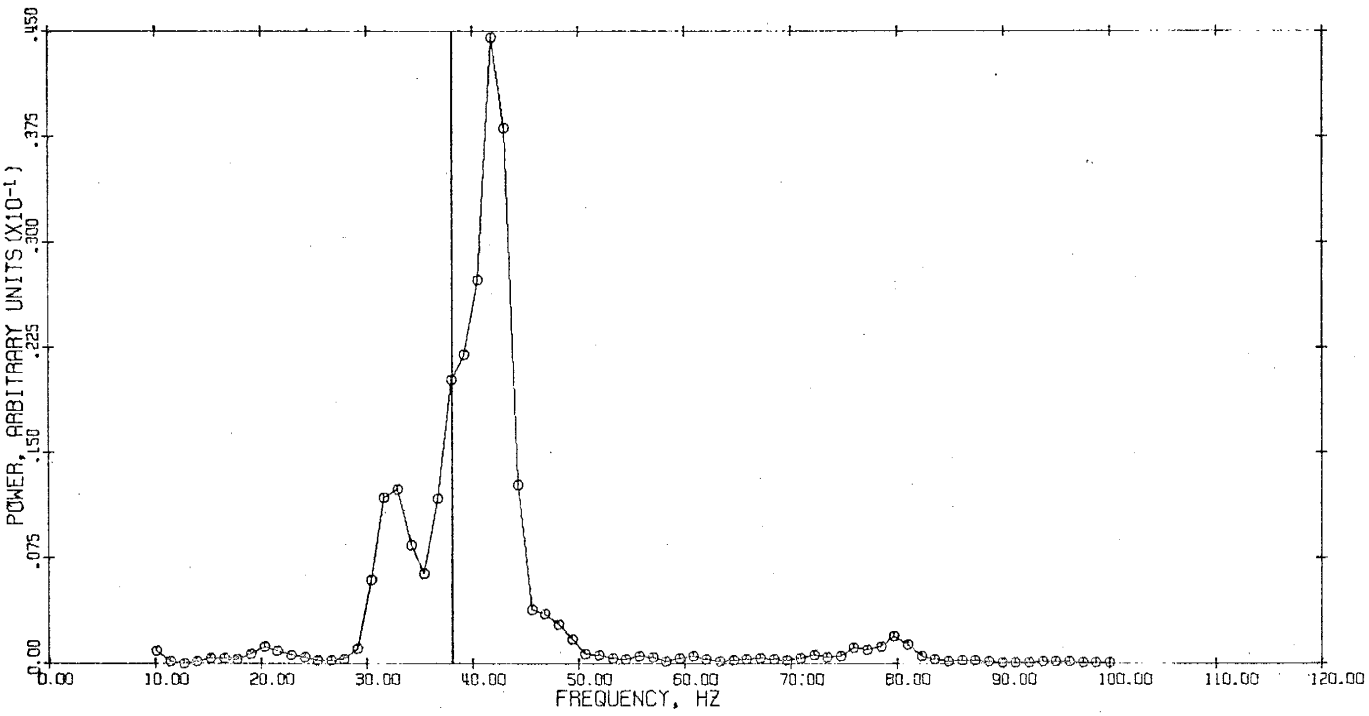

MICROWAVE SPECTRUM WEIGHT .0434 G.

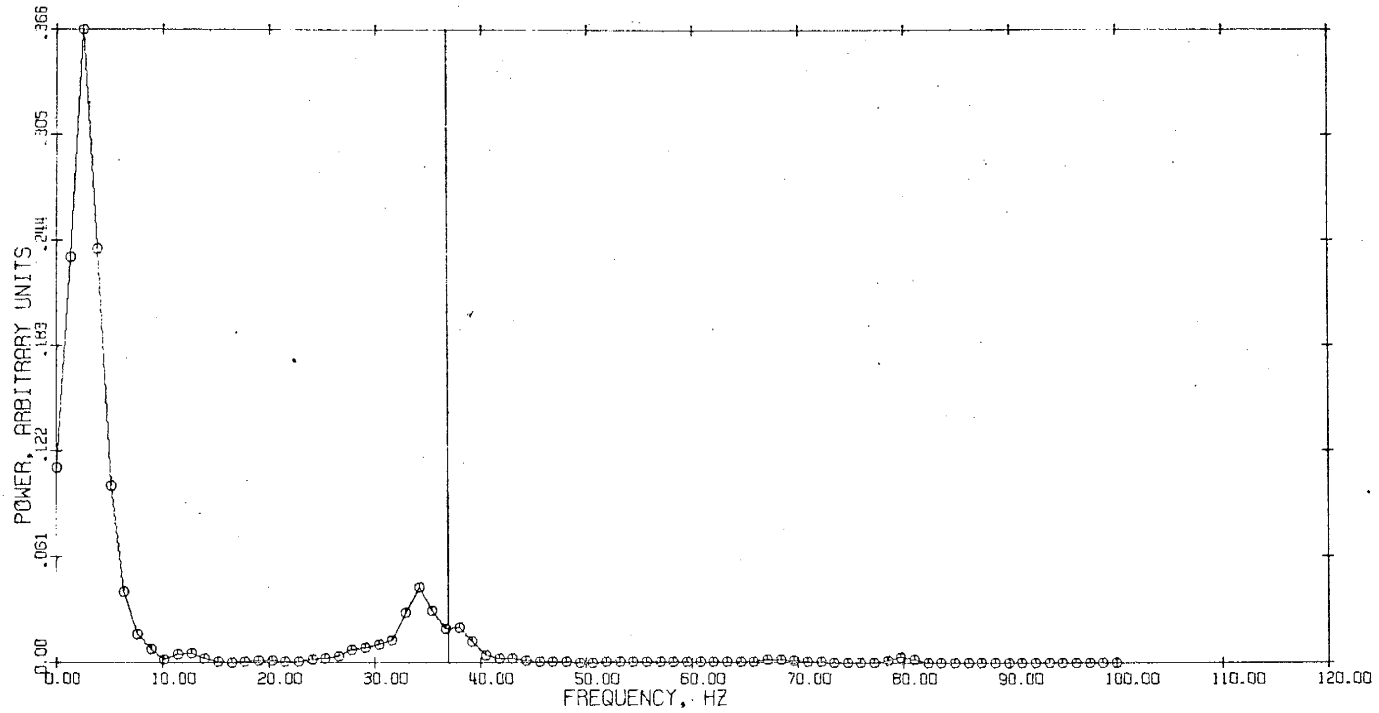

MICROWAVE SPECTRUM WEIGHT .0459 G.

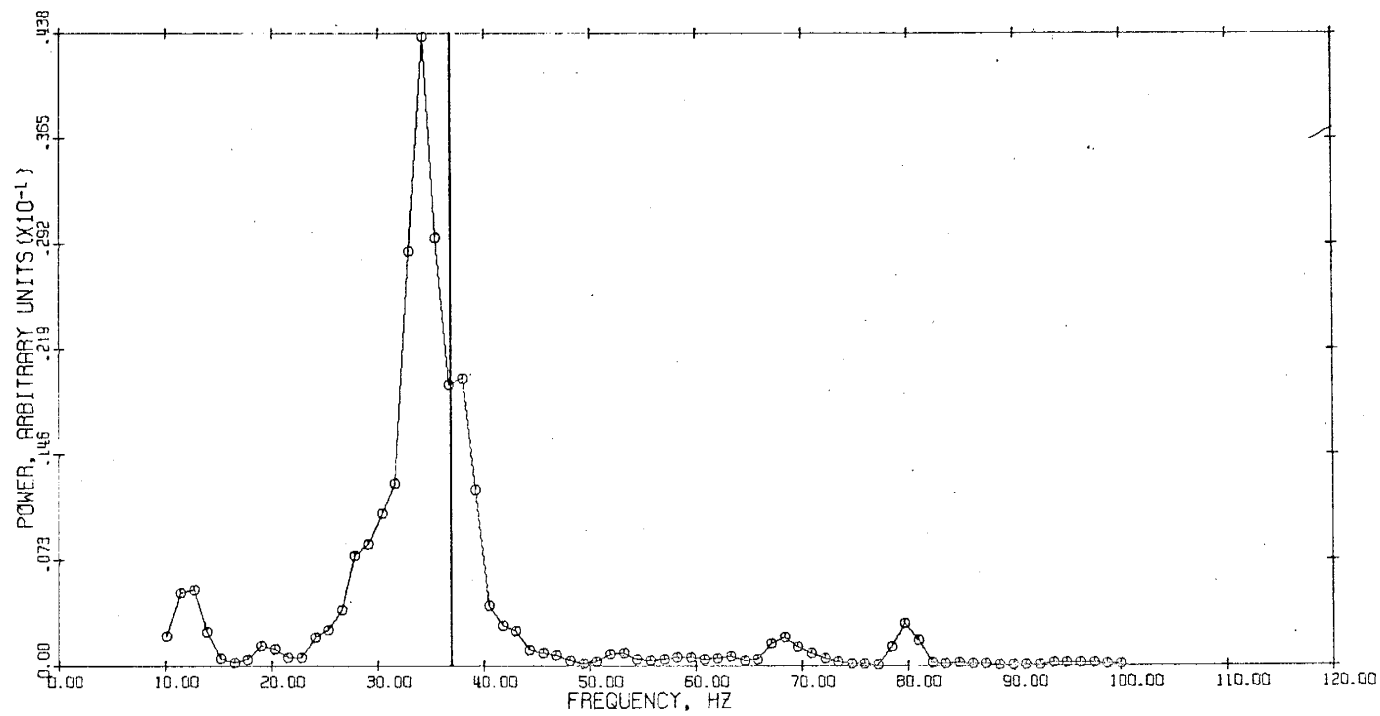

MICROWAVE SPECTRUM WEIGHT .0459 G.

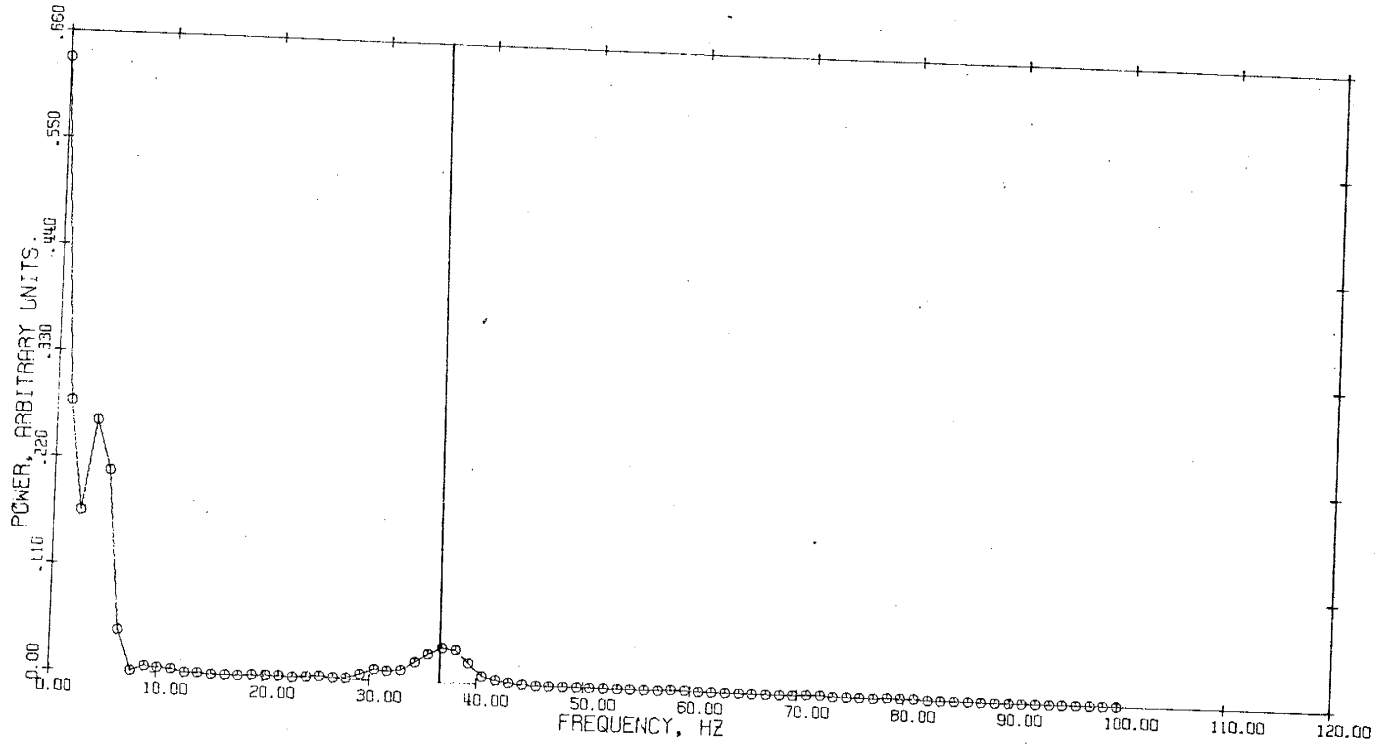

MICRØWAVE SPECTRUM WEIGHT .0467 G.

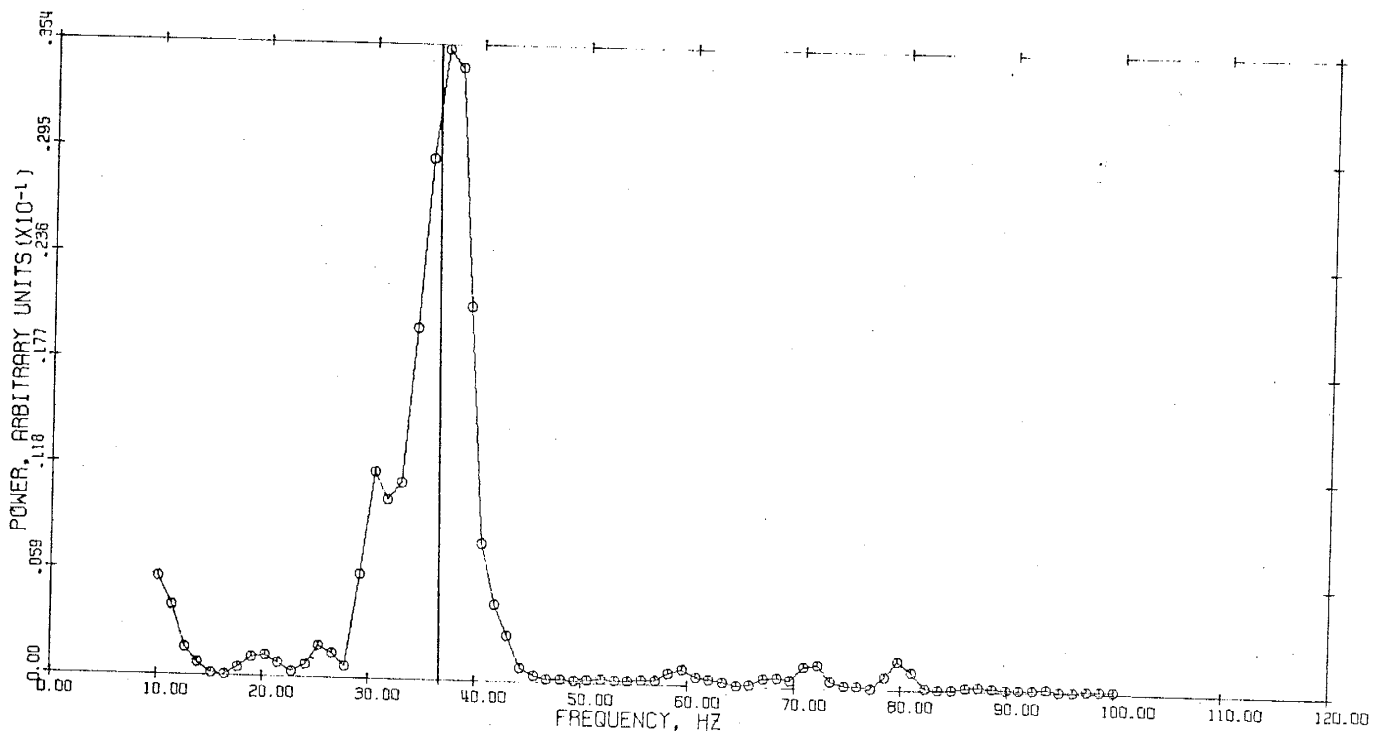

MICROWAVE SPECTRUM WEIGHT .0467 G.

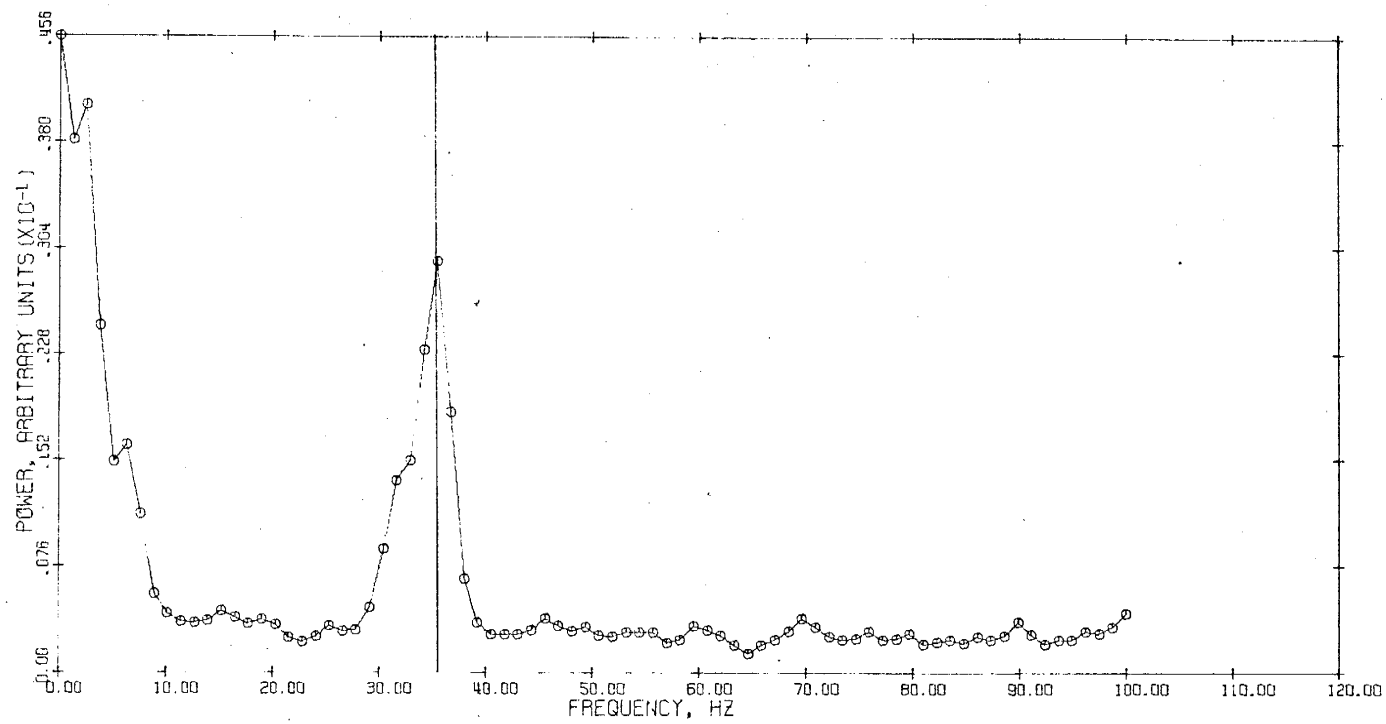

MICROWAVE SPECTRUM WEIGHT .0515 G.

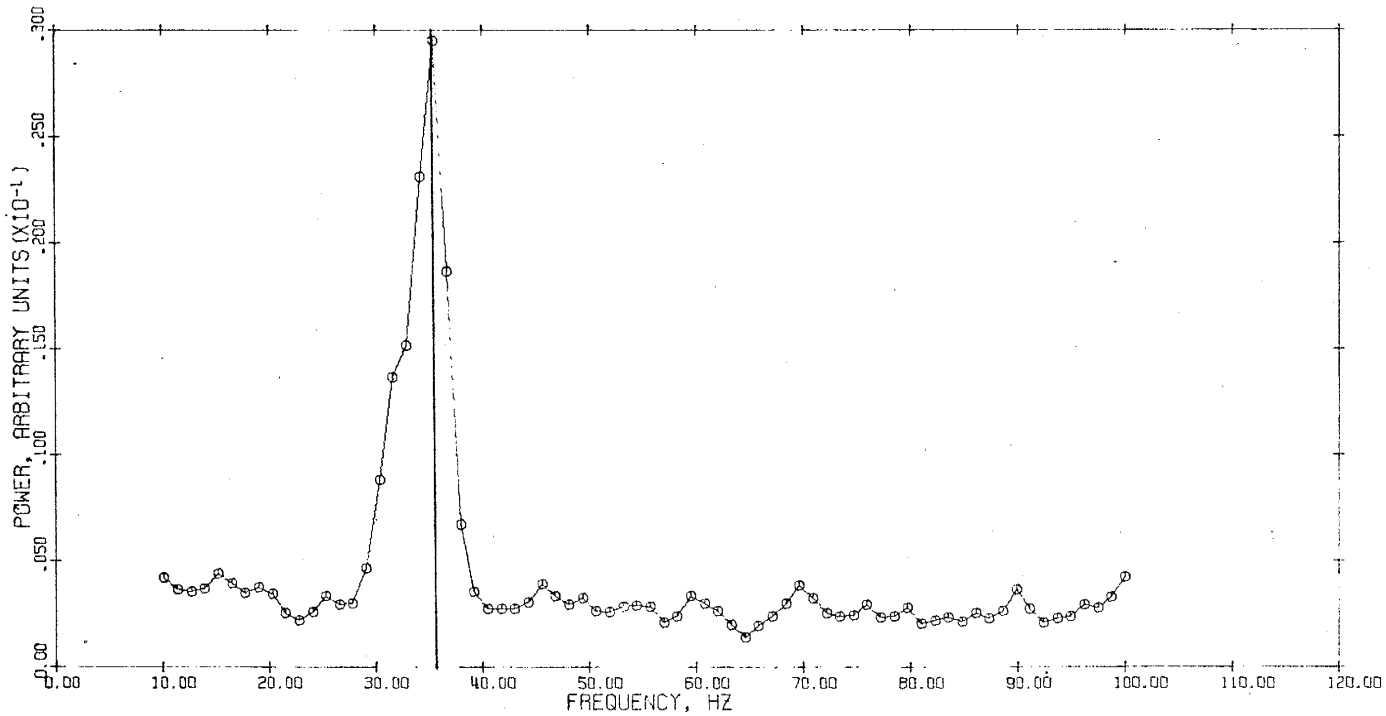

MICROWAVE SPECTRUM WEIGHT .0515 G.

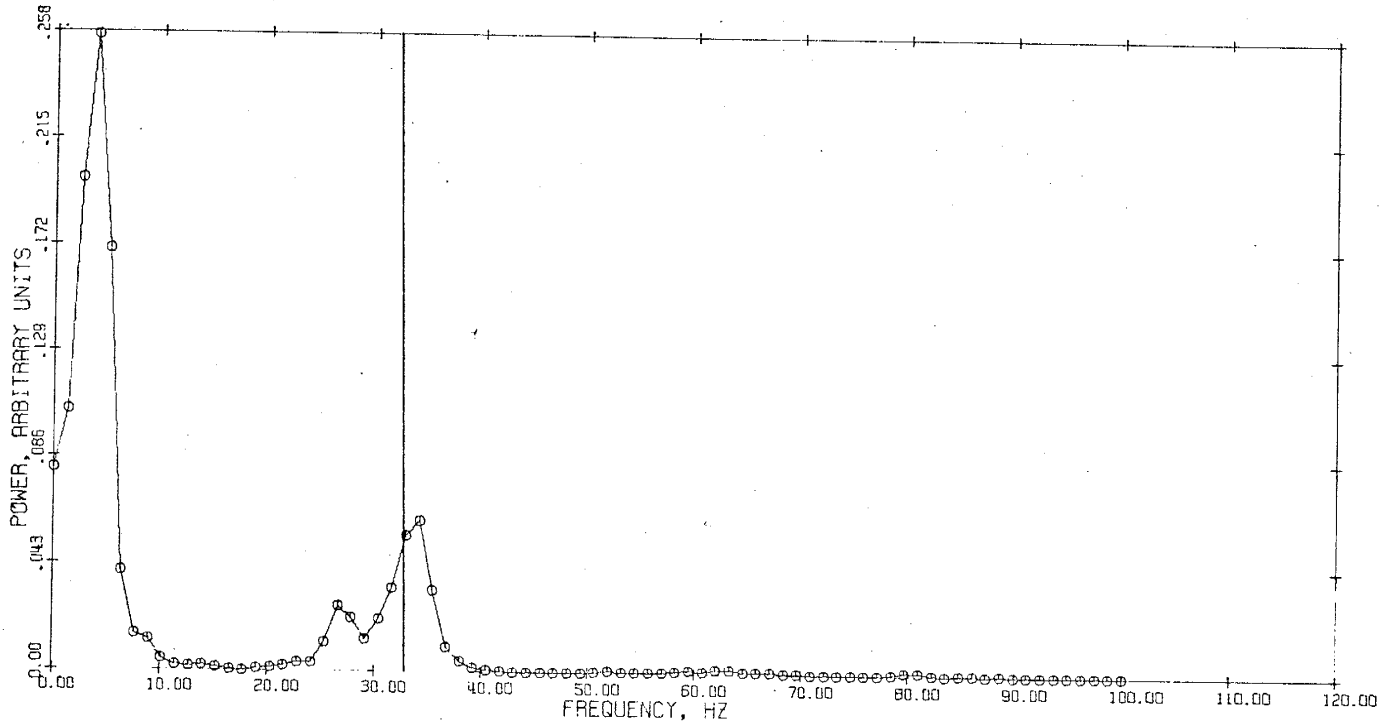

MICROWAVE SPECTRUM WEIGHT .0579 G.

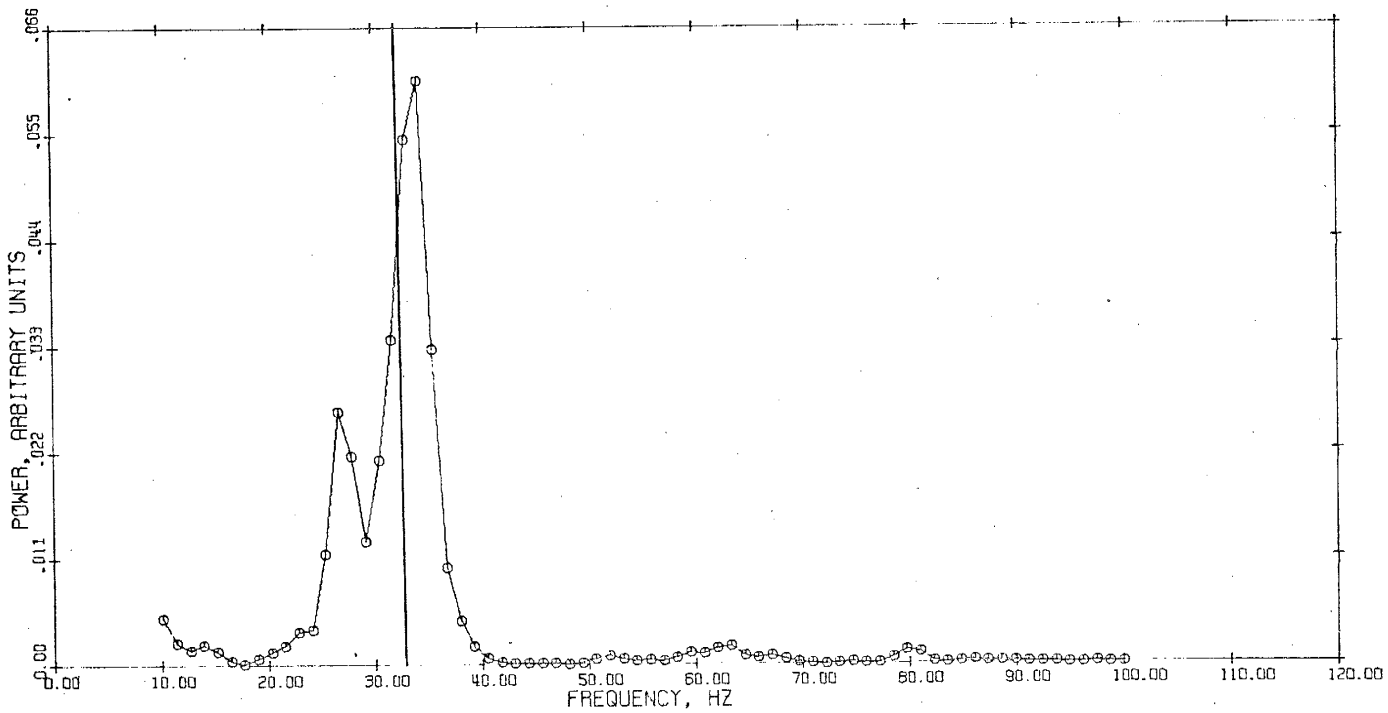

MICROWAVE SPECTRUM WEIGHT .0579 G.

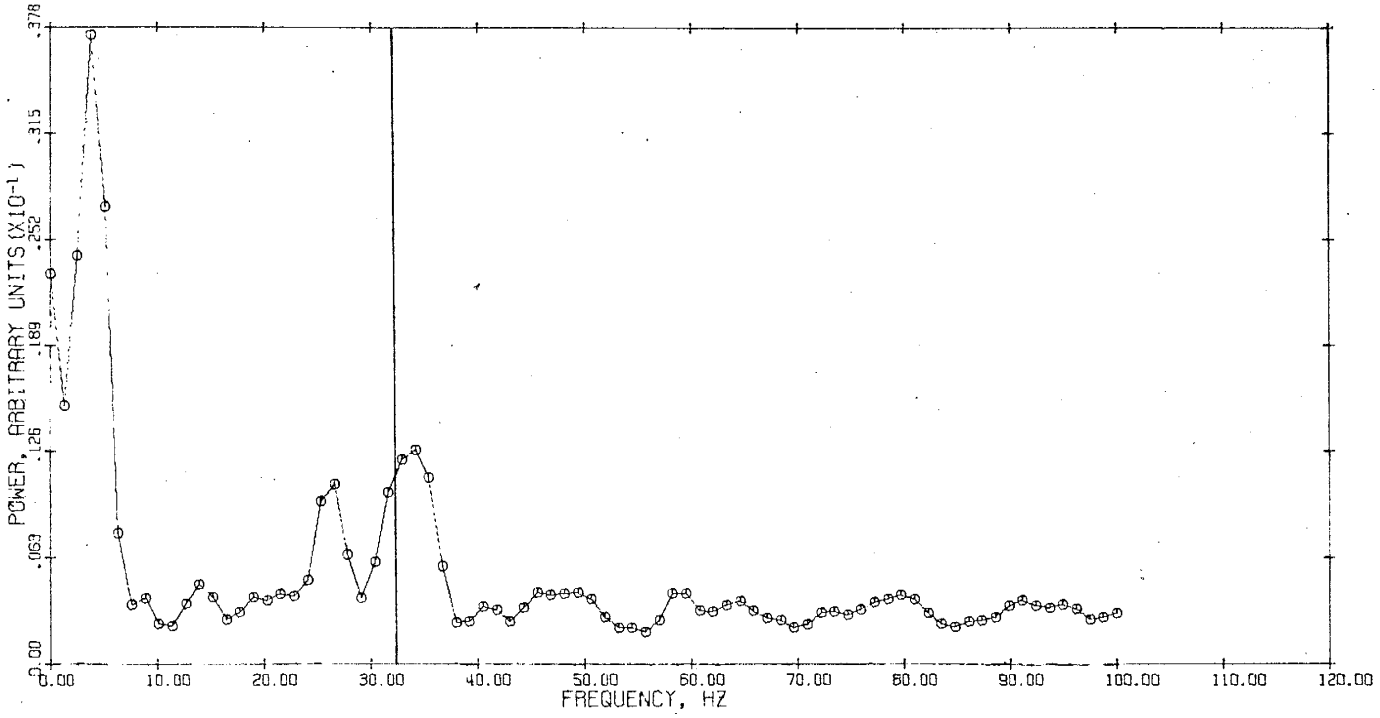

MICROWAVE SPECTRUM WEIGHT .0587 G.

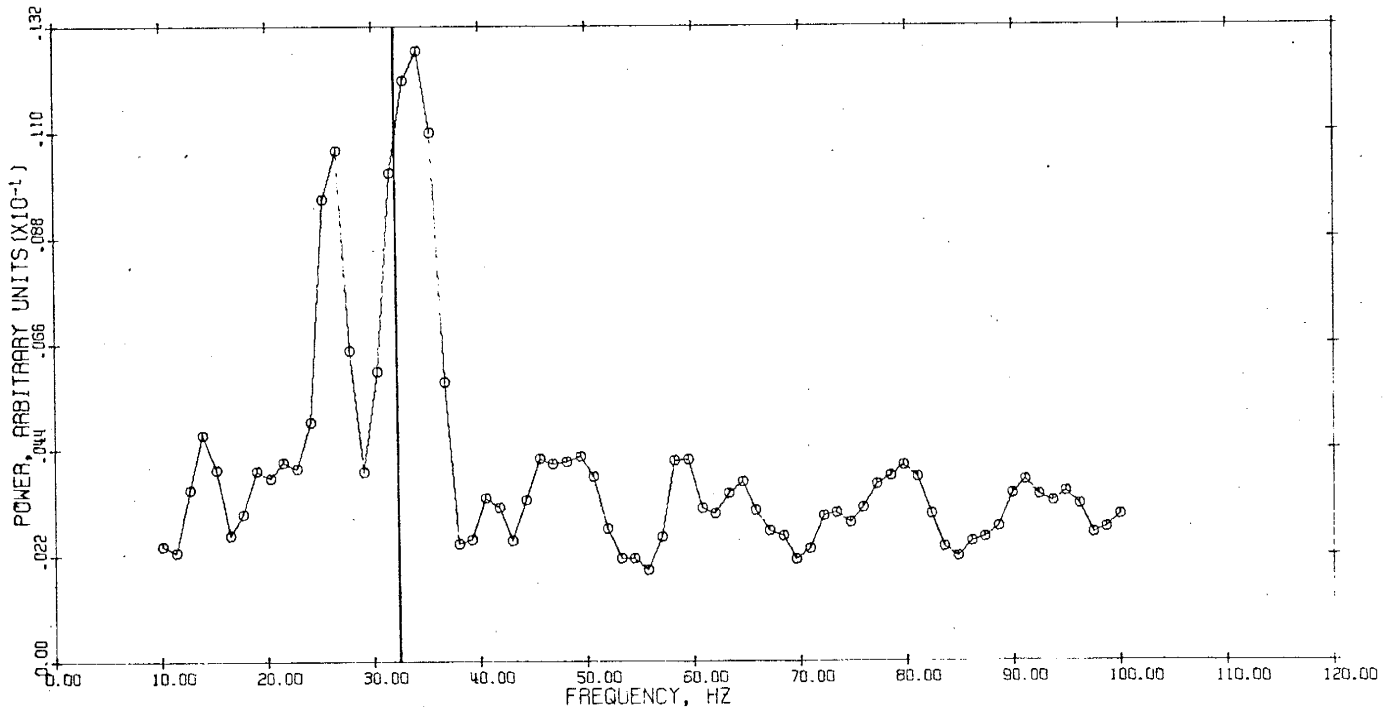

MICROWAVE SPECTRUM WEIGHT .0587 G.

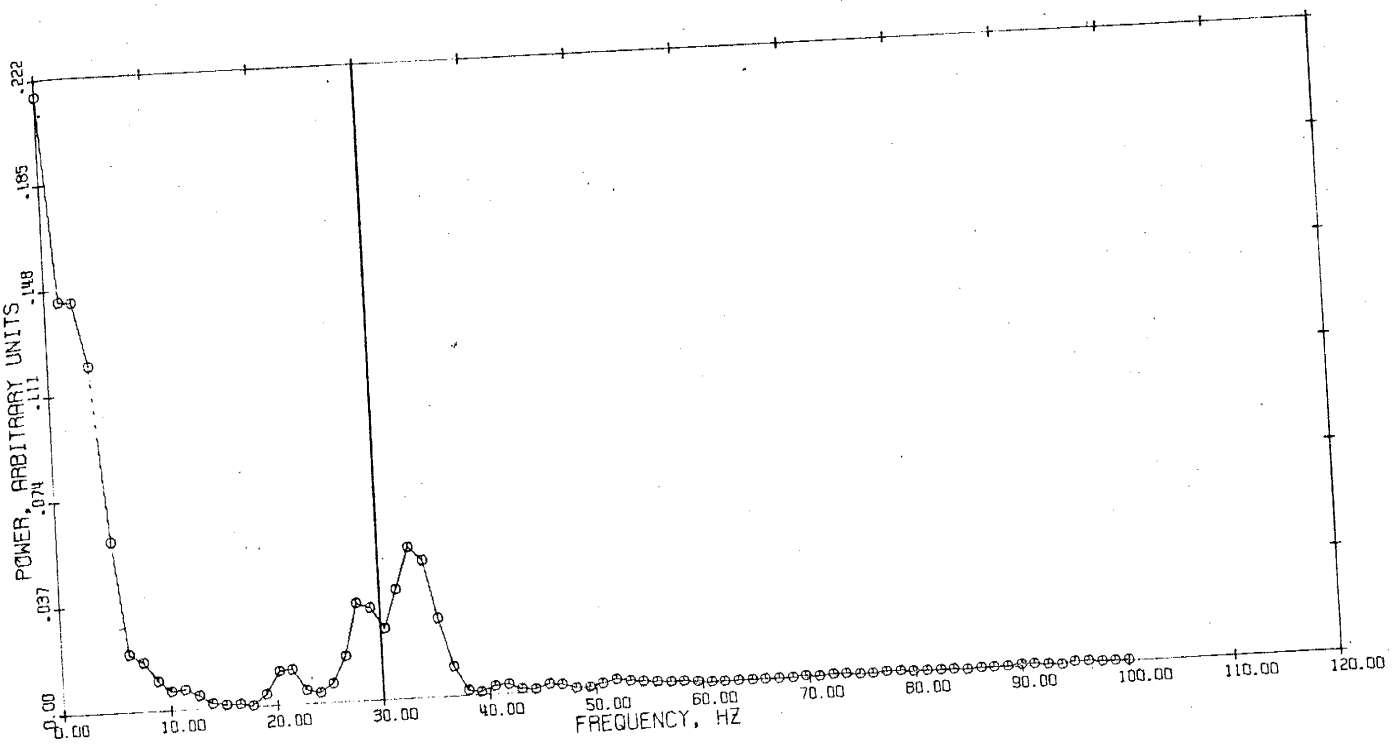

MICROWAVE SPECTRUM WEIGHT .0692 G.

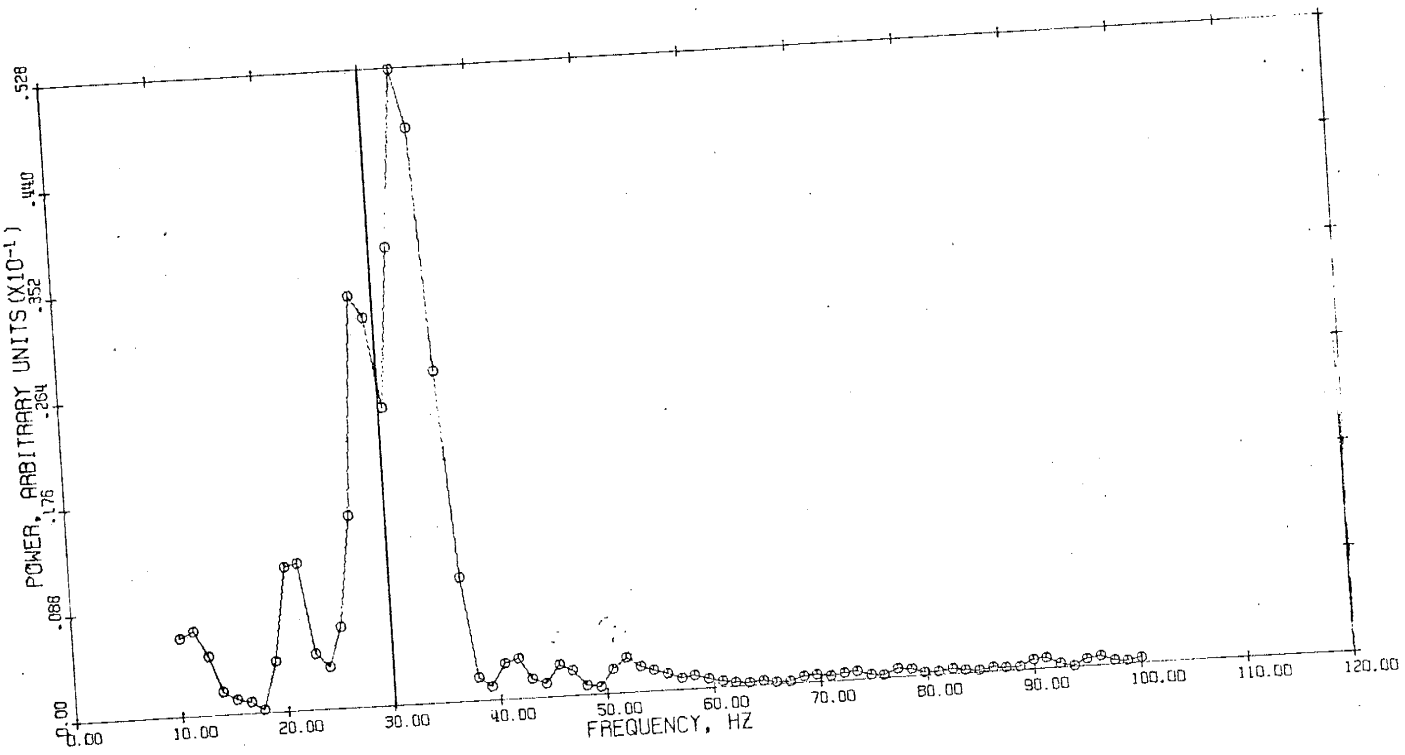

MICROWAVE SPECTRUM WEIGHT .0692 G.

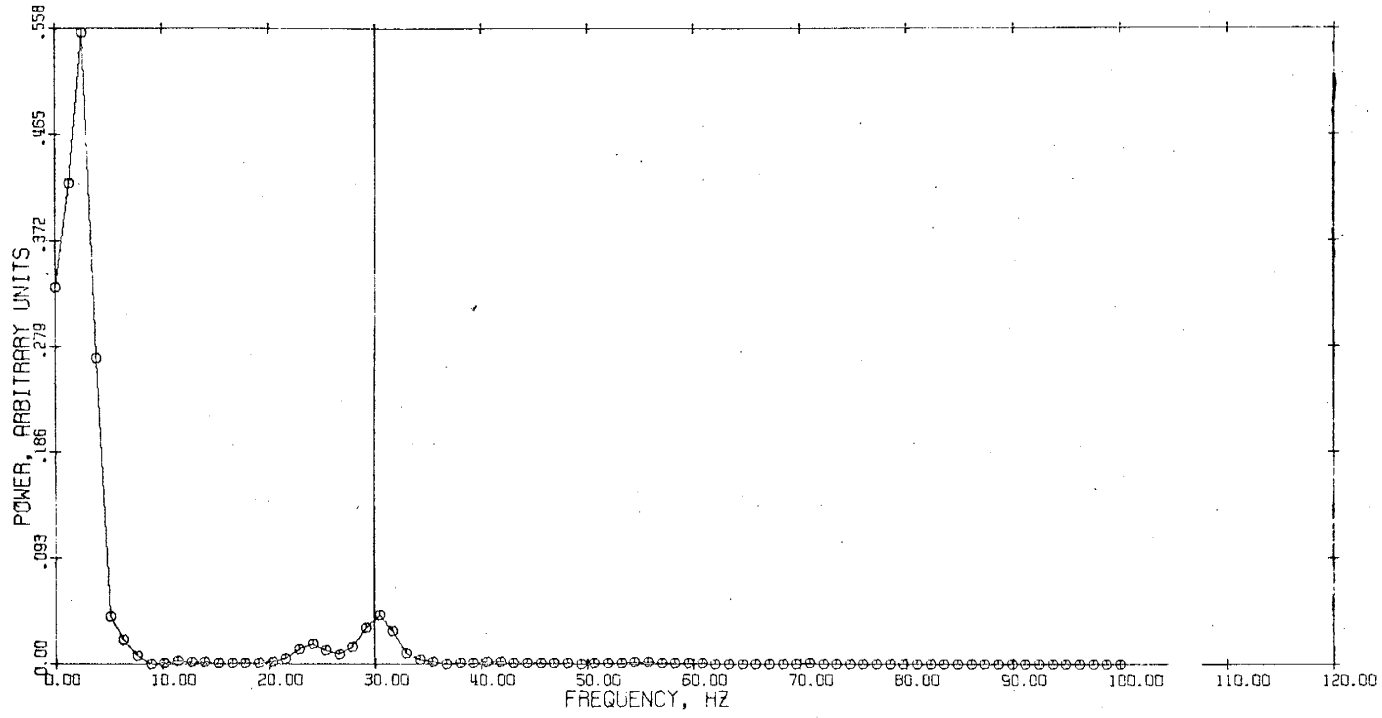

MICROWAVE SPECTRUM WEIGHT .0693 G.

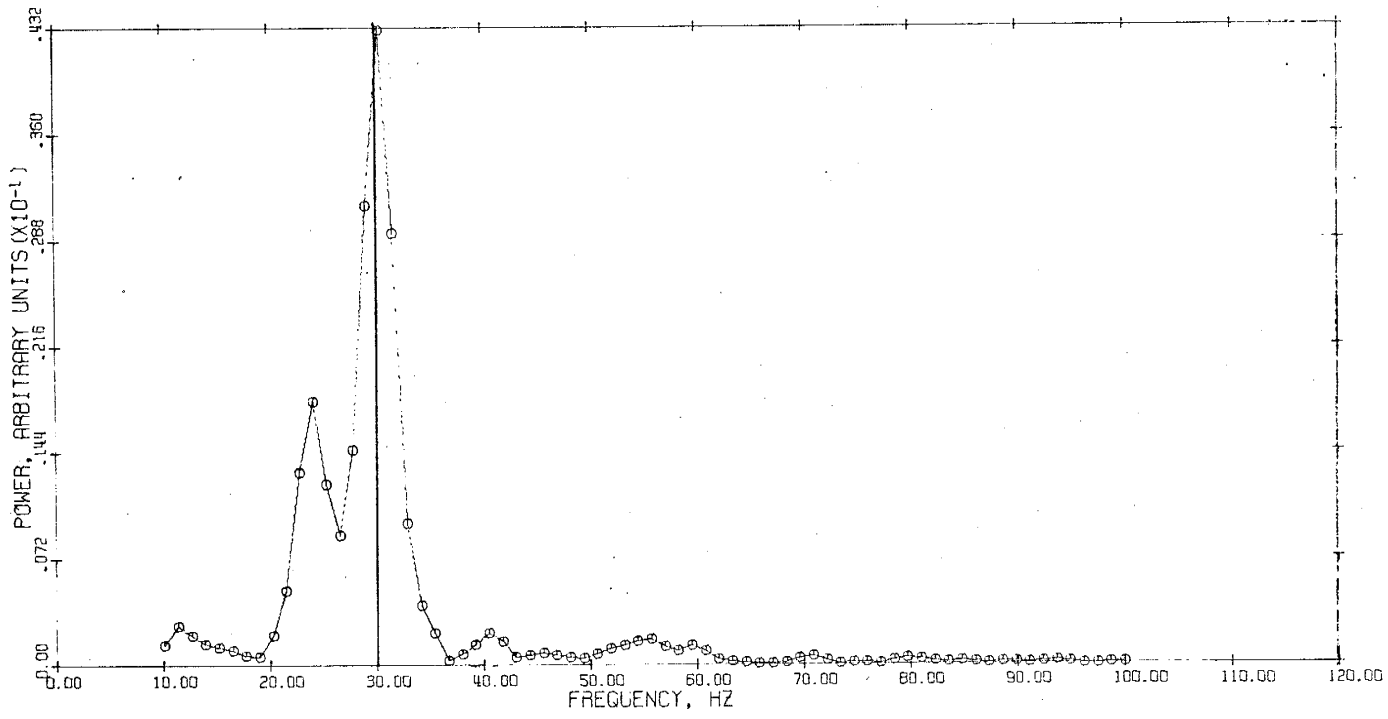

MICROWAVE SPECTRUM WEIGHT .0693 G.

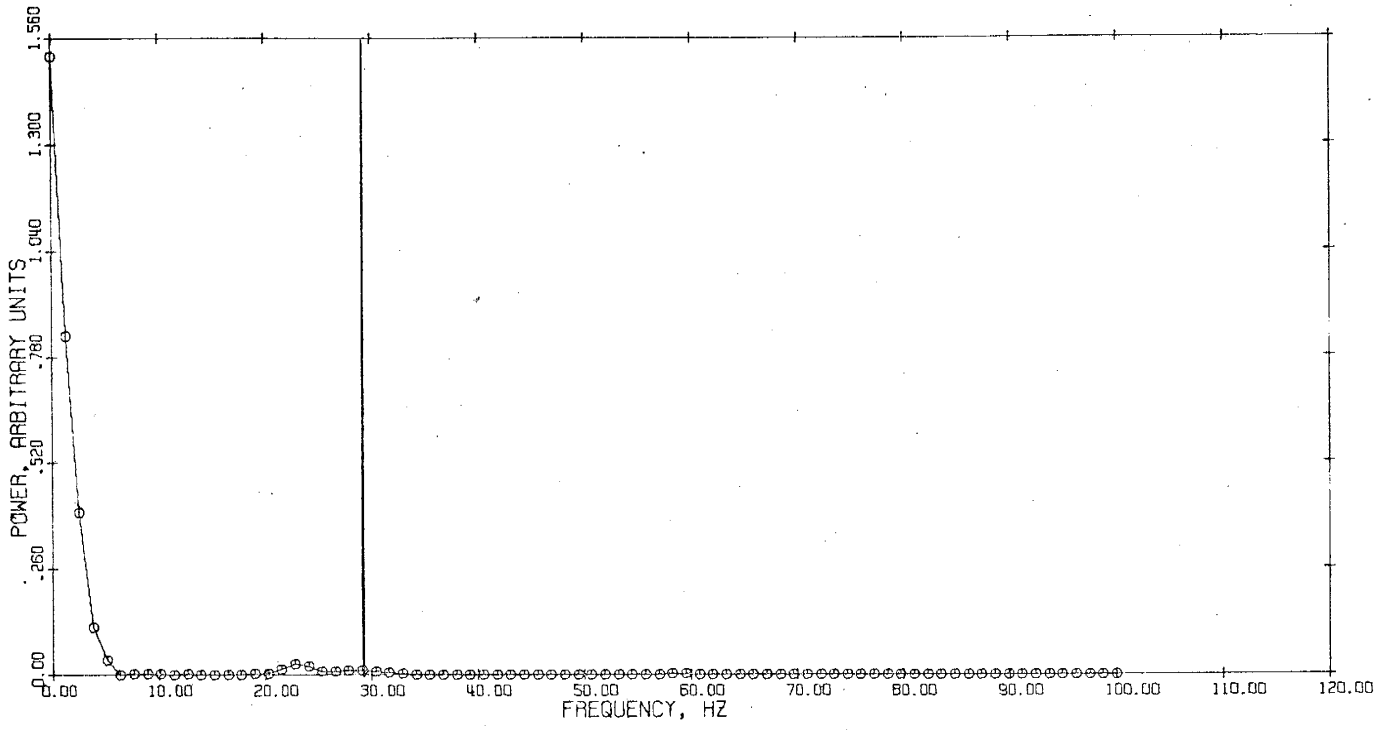

MICROWAVE SPECTRUM WEIGHT .0743 G.

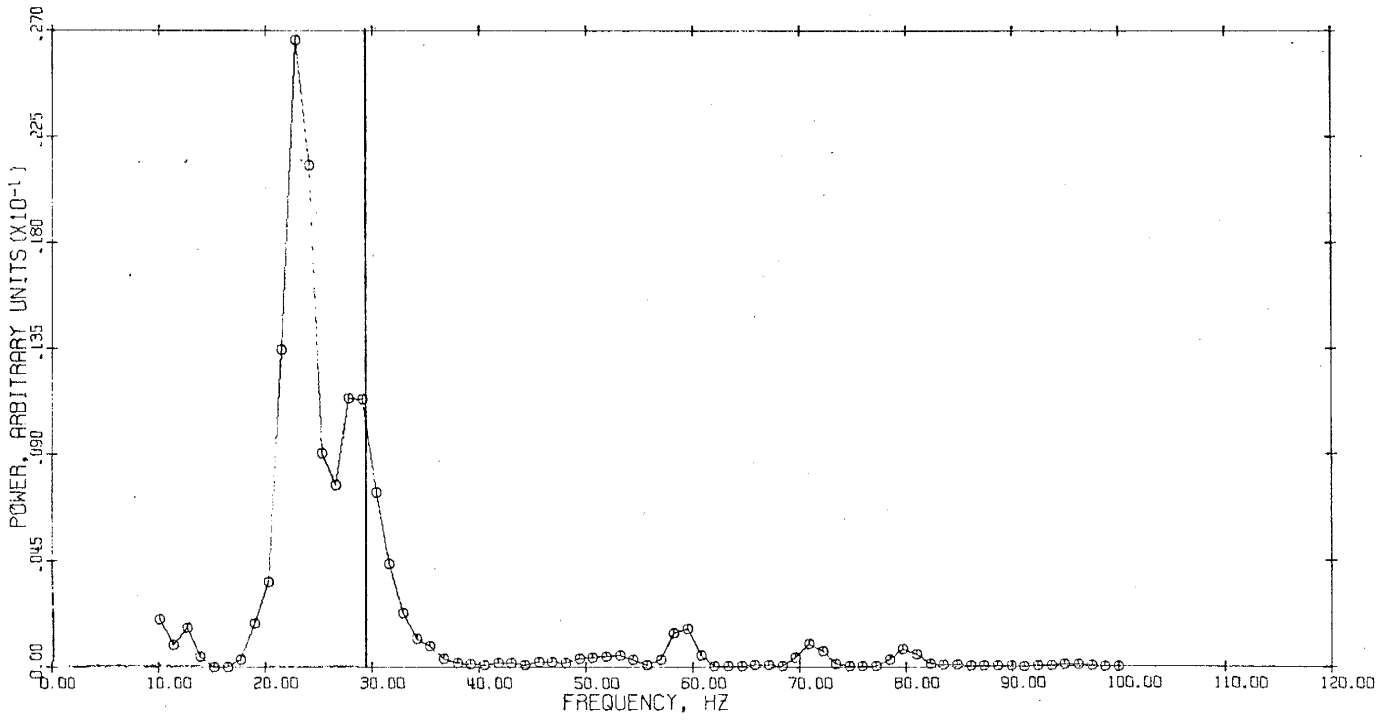

MICROWAVE SPECTRUM WEIGHT .0743 G.

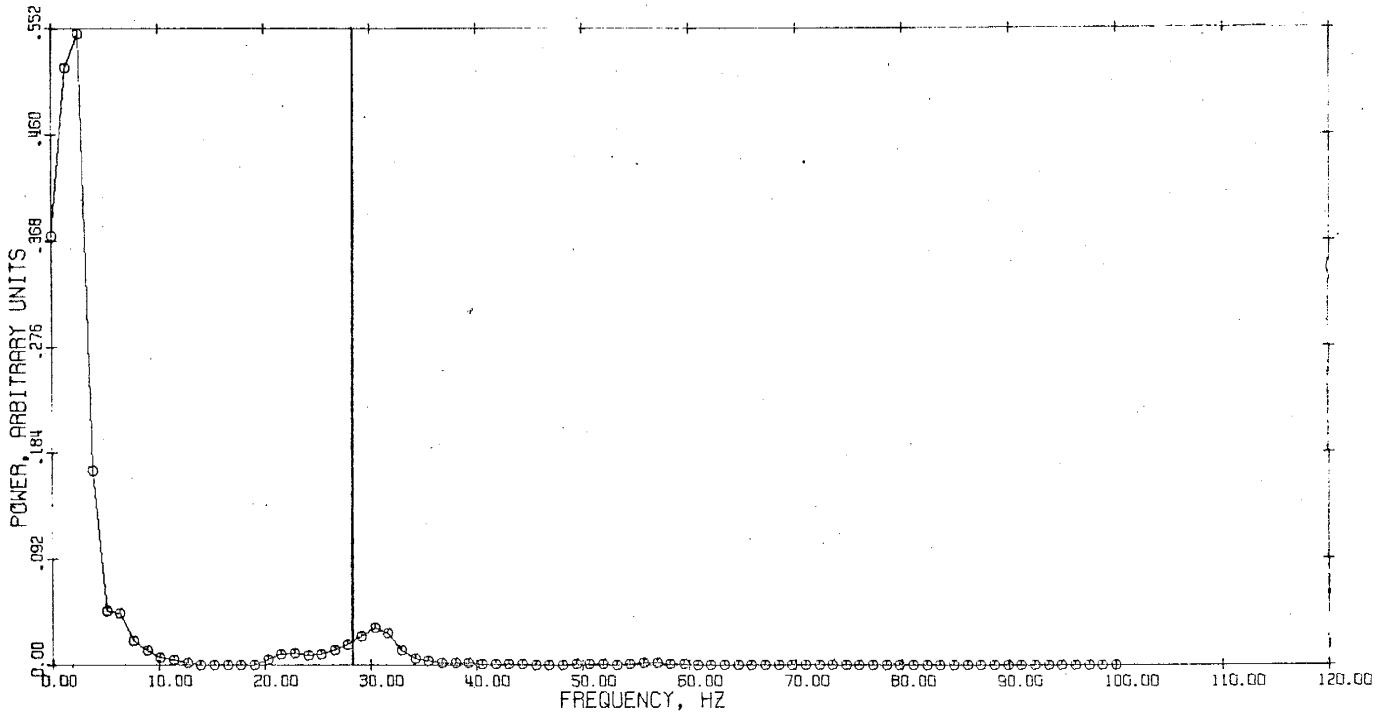

MICROWAVE SPECTRUM WEIGHT .0793 G.

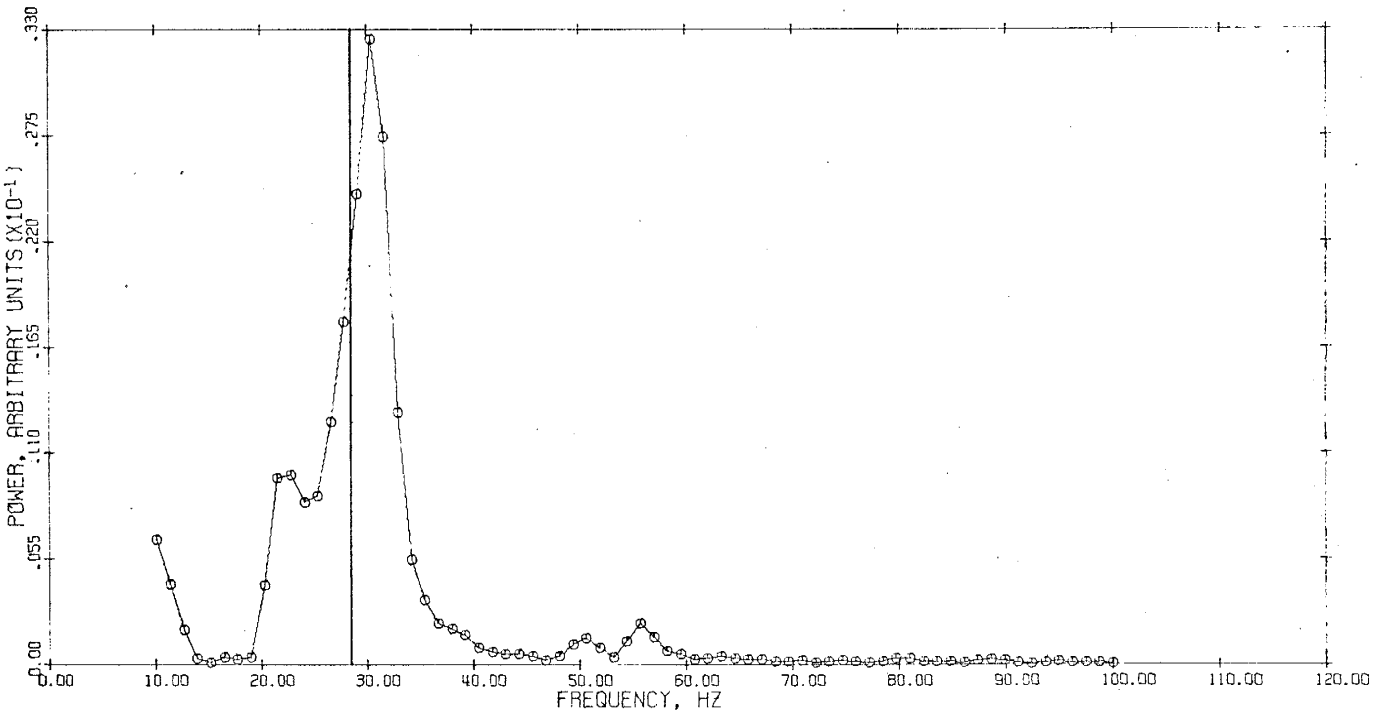

MICROWAVE SPECTRUM WEIGHT .0793 G.

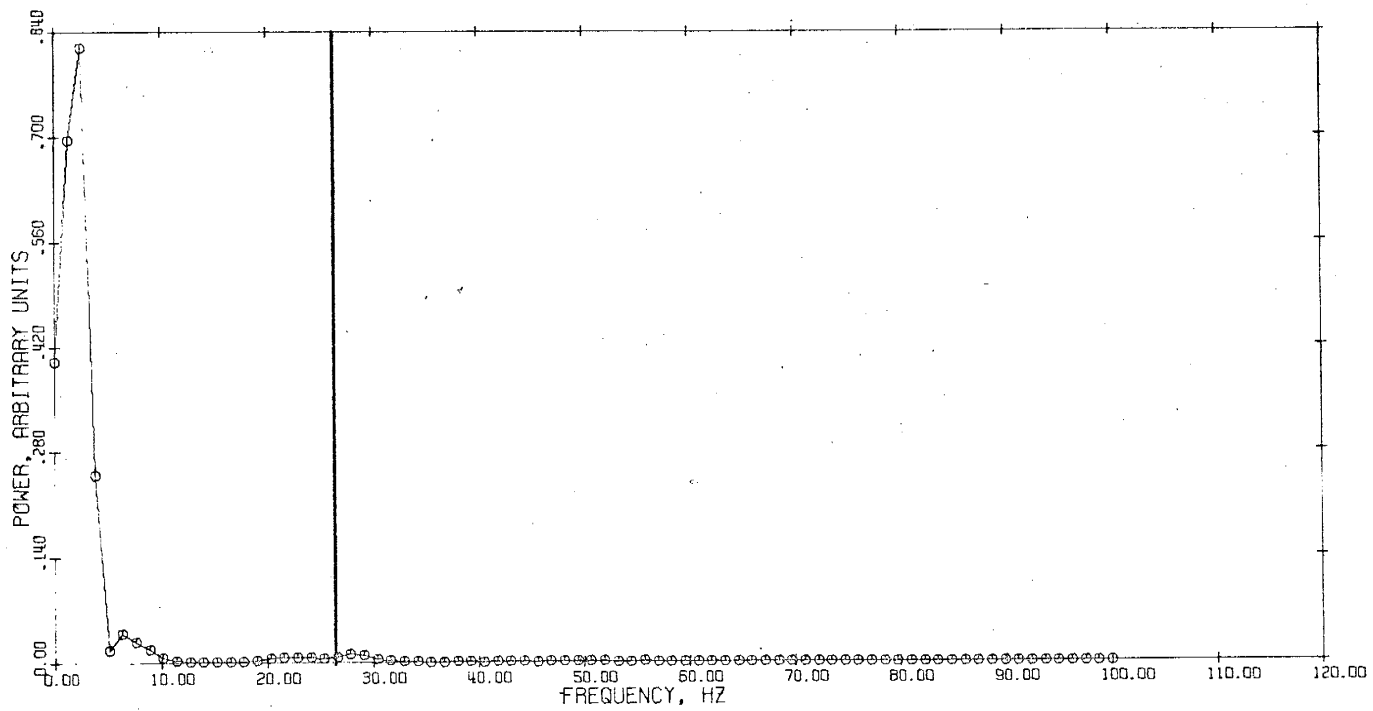

MICROWAVE SPECTRUM WEIGHT .0900 G.

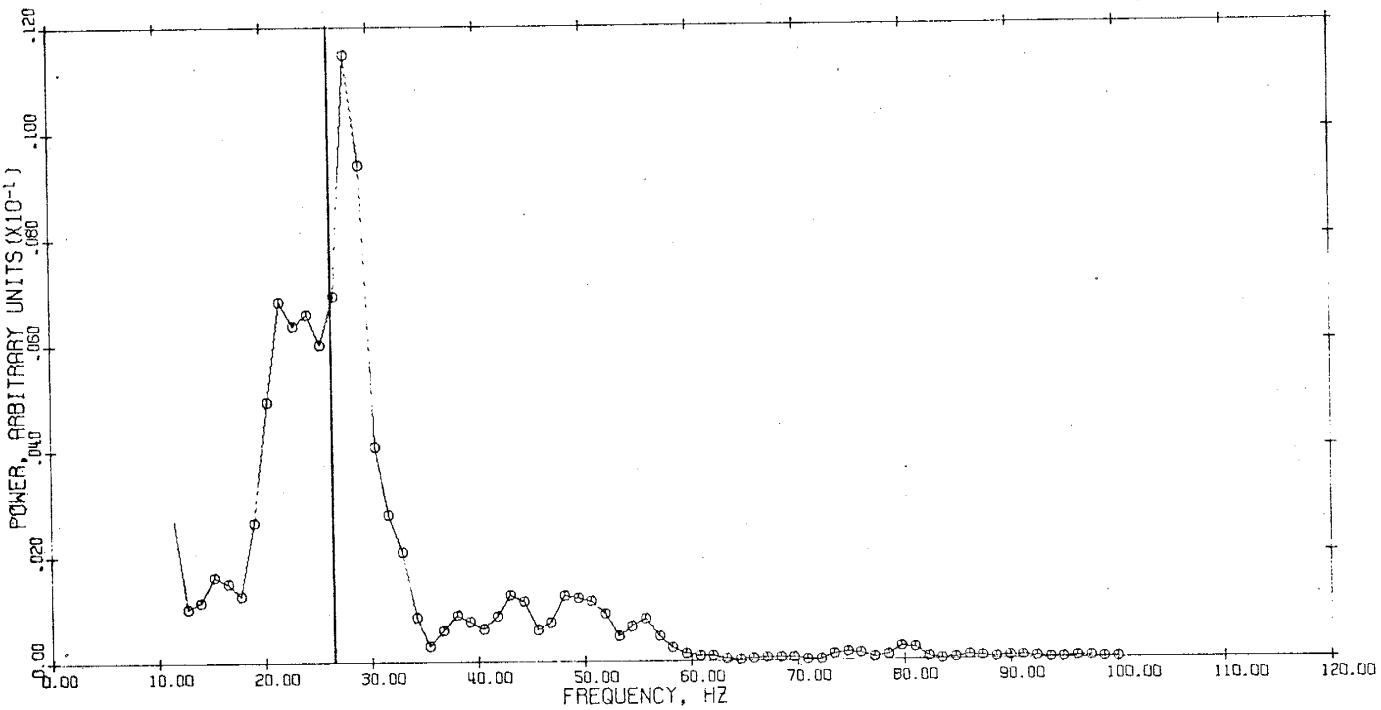

MICROWAVE SPECTRUM WEIGHT .0900 G.

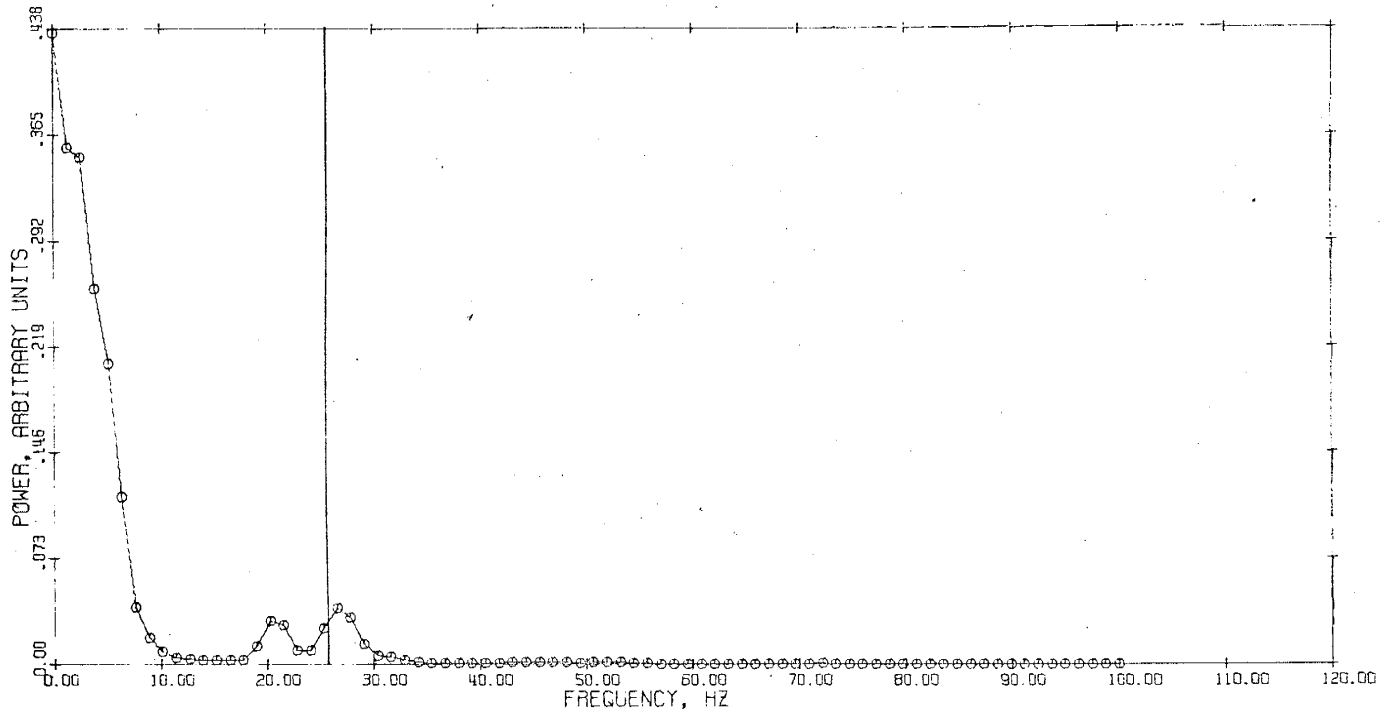

MICROWAVE SPECTRUM WEIGHT .0947 G.

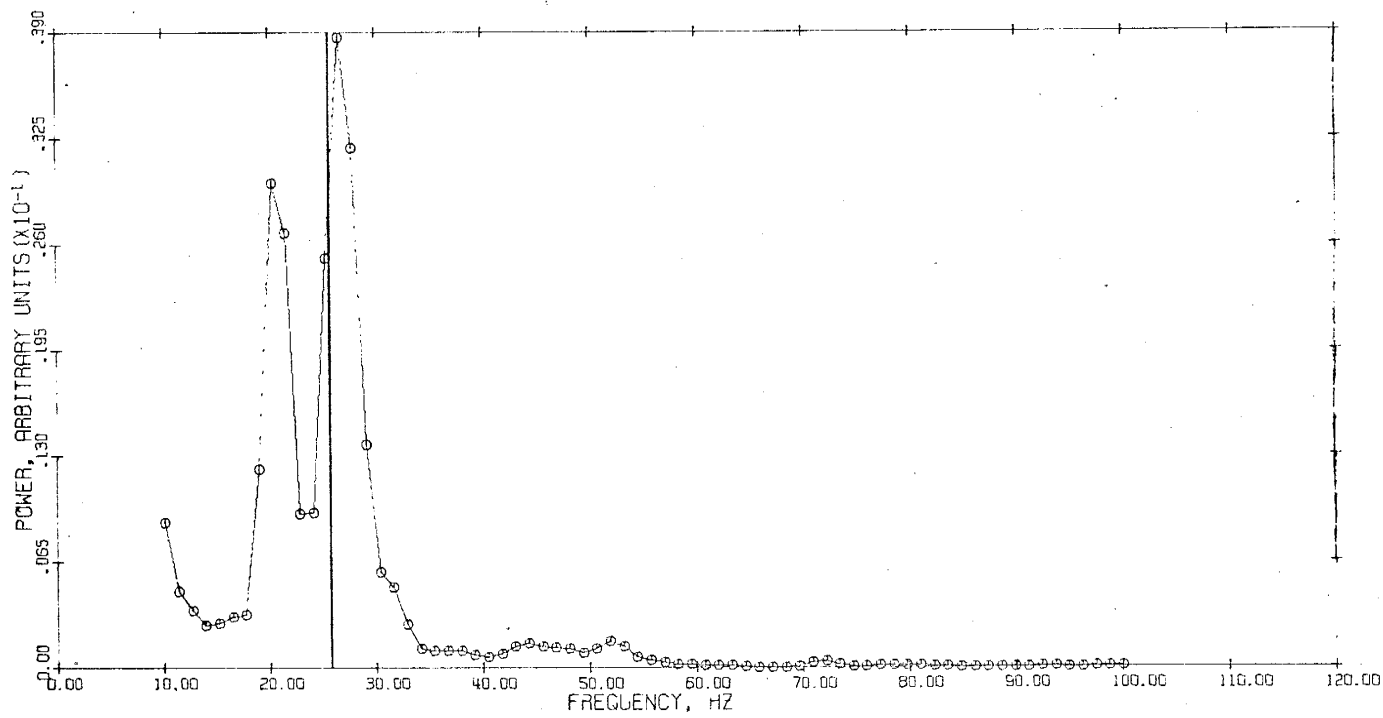

MICROWAVE SPECTRUM WEIGHT .0947 G.

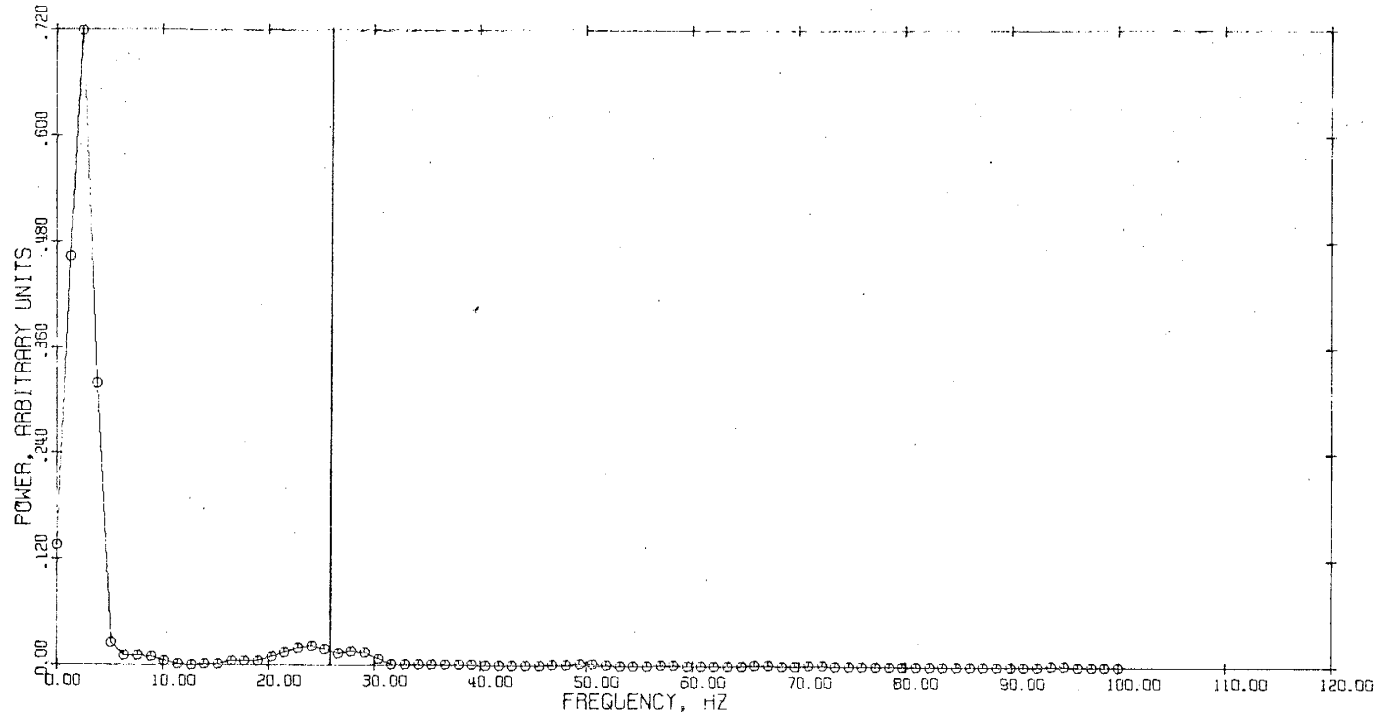

MICROWAVE SPECTRUM WEIGHT .0995 G.

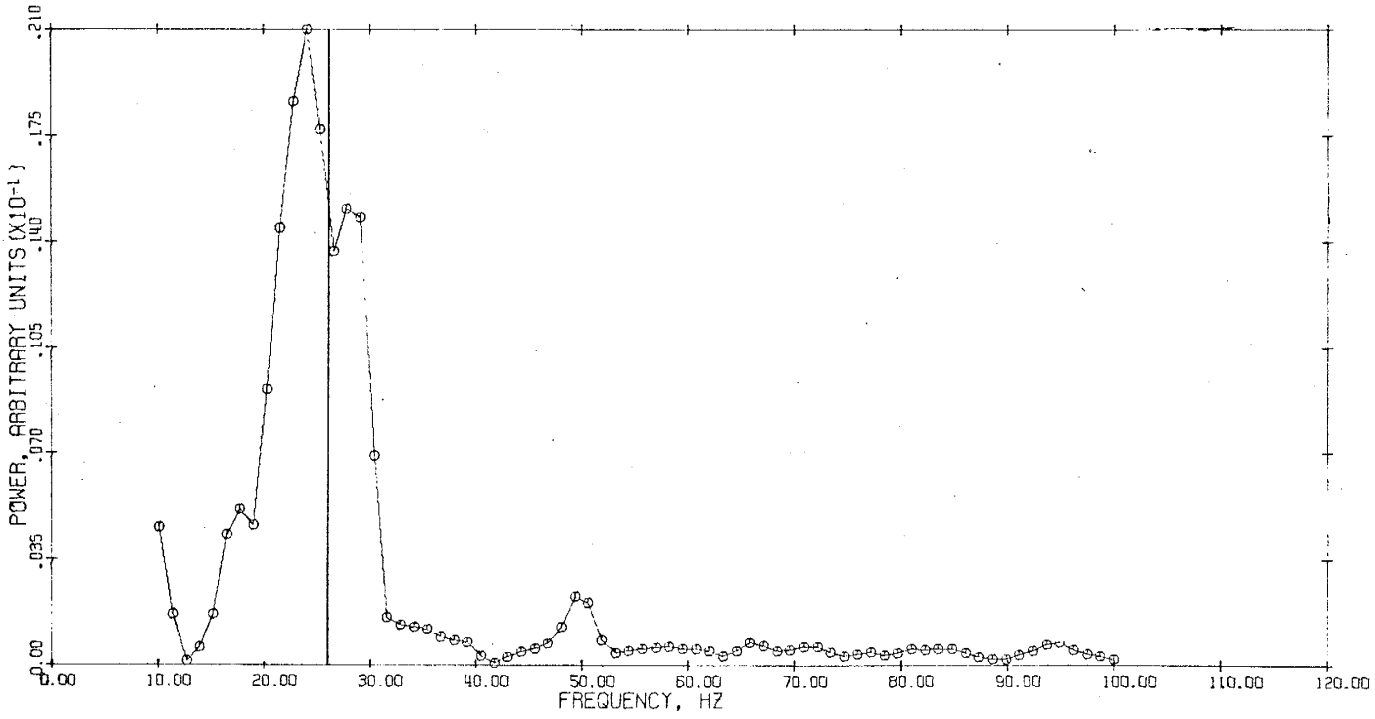

MICROWAVE SPECTRUM WEIGHT .0995 G.

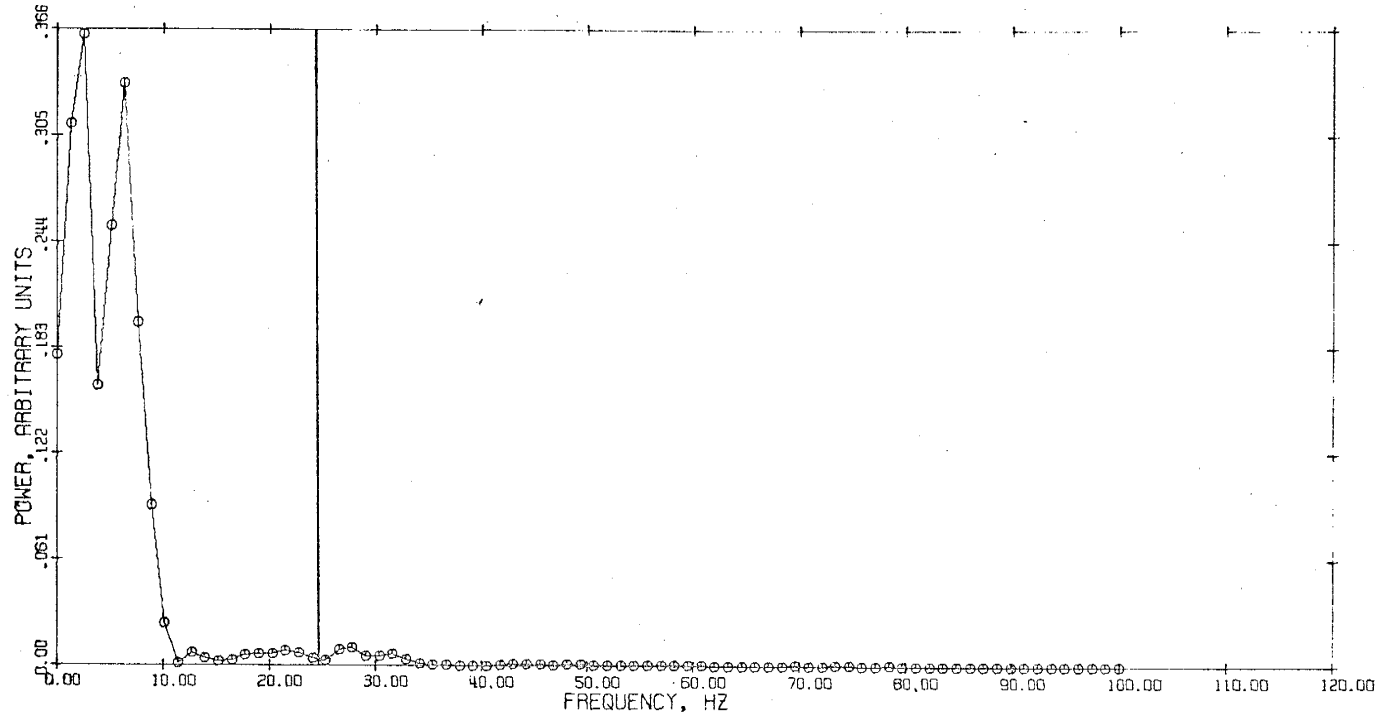

MICROWAVE SPECTRUM WEIGHT .1021 G.

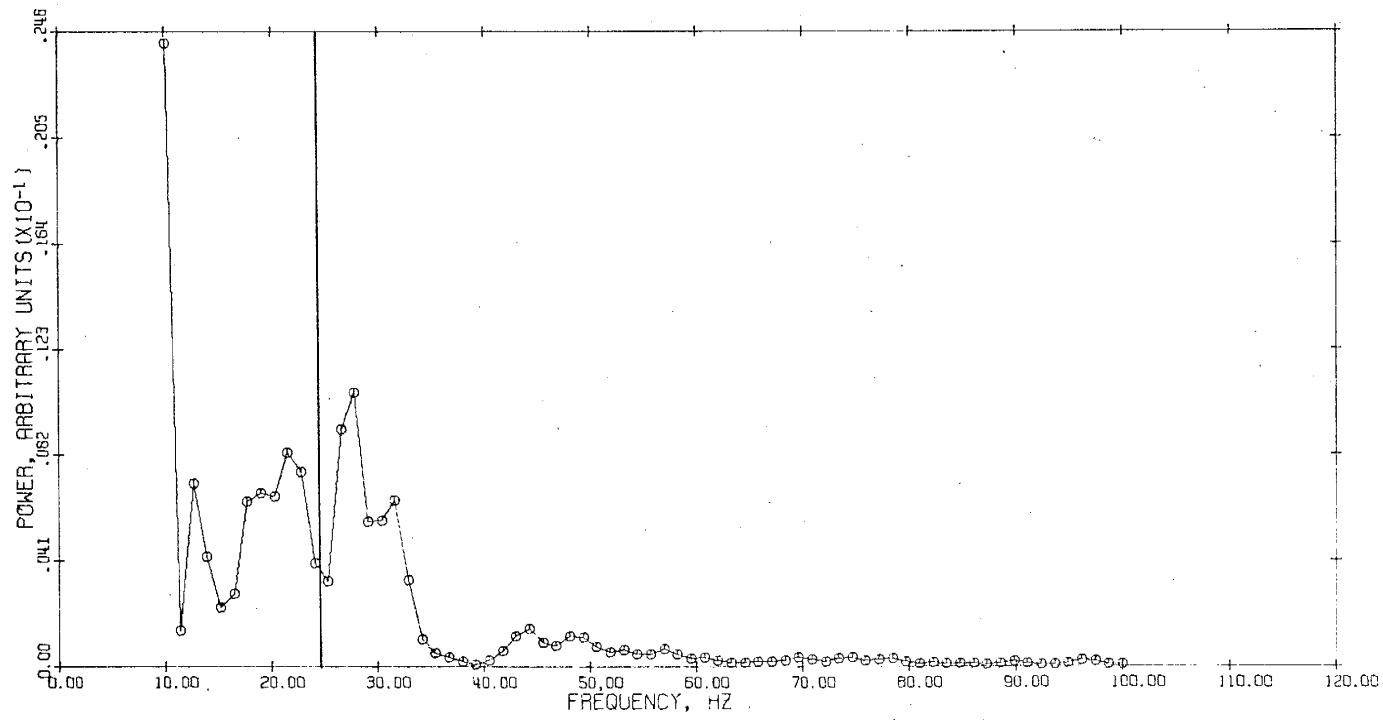

MICROWAVE SPECTRUM WEIGHT .1021 G.

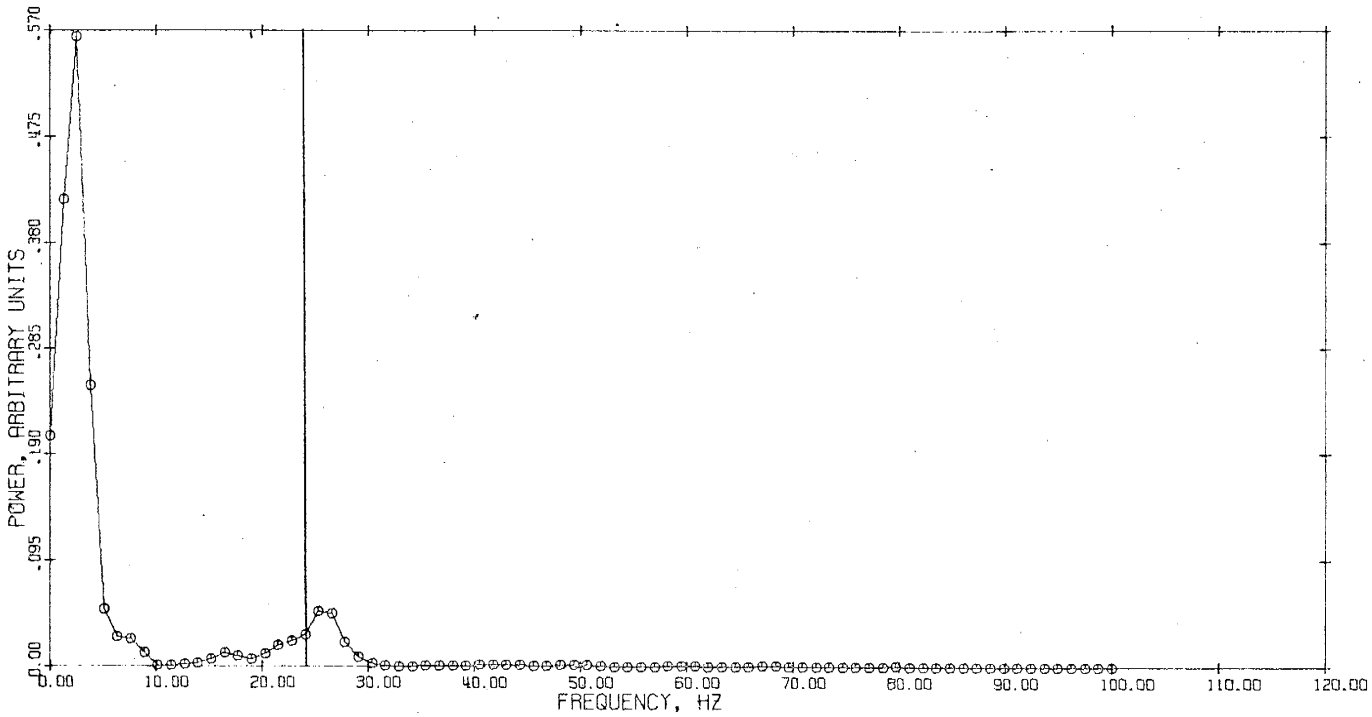

MICROWAVE SPECTRUM WEIGHT .1088 G.

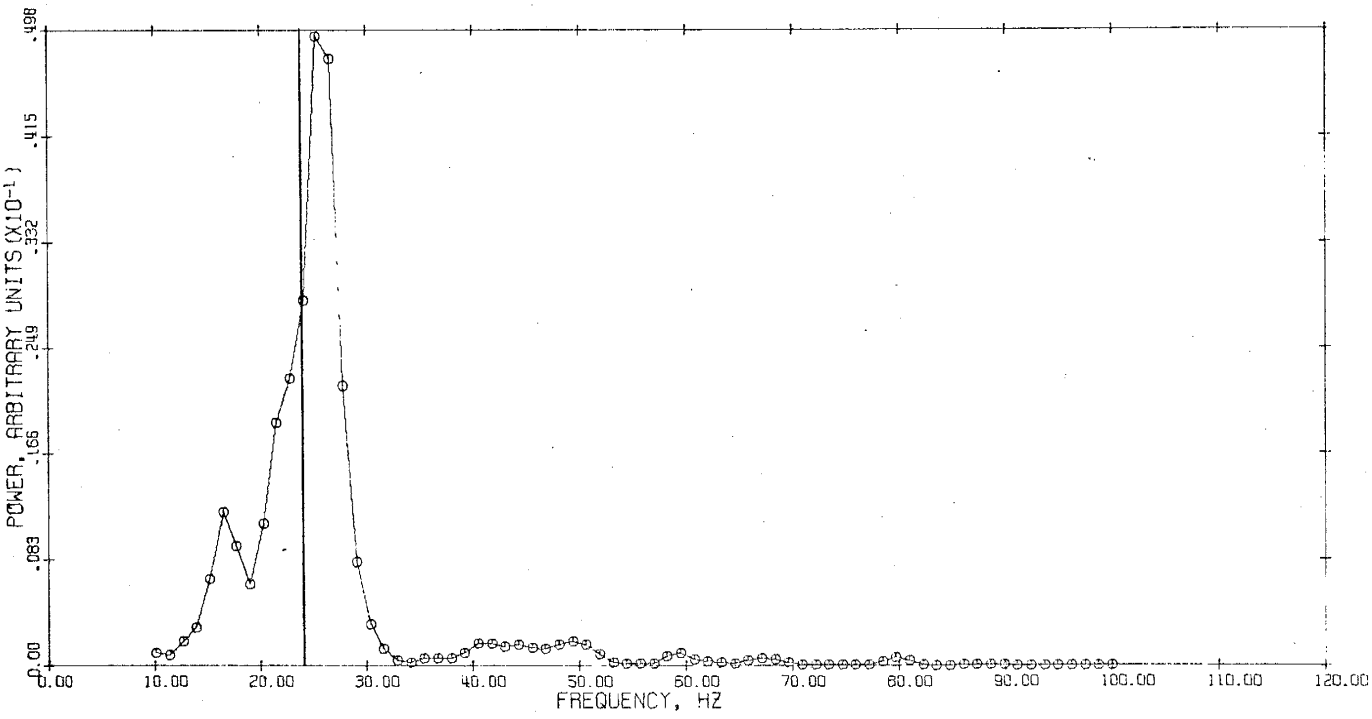

MICROWAVE SPECTRUM WEIGHT .1088 G.

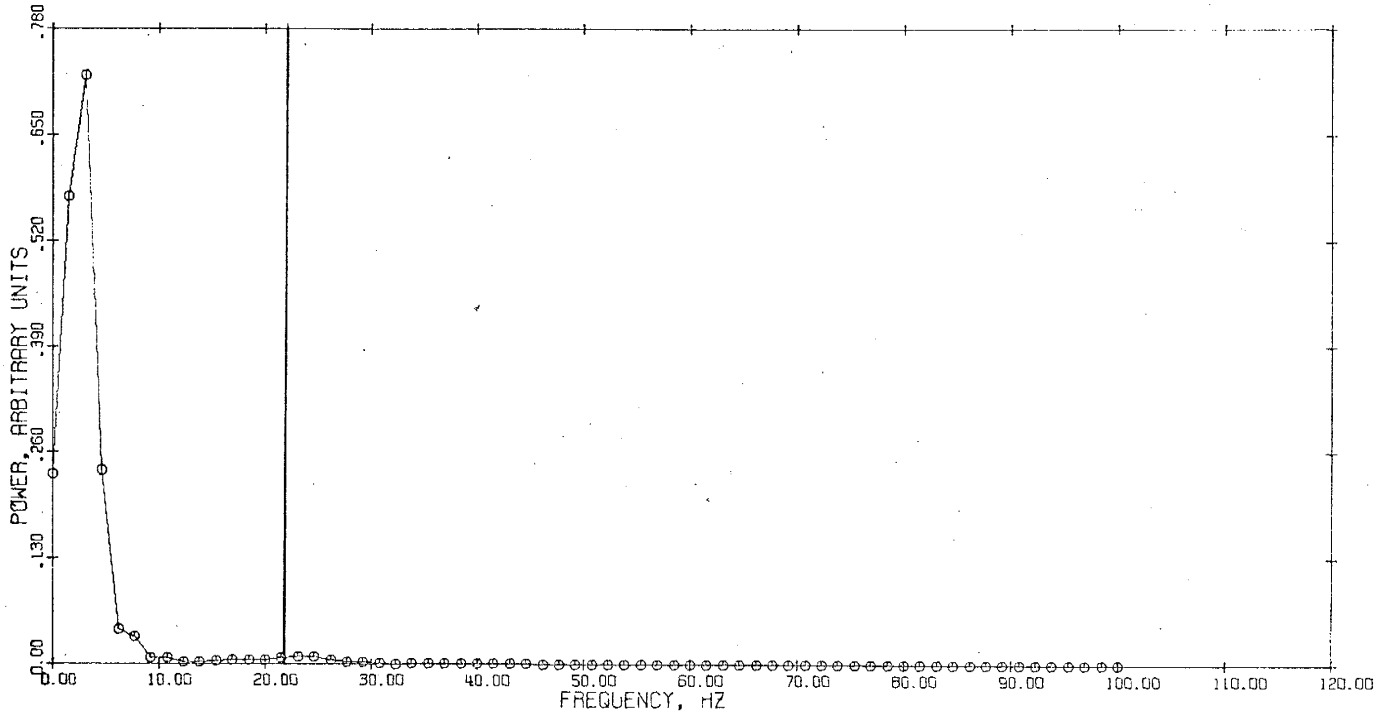

MICROWAVE SPECTRUM WEIGHT .1306 G.

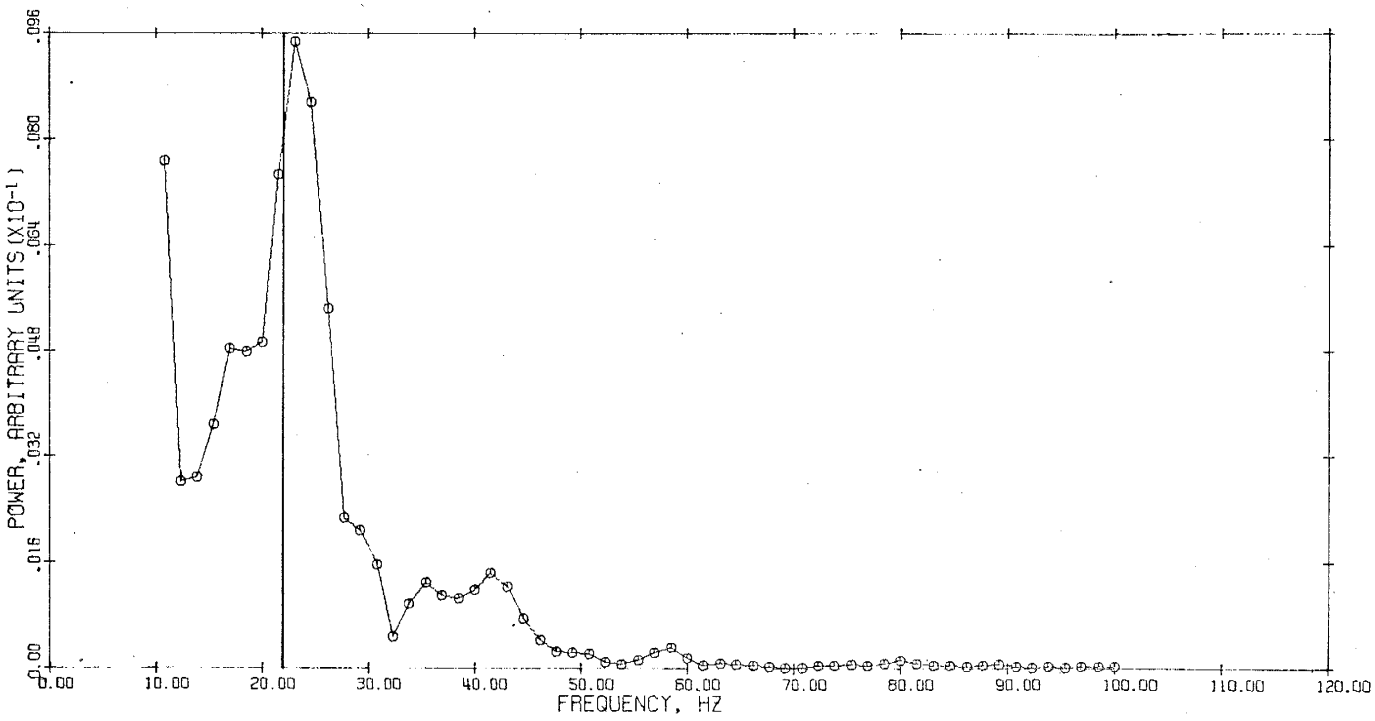

MICROWAVE SPECTRUM WEIGHT .1306 G.

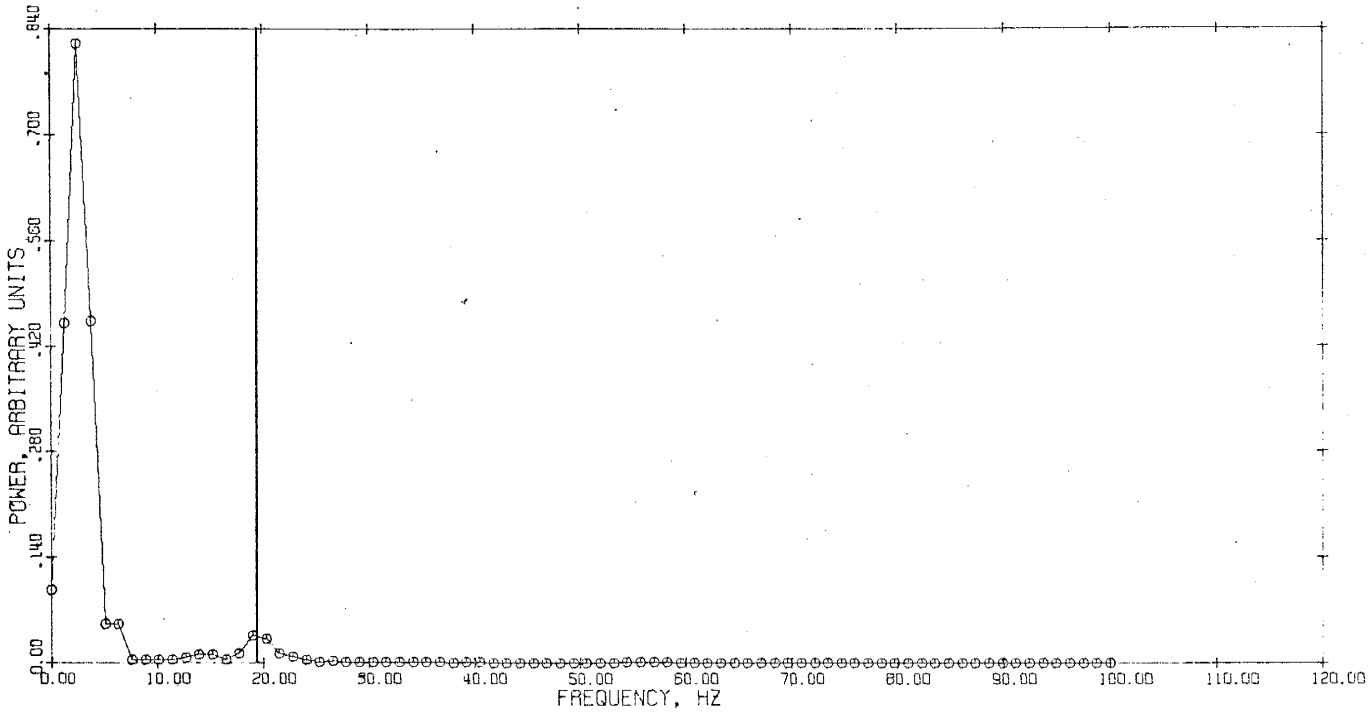

MICROWAVE SPECTRUM WEIGHT .1630 G.

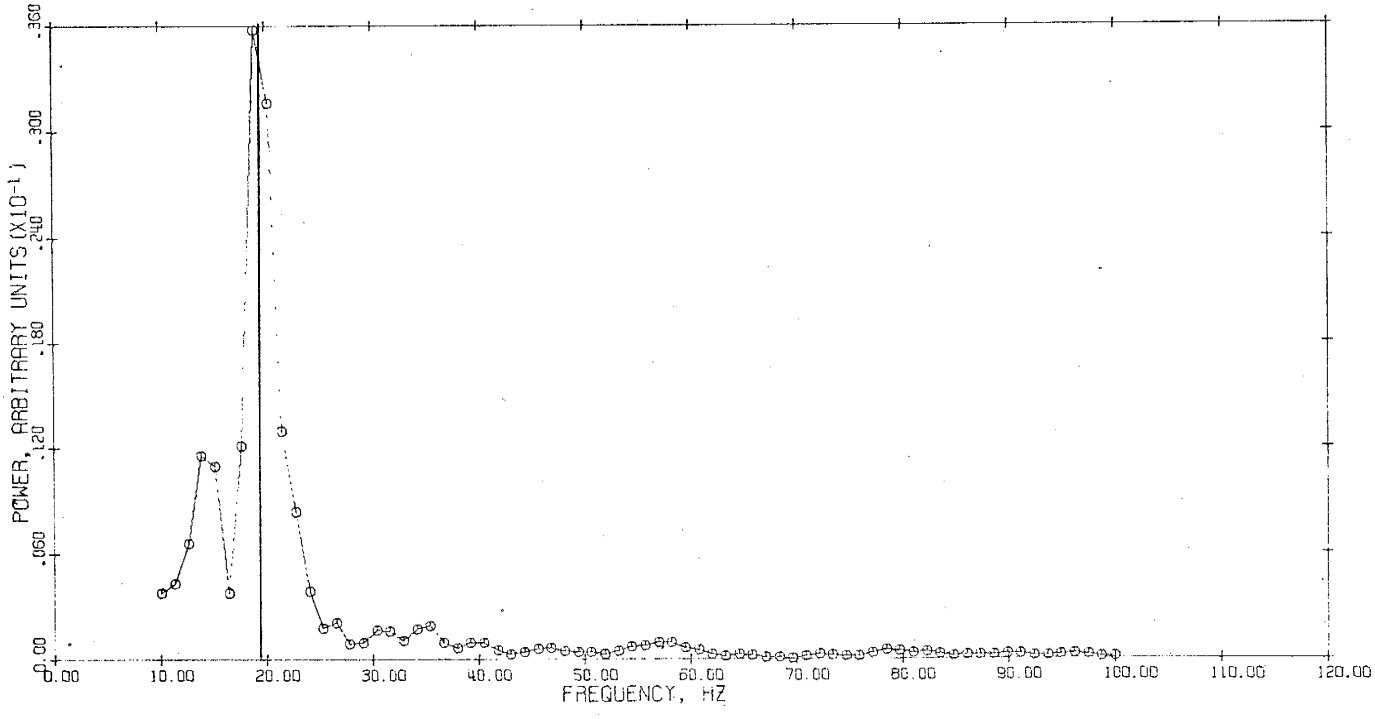

MICROWAVE SPECTRUM WEIGHT .1630 G.

BIBLIOGRAPHY

Atlas, D., Advances in radar meteorology, Advances in Geophysics, 10, Academic Press, 1964.

Atlas, D., M. Kerker, and W. Hitschfeld, Scattering and attenuation by non-spherical atmospheric particles, J. Atmos. Terr. Phys., 3, 108, 1953.

Ausman, Jr., E. L., and M. Brook, to be published, 1967.

Bartnoff, S., and D. Atlas, Microwave determination of particle-size distribution, J. Meteor., 8, 130, 1951.

Best, A. C., Empirical formulae for the terminal velocity of water drops falling through the atmosphere, Quart. J. Roy. Met. Soc., 76, 302, 1950.

Blanchard, D. C., Experiments with water drops and the interaction between them at terminal velocity in air, Project Cirrus occasional report No. 17, 1949.

Blanchard, D. C., The behavior of water drops at terminal velocity in air, Trans. A. G. U., 31, 836, 1950.

Boyenval, E. H., Echoes from precipitation using pulsed doppler radar, Proc. 8th Weather Radar Conf., Am. Met. Soc., Boston, 65, 1960.

Bridges, J. E., and J. R. Feldman, Radar attenuation-reflectivity technique for the remote measurement of drop-size distributions of rain, J. Appl. Met., 5, 349, 1966.

Cartmill, R. H., Rainfall rate measurement using two radar sets of different wavelengths-theory, Proc. 10th Weather Radar Conf., 265, 1963.

Chandrasekhar, S., The oscillations of a viscous liquid globe, Proc. London Math. Soc., 9, 141, 1959.

Colgate, S. A., Enchanced drop coalescence by electric fields in equilibrium with turbulence, J. Geophys. Res., 72, 479, 1967.

Edgerton, E. K., and J. R. Killian, Flash: seeing the unseen by ultra high-speed photography, Hale Publishing Co., New York, New York, 1939.

Finlay, B. A., A study of liquid drops in an air stream, Ph. D. Thesis, Univ. of Birmingham, Birmingham, England, 1957.

Flower, W. D., The terminal velocity of drops, Phys. Soc. London, Proceedings, 40, 167, 1928.

Garner, F. H., and P. Kendrik, Mass transfer to drops of liquid suspended in a gas stream, Part I "A wind tunnel for the study of individual liquid drops," Trans. Instn. Chem. Engrs., 37, 155, 1959.

Garner, F. H., and J. J. Lane, Mass transfer to drops of a liquid suspended in a gas stream, Part II "Experimental work and results", Trans. Instn. Chem. Engrs., 37, 162, 1959.

Gerhardt, J. R., C. W. Tolbert, S. A. Brunstein, and W. W. Bahn, Experimental determinations of the back-scattering cross-sections of water drops and of wet and dry ice spheres at 3.2 cm, J. Met., 18, 340, 1961.

Goldburg, A., and B. H. Florsheim, Transition and strouhal number for the incompressible wake of various bodies, Phys. Fluids, 9, 45, 1966

Golvin, A. M., The theory of the vibration and breakdown of droplets in a gas stream in the presence of rotational motion inside the droplets, IZV. Geophys. Ser. #7, 1084, 1964.

Golovin, A. M., On the theory of oscillations and fractioning of a drop in a gas stream with a potential movement within the drop, IZV. Geophys. Ser. #8, 1269, 1964b.

Gunn, R., Mechanical resonance in freely falling raindrops, J. Geophys. Res., 54, 383, 1949.

Gunn, R. and G. D. Kinzer, The terminal velocity of fall for water droplets in stagnant air, J. Met., 6, 243, 1949.

Herman, B. M., S. R. Browning, and L. J. Battan, Tables of the radar cross-sections of water spheres, Tech. Rep. No. 9, Univ. of Arizona, Inst. of Atmospheric Physics, 1961.

Hinze, J. O., Forced deformations of viscous liquid globules, Appl. Sci. Res., A1, 263, 1949a.

Hinze, J. O., Critical speeds and sizes of liquid globules, Appl. Sci. Res., A1, 273, 1949b.

Hitschfeld, W., Free fall of drops through air, Trans. A.G.U., 32 697, 1951.

Hodgkinson, T. G., The response of a spherical fluid particle suspended in air to irradiation with sound at the natural frequency of the particle, Acustica, 3, 383, 1953.

Hughes, R. R., and E. R. Gilliland, The mechanics of drops, Chem. Engrg. Prog., 48, 497, 1952.

Imai, I., On the velocity of falling raindrops, J. Meteor. Soc., Japan, 28, 43, 1950.

Jones, D. M. A., The shape of raindrops, J. Met., 16, 504, 1959.

Kaparthi, R., and W. Licht, Deformation and oscillation of liquid drops falling through water, J. Sci. Indust. Res., 21B, 565, 1962.

Kinzer, G. D., and R. Gunn, The evaporation, temperature, and thermal relaxation-time of freely falling waterdrops, J. Met., 8, 71, 1951.

Labrum, N. R., The scattering of radio waves by meteorological particles, J. Appl. Phys., 23, 1324, 1952.

Lamb, H., Hydrodynamics, 1879 (as reprinted by Dover Press, 1945.)

Lane, W. R., and H. L. Green, The mechanics of drops and bubbles, in Surveys in Mechanics, Cambridge Univ. Press, 1956.

Laws, J. O., Measurements of the fall-velocity of water-drops and raindrops, Trans. A.G.U., 709, 1941.

Lenard, P., Uberdie schivingungen fallender tropfen, Ann. der Phys., 30, 209, 1887.

Lenard, P., Uber Regen, Met. Zeit., 21, 248, 1904.

Lhermitte, R., New developments of the echo fluctuations theory and measurements, Proc. 8th Weather Radar Conf., San Francisco, 263, 1960.

Lumley, J. L., Passage of a turbulent stream through honeycomb of large length-to-diameter ratio, Trans. ASME, J. Basic Engrg., 9, 218, 1964.

McDonald, J. E., The shape and aerodynamics of large raindrops, J. Met., 11, 478, 1954.

Margarvey, R. H., and R. L. Bishop, Wakes in liquid-liquid systems, Phys. Fluids, 4, 800, 1961.

Magono, C., On the shape of water drops falling in stagnant air, J. Met., 11, 77, 1954.

Mathur, N., and E. A. Mueller, Radar back-scattering from non-spherical particles, Rep. of Investigation #28, Illinois State Water Survey Div., Univ. of Illinois, Urbana, 1955.

Matunobu, Y., Motion of a deformed drop in Stokes flow, J. Phys. Soc., Japan, 21, 1596, 1966.

Möller, V. W., Experimentelle untersuchungen zur hydrodynamuk der kugel, Physik. Zeit., 39, 57, 1938.

Morse, P. M., Vibration and sound, McGraw Hill, 234, 1948.

Pai, S., The fluid dynamics of jets, Van Nostrand, New York, New York, 1954.

Rayleigh, J. W. S., The theory of sound, II, (1877) (Reprinted by Dover Press, 1945.

Reid, W. H., The oscillations of a viscous liquid drop, Quart. Appl. Math., 18, 86, 1960.

Saito, S., On the deformation of a fluid drop at low Reynolds number, Sci. Rep. Tohoku Imp. Univ., Sendai, Japan, 2, 179, 1913.

Sample, S. B., Static and dynamic behavior of liquid drops in electric fields, Charged Particle Res. Lab., Rep #7-65 CPRL, Univ. of Illinois.

Savic, P., Circulation and distortion of liquid drops falling through a viscous medium, National Res. Council of Canada, Mech. Engrg. Rep. #MT-22, 1953.

Schmidt, W., Die gestalt fallender regentropfen, Met. Zeit., 30, 456.

Schroeder, R. R., and R. C. Kintner, Oscillations of drops falling in a liquid field, A.I.CH.E. J., 11, 5, 1965.

Senior, T. B. A., The scattering of an electromagnetic wave by a spheroid, Can. J. Phys., 44, 1353, 1966.

Shafrir, U., Horizontal oscillations of falling spheres, Final Rep. Contract AF 19 (628) - 3993 AFCRL, 1965.

Sphilaus, A. F., Raindrop size, shape, and falling speed, J. Met., 5, 108, 1948.

Squire, H. B., The round laminar jet, Quart. Journ. Mech. and Appl. Math., IV, 321, 1951.

Stephens, J. J., Radar cross-sections for water and ice spheres, J. Meteor., 18, 348, 1961.

Stevenson, A. F., Solution of electromagnetic scattering problems as power series in the ratio (dimension of scatterer)/ wave length, J. Appl. Phys., 24, 1134, 1953a.

Stevenson, A. F., Electromagnetic scattering by an ellipsoid in the third approximation, J. Appl. Phys., 24, 1143, 1953.

Taylor, T. D., and A. Acrivos, On the deformation and drag of a falling viscous drop at low Reynolds number, J. Fluid Mech., 18, 466, 1964.

Telford, J. W., W. S. Thorndike, and E. G. Bowen, The coalescence between small water drops, Quart. J. Roy. Meteorol. Soc., 81, 241, 1955.

Van der Leeden, P., L. D. Nio, and P. C. Suratman, The velocity of free falling droplets, Appl. Sci. Res., Sect. A., 5, 338, 1956.

Wexler, R. and D. Atlas, Radar reflectivity and attenuation of rain, J. Appl. Met. , 2, 276, 1963.

Winnikow, S., and B. T. Chao, Droplet motion in purified systems, Phys. Fluids, 9, 50, 1966.

This thesis is accepted on behalf of the faculty of the Institute by the following committee:

Albert J. Petzold

Charles R. Holmes

Marvin H. Wilkening

C. B. Moore

Max Brook

Martin S. Friday

Date: 7 Sept 1967